

https://dspace.org/

Functional impact of IGHG3 genetic variation in HIV-1 infection

Spencer, Holly

2022
https://hdl.handle.net/10539/34229

Downloaded from a DSpace repository. https://dspace.org/

FUNCTIONAL IMPACT OF *IGHG3* GENETIC VARIATION IN HIV-1 INFECTION

Holly Spencer

A Dissertation submitted to the Faculty of Health Sciences, University of the Witwatersrand, Johannesburg, in fulfilment of the requirements for the degree of Master of Science in Medicine.

Johannesburg, 2022

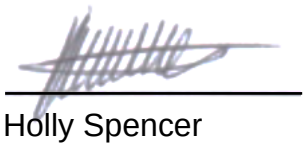
Declaration

UNIVERSITY OF THE WITWATERSRAND, JOHANNESBURG

FACULTY OF HEALTH SCIENCES

I, Holly Spencer (Student number: 1076013) am a student registered for MSc (MED) in the academic year 2021. I hereby declare the following:

- I am aware that plagiarism (the use of someone else's work without their permission and/or without acknowledging the original source) is wrong.
- I confirm that the work submitted for assessment for the above degree is my own unaided work except where I have explicitly indicated otherwise.
- I have followed the required conventions in referencing the thoughts and ideas of others.
- I understand that the University of the Witwatersrand may take disciplinary action against me if there is a belief that this is not my own unaided work or that I have failed to acknowledge the source of the ideas or words in my writing.
- I have included as an appendix a report from "Turnitin" (or other approved plagiarism detection) software indicating the level of plagiarism in my research document.



Holly Spencer

15th February 2022

Date

Presentations

Spencer, H., Richardson, S. I., Lambson, B. E., Morris, L., Moore, P. L., Scheepers, C. (2021) 'High Levels of Diversity in IgG3 Constant Region Antibody Genes', 4th HIVR4P // Virtual. 2021. Publication-only abstract.

Spencer, H., Richardson, S. I., Lambson, B. E., Morris, L., Moore, P. L., Scheepers, C. (2020) '*IGHG3* Genetic Variation in HIV-1 Infected Individuals', Wits Faculty of Health Sciences Virtual Research Day & Postgraduate Expo. 2020. Oral presentation.

Spencer, H., Richardson, S. I., Lambson, B. E., Morris, L., Moore, P. L., Scheepers, C. (2019) 'Functional Impact of *IGHG3* Genetic Variation in HIV-1 Infection', 9th Infectious Diseases in Africa Symposium. 2019. Oral presentation and poster.

Spencer, H., Richardson, S. I., Lambson, B. E., Morris, L., Moore, P. L., Scheepers, C. (2019) 'Functional Impact of *IGHG3* Genetic Variation In HIV-1 Infection', 14th Meeting of the H3Africa Consortium. 2019. Oral presentation.

Abstract

IgG3 antibodies are able to mediate a broad range of potent Fc effector functions. Several of which have been associated with reduced risk of infection following HIV vaccination. Furthermore, *IGHG3* (the gene encoding IgG3) contains the highest level of reported allelic diversity, with 29 documented alleles in the international immunogenetics database (IMGT). While there is some evidence that key IgG3 mutations can alter antibody half-life and effector function, the functional impact of these alleles is generally poorly characterized. Additionally, the diversity of *IGHC* genes has not been investigated in Southern African populations. The aim of this project was to sequence the full-length *IGHG3* in the CAPRISA cohort and to test their functional relevance in the context of HIV. Using Sanger and PacBio platforms, five novel *IGHG3* alleles were identified, three of which contained amino acid substitutions in coding regions. A further ten documented alleles were identified from nine participants. The alleles identified were used to clone participant-matched HIV-specific antibodies previously isolated from the nine individuals sequenced, alongside IgG1*01 and IgG3*01 controls. The ability of these antibodies to induce antibody-dependent cellular phagocytosis (ADCP), to neutralize, to bind to FcγRIIA; and their susceptibility to protease digestion was tested. Overall, IgG3 antibodies exhibited equivalent or enhanced ADCP, neutralization and FcγRIIA-binding compared to IgG1 antibodies, while the functional differences between *IGHG3* alleles were subtle. This was observed across multiple strain-specific and broadly neutralizing antibodies targeting various HIV epitopes. Altogether, we found a high level of genetic diversity in a small sample-size, motivating for further investigation into *IGHG3* diversity within understudied populations. The outcomes of this project contribute to our understanding of how genetic diversity affects function in IgG3 antibodies, in line with a growing body of research supporting the use of IgG3 antibodies in passive immunization for HIV prevention.

295/350 words

Acknowledgments

A wise supervisor once said “it takes a village to raise a child”. Thank you to the village that is the Antibody Immunity Research Unit for all the advice, for providing inspiration and role models – and of course for all the cake.

Thank you to my three science mothers for sharing their expertise, their endless patience, and for motivating me to be a better scientist. I am grateful to…

- Dr Simone Richardson for being my Patronus to the dementors that are Fc assays.
- Dr Cathrine Scheepers for providing honest advice both in science and in life, and for sharing all the best memes.
- Prof. Penny Moore for creating the remarkable culture in this lab, and for showing me the importance of collaborations.

I’d also like to thank the National Research Foundation (NRF), the Poliomyelitis Research Foundation (PRF) and the University of the Witwatersrand Postgraduate Merit Award for their funding support, without whom this project would not have been possible.

Finally, thank you to my family for their unconditional support, and for doing their best to understand why I get excited about dot plots.

Contents

Declaration ii
Presentations iii
Abstract iv
Acknowledgments v
Contents vi
List of Figures ix
List of Tables xi
List of Equations xii
Abbreviations xiii
1. Introduction 2
1.1. HIV: the pandemic 2
1.2. Broadly Neutralizing Antibodies in HIV prevention and treatment 2
1.3. The role of bNAbs in HIV vaccines 4
1.4. Strain-specific neutralizing antibodies in HIV 5
1.5. The role of non-neutralizing antibody function in HIV 5
1.6. The structure of antibodies 6
1.7. Antibody Fc effector functions 7
1.7.1. Antibody-dependent cellular phagocytosis (ADCP) 7
1.7.2. Antibody-dependent cellular cytotoxicity (ADCC) 8
1.7.3. Antibody-dependent complement deposition (ADCD) 8
1.7.4. Antibody-dependent cellular trogocytosis (ADCT) 8
1.8. Modulators of antibody function 8
1.8.1. Fc receptors 9
1.8.2. Glycosylation 10
1.8.3. Antibody Isotype 10
1.9. IgG3 antibodies and their therapeutic potential 13
1.10. *IGHG3* Allelic diversity 13
1.11. Genetic diversity in African populations 13
1.12. Study objectives 15
1.12.1. Sequencing *IGHG3* in 10 CAPRISA participants 15
1.12.2. To characterize the impact of *IGHG3* alleles in this population on phagocytosis, Fc-receptor-binding, antibody cleavage and neutralization 15
2. Materials and methods 16

2.1. Ethics and the CAPRISA cohort 16
2.2. *IGHG3* sequencing protocol 16
2.2.1. Sample DNA extraction 16
2.2.2. Polymerase Chain Reaction 17
2.2.3. Gel imaging and amplicon DNA extraction 17
2.2.4. Separation of alleles through bacterial cloning 18
2.2.5. Screening of colonies for *IGHG3* inserts 18
2.2.6. Plasmid DNA extraction and isolation (MiniPrep) 18
2.2.7. Sanger sequencing 19
2.2.8. PacBio Sequencing 20
2.2.9. Sequencing analysis 22
2.3. Assessing the impact of allelic variation on antibody function 23
2.3.1. Antibody subclass/allelic variant engineering and expression 23
2.3.2. Antibody plasmid transfection and protein expression 30
2.3.3. Antibody purification 31
2.3.4. ADCP assay 31
2.3.5. ADCP analysis 32
2.3.6. ADCP assay statistics 34
2.3.7. TZM-bl neutralization assay and analysis 34
2.3.8. FcγRIIA-binding ELISA 35
2.3.9. Fc region enzyme digest 35
3. Results 37
3.1. Sanger sequencing results 37
3.2. PacBio sequencing results 38
3.3. *IGHG3* haplotypes in CAPRISA participants 40
3.4. Characterizing *IGHG3* functional diversity 44
3.4.1. The impact of allelic diversity on protein structure 44
3.4.2. Converting alleles to participant-matched HIV-specific antibodies 45
3.4.3. The variable region differences between participants 46
3.4.4. The impact of *IGHG3* allelic variation on phagocytosis 47
3.4.5. The influence of Fc region variation on pseudovirus neutralization 49
3.4.1. Reduced FcγRIIA-binding by novel *IGHG3* alleles containing an L234F mutation 51
3.4.2. Investigating the impact of allelic diversity on IdeS cleavage 52
4. Discussion 54

5. Conclusion 61
References 62
Supplementary 79
Appendix A: CAPRISA Letter of Permission 91
Appendix B: Ethics Clearance Certificate 92
Appendix C: Turnitin Report Cover Page 93

List of Figures

Figure 1.1. HIV Env trimer with shaded bNAb epitopes. 3
Figure 1.2. The structure of an antibody. 6
Figure 1.3. The functions of an antibody. 7
Figure 1.4. The FcγR affinity for each IgG subclass. 9
Figure 1.5. The secreted forms of different antibody isotypes and subclasses. 10
Figure 1.6. Class switch recombination within the *IGHC* locus 11
Figure 2.1. PCR conditions used to amplify *IGHG3*. 17
Figure 2.2. The primers and the thermocycler conditions used in the colony PCR. ..18
Figure 2.3. BigDye™ Terminator v3.1 Cycle Sequencing conditions. 19
Figure 2.4. The library preparation process for PacBio sequencing. 20
Figure 2.5. The thermocycler conditions for both the first (orange) and second (black) round PacBio PCRs. 21
Figure 2.6. The sequences and binding sites of the primers used to confirm both HC and LC plasmid identities. 24
Figure 2.7. The digestion and ligations to make HC and LC plasmids for this project. 25
Figure 2.8. CMV/R heavy chain plasmid structure and elements. 26
Figure 2.9. The SEK and pLM2 mutagenesis primers and the SEK and pLM2 plasmid structures with the primer binding sites. 27
Figure 2.10. Thermocycler conditions used to amplify in CMV/R restriction enzyme sites. 28
Figure 2.11. The thermocycler conditions used in Site-Directed Mutagenesis. 30
Figure 2.12. The gating used to analyse the ADCP assay in FlowJo™ 10 Software. 33
Figure 3.1. The results of the *IGHG3* PCR. 37
Figure 3.2. A subset of colony PCR results for CAP206. 38
Figure 3.3. The size of the product generated in both first and second round PCRs in preparation for PacBio sequencing. 39
Figure 3.4. A density plot of the TapeStation results from each CAPRISA participant after the second round PacBio PCR. 40
Figure 3.5. *IGHG3* alleles sequenced using both Sanger and PacBio techniques. 42
Figure 3.6. Schematic of the five novel alleles detected in nine CAPRISA participants. 43

Figure 3.7. The allele structure and SNPs that differ between *IGHG3*01*, *IGHG3*05* and *IGHG3*01m*.....44
Figure 3.8. The amino acid differences between all 29 documented *IGHG3* alleles, and the five novel alleles.....44
Figure 3.9. An example gel of the plasmid digestion fragments.....45
Figure 3.10. The antibodies and the subclass variants made for each participant.....46
Figure 3.11. The HIV epitopes of the CAPRISA antibodies studied.....47
Figure 3.12. The AUC for each set of antibodies where differences between subclass/allele reached statistical significance.....48
Figure 3.13. The fold change between IgG1*01 and all IgG3 antibodies.....49
Figure 3.14. The neutralization titres of the four groups of antibodies tested.....50
Figure 3.15. L234F SNP in *IGHG3*11mm* and *IGHG3*11mm1* influences FcγRIIA-binding.....51
Figure 3.16. The mechanism of IdeS mAb digestion followed by the SDS-PAGE results.....52

List of Tables

Table 1.1. The structure and polyfunctionality of IgG subclasses.....12
Table 2.1. CAPRISA participant and monoclonal antibody (mAb) characteristics.....16
Table 2.2. First round PacBio PCR primer names and sequences. 20
Table 2.3. The antigens used for each participant in the ADCP assay.....31
Table 3.1. The technique used, and participant each allele was identified in. 41

List of Equations

Equation 1. The equation used to calculate the phagocytosis score for each sample. 33
Equation 2. The dilution calculation used in all neutralization assays. 34

Abbreviations

ADCC: Antibody-dependent cellular cytotoxicity

ADCD: Antibody-dependent complement deposition

ADCP: Antibody-dependent cellular phagocytosis

ADCT: Antibody-dependent cellular trogocytosis

AID: activation-induced cytidine deaminase

AIDS: acquired immunodeficiency syndrome

AUC: area under the curve

BCRs: B-cell receptors

bNAbs: broadly neutralizing antibodies

C: constant region

CAPRISA: Centre for the AIDS Programme of Research in South Africa

CD4bs: CD4 binding site

CDR: complementarity-determining regions

CH: constant heavy

CL: constant light

ConC: consensus C

CSR: class-switch recombination

D: diversity region

ELISA: enzyme-linked immunosorbent assay

Fab: antigen-binding fragment

Fc: fragment crystallisable

FcR: Fc receptor

FcRn: neonatal Fc receptor

GM: gamma markers

HIV: Human Immunodeficiency Virus

IdeS: IgG-degrading enzyme of *Streptococcus pyogenes*

IGHC: immunoglobulin heavy constant gene

IGHG3: immunoglobulin 3 heavy constant gene

IGHV: immunoglobulin heavy variable gene

IGKV: immunoglobulin kappa variable gene

IGLV: immunoglobulin lambda variable gene

IMGT: the Immunogenetics Database

J: Joining

LC: light chain

mAbs: monoclonal antibodies

MPER: Membrane-proximal external region

Nab: neutralizing antibody

NHP: non-human primate

NK: natural killer cells

PacBio: Pacific Biosciences

PBMCs: peripheral blood mononuclear cell

RE: restriction enzyme

RLU: relative light units

SHM: somatic hypermutation

SNP: single nucleotide polymorphism

UBP: Unique Barcode Primers

V: variable

VH: variable heavy

VL: variable light

1. Introduction

1.1. HIV: the pandemic

The Human Immunodeficiency Virus (HIV) first identified in the 1980s has caused a global pandemic. It disproportionately affects Southern Africa, with one-third of the total disease burden occurring in this region (UNAIDS, 2021b). In 2019, South Africa had approximately 7.5 million people living with HIV - the largest HIV-infected population in the world (UNAIDS, 2021b). As a result, South Africa has the largest antiretroviral program globally (UNAIDS, 2021b). However, while antiretroviral drugs (ARVs) have been shown to reduce viral load and thus transmission, there were still 200,000 new infections in 2019 alone (UNAIDS, 2021b). The largest proportion of these new infections (35%) was in women between the ages of 15-24 (UNAIDS, 2021a). This is due to a number of factors including the reproductive tract physiology, early sexual debut, economic disempowerment and poverty (Abdool Karim, Abdool Karim and Baxter, 2015). Alternative prevention strategies have thus come to the fore, such as the use of broadly neutralizing antibodies (bNAbs) in both passive immunization and active vaccination.

1.2. Broadly Neutralizing Antibodies in HIV prevention and treatment

Neutralizing antibody responses to HIV infection are targeted towards the surface expressed envelope (Env) protein, which comprises a trimer of non-covalently associated surface glycoprotein (gp120) and transmembrane glycoprotein (gp41) heterodimers (Hoffmann and Rockstroh, 2011). Broadly neutralizing antibodies (bNAbs) target sites on Env that are conserved across clades, and confer protection through neutralization – the loss of viral infectivity due to antibody binding (Walker *et al.*, 2009). BNAbs develop in approximately 10-30% of HIV-1 infected individuals 2-3 years post-infection (Stamatatos *et al.*, 2009). There are seven known bNAb epitopes Figure 1.1): the V2/apex, N332-supersite, silent face, gp120/gp41 interface, fusion peptide, membrane-proximal external region (MPER) and the CD4 binding site (CD4bs) (Moyo, Kitchin and Moore, 2020).

The V2/apex site is targeted by bNAbs PG9, PG16 and those from the CAP256-VRC26 lineage – including CAP256-VRC26.30 (Walker *et al.*, 2009; Doria-Rose *et al.*, 2016). PG9 and PG16 were the first V2/apex directed antibodies identified, and both target conserved regions of the V2 and V3 loops (Walker *et al.*, 2009). V2/apex directed

bNAbs arise relatively early following infection, are common across individuals, and generally have long CDR3s that allow penetration of the glycan shield (Doria-rose *et al.*, 2014; Andrabi *et al.*, 2015). BNAbs directed to the N332-supersite are the most common, and include 2G12, PGT121, PGT128, CAP255.C5 and CAP255.G3 (Scanlan *et al.*, 2002; Walker *et al.*, 2011). N332-supersite bNAbs differ in their approach and mode of binding, making this an attractive target for immunization (Moyo, Kitchin and Moore, 2020). To date, only two silent face bNAbs have been identified– SF12 and VRC-PG05 (Zhou *et al.*, 2018; Schoofs *et al.*, 2019). Gp120/gp41 interface bNAbs include PGT151 and CAP248.2B, and are usually glycan-dependent (Wibmer *et al.*, 2017). BNAbs targeting MPER (such as 4E10 and 10E8) are amongst the broadest identified to date, though weak neutralizers such as CAP206-CH12 also target this site (Morris *et al.*, 2011; Krebs *et al.*, 2019). MPER-directed bNAbs commonly use VH1-69 and Vκ3-20 genes (Krebs *et al.*, 2019). Finally, CD4bs bNAbs, such as VRC01, are highly somatically mutated, and demonstrate biased heavy chain gene usage to VH1-2 and VH1-46 (Scheid *et al.*, 2012). They were amongst the earliest bNAbs identified (Saphire *et al.*, 2001), and VRC01 was the first bNAb used in an HIV prevention trial (Corey *et al.*, 2021).

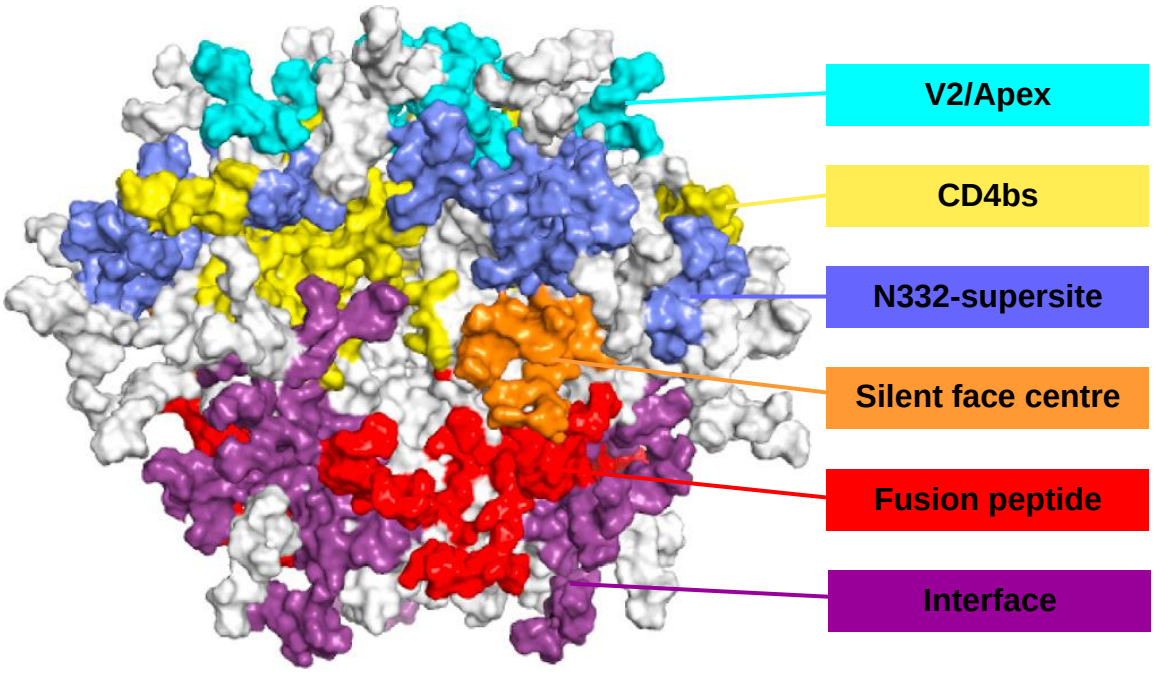


Figure 1.1. HIV Env trimer with shaded bNAb epitopes. Six of the seven bNAb epitope clusters are shown. Individual bNAbs bind to epitopes within each cluster. MPER is not shown as it is not present in the BG505.664 SOSIP trimer that is represented here. Figure adapted from Kwong and Mascola (2018).

The proof-of-concept Antibody Mediated Prevention (AMP) trials (HVTN 704/HPTN 085 and HVTN 703/HPTN 081) demonstrated that passively-infused VRC01 was effective at preventing infection from VRC01-sensitive HIV strains in humans (Corey

et al., 2021). This trial has paved the way for future trials assessing the efficacy of combinations of mAbs in preventing HIV acquisition in humans.

BNAbs are also used in treatment. When passively infused as a treatment in chronically infected virally suppressed individuals, bNAbs have been shown to maintain HIV suppression and delay viral rebound during antiretroviral therapy (ART) interruption (Lynch *et al.*, 2015; Bar *et al.*, 2016; Scheid *et al.*, 2016). Furthermore, compared to ART, bNAbs have a low risk of adverse events (Caskey *et al.*, 2015; Awi and Teow, 2018). However, the development of resistance is associated with the use of a single monoclonal antibody (mAb) (Shingai *et al.*, 2013). Thus, cocktails of antibodies have been tested *in vitro* and in animal models (Kong *et al.*, 2015; Wagh *et al.*, 2016, 2018; Shapiro *et al.*, 2020; Mahomed *et al.*, 2021) – and have progressed to ongoing phase I clinical trials in humans (CAPRISA, 2021; HPTN, 2021). Passively infused mAbs can also be modified to have half-lives of up to 6 months, offering HIV prevention or therapy as a single injection biannually – an attractive solution in settings where perceived stigma is a barrier to HIV treatment and prophylaxis (Gautam *et al.*, 2018).

1.3. The role of bNAbs in HIV vaccines

Active vaccination trials have attempted to induce bNAbs using a number of antigens including gp160 protein subunits and recombinant viral vectors – with little success (Burton, 2019). There has only been one partially effective HIV vaccine trial - RV144 - which showed 31% efficacy 42 months after vaccination (Rerks-Ngarm *et al.*, 2009). The RV144 vaccine consisted of a prime recombinant canarypox vector ALVAC® [vCP1521] HIV vaccine and a booster recombinant subunit gp120 AIDSVAX® B/E vaccine (Rerks-Ngarm *et al.*, 2009) but failed to elicit bNAbs. The latest active vaccine strategies have focused on germline targeting: the activation of bNAb-precursor B-cells with an antigen that has an affinity for specific germline genes (Jardine *et al.*, 2013; Sok *et al.*, 2016; Steichen *et al.*, 2019). Germline targeting has demonstrated activation of bNAb precursor B-cells in human tissues *in vitro* (Havenar-daughton *et al.*, 2018; Saunders *et al.*, 2019; Huang *et al.*, 2020). Recently, the IAVI G001 trial (evaluating the safety and immunogenicity of nanoparticle eOD-GT8), showed that 97% of participants developed VRC01-class IgG B cells (Schief, Jardine and Menis, 2021). eOD-GT8 is an engineered outer domain (eOD) of the Env gp120 CD4bs (ClinicalTrials.gov, 2018). While this study demonstrated that bNAb precursors can be elicited, the VRC01-class antibodies were not broad – highlighting the necessity of

sequential immunization (Steichen *et al.*, 2019). Both germline targeting and sequential immunization are underpinned by studying antibody maturation in both bNAbs and strain-specific neutralizing antibodies (NAbs).

1.4. Strain-specific neutralizing antibodies in HIV

Neutralizing antibodies (NAbs) develop in most HIV-infected individuals, and in some cases are the precursors of bNAbs (Gray *et al.*, 2007). Studying NAbs (such as CAP85-14.8, CAP88-CH06, CAP177-24G, CAP228-16H and CAP257-RH1) over the course of infection has provided important insights into both antibody maturation and viral co-evolution (Gray *et al.*, 2007, 2011; Wibmer *et al.*, 2016; van Eeden *et al.*, 2018; Scheepers *et al.*, 2020). Following HIV infection, antibodies that bind to various Env epitopes are detectable as antigen-antibody complexes at day 18, and consist of a mix of IgM and IgG antibodies (Tomaras *et al.*, 2008). Approximately 13 days later, 90% of individuals have IgG antibodies to gp41 (Tomaras *et al.*, 2008; McMichael *et al.*, 2010). The first gp120 targeted antibodies are V3 specific and occur 14 days later. These antibodies are non-neutralizing, with NAbs only detectable after day 40 (Tomaras *et al.*, 2008). However, the immune response is unable to protect from progression to AIDS. This is due to rapid viral evolution, resulting in escape mutations in Env that render the antibody response ineffective against the autologous virus – irrespective of whether or not the antibodies are bNAbs or NAbs (Gray *et al.*, 2007; Moore *et al.*, 2009).

1.5. The role of non-neutralizing antibody function in HIV

In contrast to NAbs, non-neutralizing antibodies (those that bind to, but do not impact virus infectivity) have been shown to play a role in viral control, to reduce transmission in sero-discordant couples, and to limit the number of founder viruses transmitted (Chung *et al.*, 2014, 2018; Ackerman *et al.*, 2016; Ruiz *et al.*, 2017; Smith *et al.*, 2019). Furthermore, initial analyses of the RV144 trial identified two correlates: IgG3 antibodies binding to V2/apex loops of the Env glycoprotein were protective; and IgA antibodies that bound to Env increased risk of HIV infection (Haynes *et al.*, 2012). The neutralizing ability of the IgG antibodies was low, suggesting that the protective effect was due to non-neutralizing antibody (or Fc effector) functions (Haynes *et al.*, 2012).

In passive bNAb infusion, Fc effector activity has been shown to contribute to slower disease progression, to limit the number of founder viruses transmitted, to reduce viral fitness and to clear infected cells (Hessell *et al.*, 2007; Ackerman *et al.*, 2013;

Bournazos *et al.*, 2014a; Halper-stromberg *et al.*, 2014; Santra *et al.*, 2015; Lu *et al.*, 2016). Furthermore, polyfunctional Fc effector function early in HIV infection was linked to the development of bNAbs later on in infection (Lofano *et al.*, 2018; Richardson *et al.*, 2018a).

1.6. The structure of antibodies

Antibodies are Y-shaped proteins made up of two identical light chains (LCs), and two identical heavy chains (HCs) (Figure 1.2). These can be divided into Constant (C) and Variable (V) regions based on the genes encoding each section. Alternatively, based on papain cleavage, antibodies can be divided into a Fab region and an Fc region - linked by a flexible hinge (Murphy and Weaver, 2017).

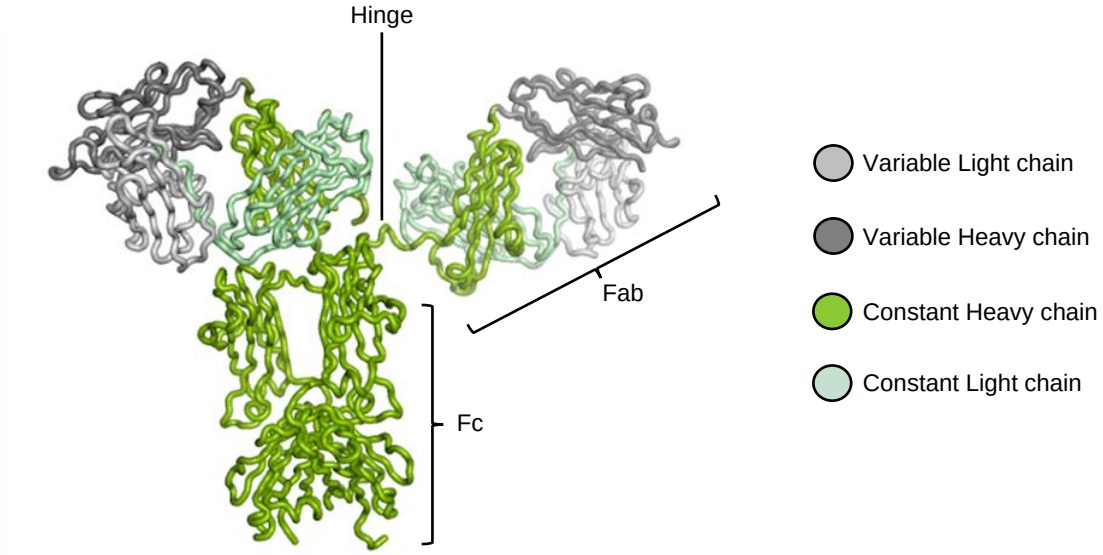


Figure 1.2. The structure of an antibody. The V regions and the first C region (CH1 or CL) of both chains form the antigen binding domain (Fab). The Fc region comprises the remaining CHs. The Fab and Fc are connected by the hinge. PDB accession code 1hzh.

Functionally, the Fab portion is predominantly protective through neutralization, while the Fc portion induces a wide range of cellular effector functions through binding to the Fc Receptors (FcR) on the surface of the cells of the innate immune cells (Pincetic *et al.*, 2014). Traditionally, the Fab region of antibodies has been the focus of research in infectious diseases due to the ability to prevent infection. However, the Fc region has also been shown to influence antigen binding and neutralization (Tudor *et al.*, 2012; Bournazos *et al.*, 2014b; Richardson *et al.*, 2019; Scheepers *et al.*, 2020).

1.7. Antibody Fc effector functions

There are four main Fc effector functions that play a role in infectious disease: antibody-dependent cellular phagocytosis (ADCP), antibody-dependent cellular cytotoxicity (ADCC), antibody-dependent complement deposition (ADCD) and antibody-dependent cellular trogocytosis (ADCT) (Figure 1.3).

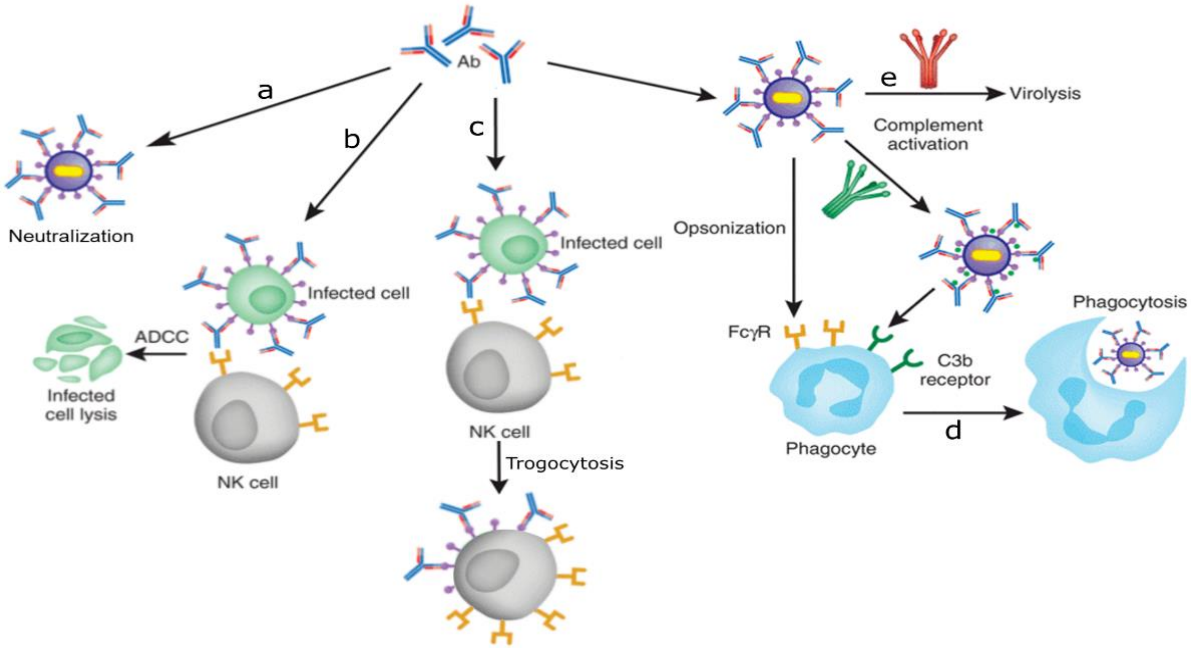


Figure 1.3. The functions of an antibody. A) Neutralization which is predominantly mediated by the Fab region. B-D are Fc effector functions. B) Antibody-dependent cellular cytotoxicity mediated by NK cells. C) Antibody-dependent cellular trogocytosis – the nibbling of the cell membrane. D) Antibody-dependent complement deposition and subsequent phagocytosis or infected cell lysis by the membrane attack complex (E). Figure adapted from Marasco and Sui (2007).

1.7.1. Antibody-dependent cellular phagocytosis (ADCP)

ADCP is the engulfment and intracellular lysis of pathogens or infected cells by monocytes, macrophages or neutrophils that have been opsonized by an antibody (Richards and Endres, 2014; Tay, Wiehe and Pollara, 2019). ADCP occurs when immune complexes bind to Fc-gamma Receptor 2 (FcγRIIA or FcγRIIB) or Fc-gamma Receptor 3 (FcγRIIIA or FcγRIIIB), triggering signal cascades within effector cells (Richards and Endres, 2014; Sips *et al.*, 2016).

As HIV is frequently transmitted vaginally and rectally, antibodies that induce ADCP at this surface represent an important defence mechanism (Sips *et al.*, 2016; Tay, Wiehe and Pollara, 2019). Additionally, non-human primate (NHP) models have shown that vaccines eliciting antibodies that mediate ADCP were protective against intrarectal challenges (Barouch *et al.*, 2013; Ackerman *et al.*, 2018). Finally, ADCP was identified as one of the mechanisms through which the non-neutralizing V2/apex-directed

antibodies were protective in the RV144 vaccine trial (Haynes *et al.*, 2012; Chung *et al.*, 2014).

1.7.2. Antibody-dependent cellular cytotoxicity (ADCC)

ADCC is the perforation and subsequent destruction of target cells by secretion of cytotoxic chemicals by effector cells. It is most commonly induced following immune-complex binding to FcγRIIIA on Natural Killer (NK) cells (Ackerman and Nimmerjahn, 2013).

ADCC (in addition to ADCP) was a correlate of protection in the RV144 trial (Haynes *et al.*, 2012; Yates *et al.*, 2014). Furthermore, ADCC activity has been shown to slow disease progression (Forthal, Landucci and Daar, 2001; Lambotte *et al.*, 2009; Chung *et al.*, 2011) and to reduce the risk of HIV transmission between sero-discordant partners (Ruiz *et al.*, 2017).

1.7.3. Antibody-dependent complement deposition (ADCD)

ADCD results in pathogen destruction and initiation of a pro-inflammatory state by plasma proteins that interact when cleaved by kinases (Goldberg and Ackerman, 2020).

Early ADCD activity in HIV infection was correlated with the development of bNAbs (Lofano *et al.*, 2018). Furthermore, in both a NHP vaccine trial and the RV144 human trial, ADCD by non-neutralizing antibodies was a correlate of protection - alongside ADCC (Barouch *et al.*, 2013; Perez *et al.*, 2017).

1.7.4. Antibody-dependent cellular trogocytosis (ADCT)

ADCT involves the nibbling and subsequent transfer of the target cell membrane to an effector cell, which can result in antigen-presentation and the induction of cell death (Joly and Hudrisier, 2003; Bettadapur, Miller and Ralston, 2020).

ADCT has only recently been described in HIV (Richardson *et al.*, 2018b). As in ADCD, there is a significant correlation between antibodies capable of ADCT in early infection and bNAb development (Richardson *et al.*, 2018a). Such correlations may have implications in the pursuit of active vaccines where eliciting bNAbs is the goal.

1.8. Modulators of antibody function

The combination of Fc effector functions, neutralization and antigen binding specificity of an antibody can be modulated by FcR variation, Fc glycosylation, and antibody isotype and subclass.

1.8.1. Fc receptors

FcRs are a group of lymphocytic cell surface proteins that contribute to the adaptive immune response through binding to the Fc region of antibodies (Mkaddem, Benhamou and Monteiro, 2019). There are two categories of FcRs based on their functional roles: transport receptors which carry antibodies across epithelial surfaces, and the receptors responsible for effector functions, expressed on the surface of leukocytes (Crowley and Ackerman, 2019). The neonatal FcR (FcRn) is expressed on the surface of the intestinal epithelium, the placenta and the endothelium, binds to IgG and is responsible for antibody recycling as well as transport (Raghavan and Bjorkman, 1996; Mkaddem, Benhamou and Monteiro, 2019).

The effector function FcRs can be subdivided into two types based on the conformation of the antibody Fc region they bind. The canonical Type-I FcRs bind to open conformation Fc regions, and are named according to the antibody subclass with which they interact (Pincetic *et al.*, 2014). The non-canonical Type-II FcRs bind to the Fc region of antibodies in the closed conformation (Pincetic *et al.*, 2014). The Type-I FcRs are either high-affinity or low-affinity receptors (such as FcγRIIA – the receptor predominantly responsible for ADCP) (Bruhns *et al.*, 2009; Bruhns and Jönsson, 2015). Both types of receptors bind to multivalent immune complexes with high avidity, however only high-affinity receptors bind well to monomeric antibodies (Tay *et al.*, 2016). Furthermore, there is allelic diversity within FcγRIIA, which impacts Fc binding affinity and thus ADCP. In HIV, individuals homozygous for the low-affinity $FcγRIIA_{R131}$ had accelerated disease progression compared to those with the high-affinity $FcγRIIA_{H131}$ (Forthal *et al.*, 2007). The comparative affinity between the documented FcγRs for each IgG subclass is shown in Figure 1.4.

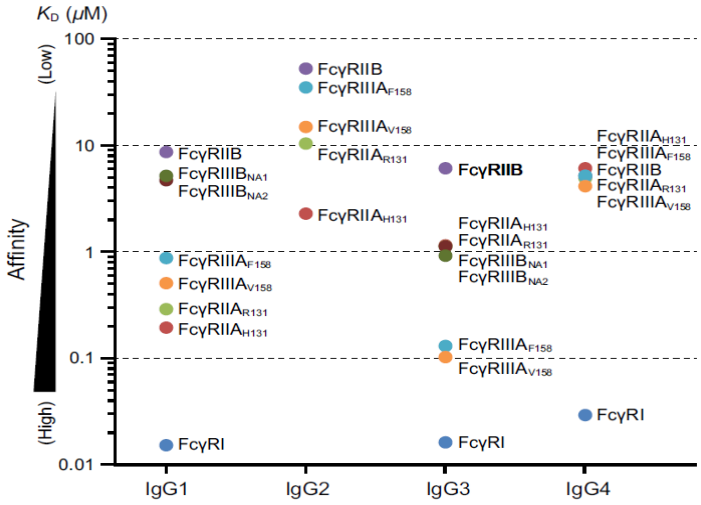


Figure 1.4. The FcγR affinity for each IgG subclass. The strength of the affinity for each receptor is represented by the dissociation constant (K_D). The major genetic variants of each receptor are shown in the subscript after the receptor's name (Caaveiro, Kiyoshi and Tsumoto, 2015).

The open or closed conformation of an antibody's Fc region (and thus whether Type-I or Type-II FcRs are bound) is determined by Fc region glycosylation.

1.8.2. Glycosylation

There is a conserved N-linked glycan in the Fc at position 297 of all IgG antibodies (Krapp *et al.*, 2003). The presence of this glycan keeps the CH2 domains in an open conformation - which is essential for Type-I FcR-binding, and therefore plays a key role in function (Krapp *et al.*, 2003; Vidarsson, Dekkers and Rispens, 2014; Kretschmer *et al.*, 2017). The structure of N-linked glycans differs based on the sugars incorporated during synthesis (Taylor and Drickamer, 2003). This can further modify antibody function - for example, fucosylation of IgG antibodies interferes with FcγRIIIA-binding, thus hindering ADCC (Shields *et al.*, 2001; Ferrara *et al.*, 2011).

1.8.3. Antibody Isotype

The Fc portion of antibodies are encoded by constant region (*IGHC*) genes. There are nine genes (*IGHM*, *IGHA1, IGHA2, IGHG1, IGHG2, IGHG3, IGHG4, IGHE* and *IGHD*) which define the antibody isotype (IgM, IgA, IgG, IgE and IgD) and subclass - (IgA1, IgA2, IgG1, IgG2, IgG3 and IgG4) (Figure 1.5) (Murphy and Weaver, 2017).

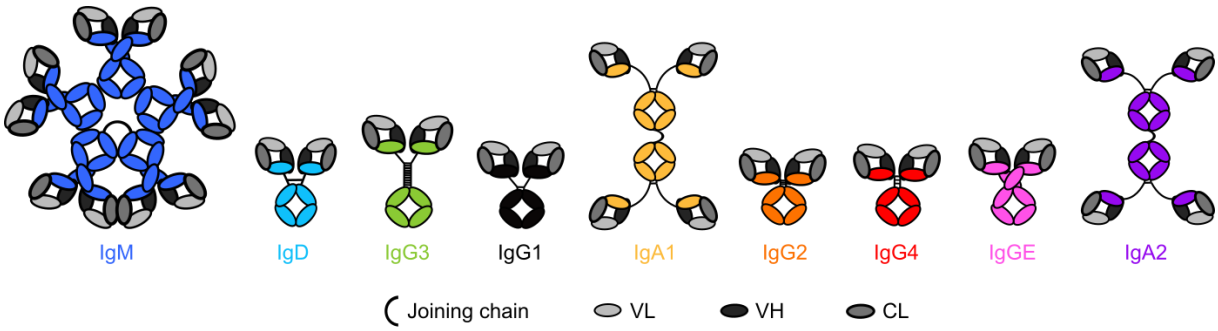


Figure 1.5. The secreted forms of different antibody isotypes and subclasses. All antibodies consist of a Fab and an Fc region, although the number and structure of the Fc domains differs between isotypes. The majority of the isotypes are expressed in monomeric form; however, IgM are expressed as a pentamer and IgA1 and IgA2 are expressed in both monomeric and dimeric form, joined by a Joining chain.

Antibodies have the ability to switch irreversibly between isotypes through a process known as class switch recombination (CSR). This occurs through the activity of the cleavage enzyme Activation-induced cytidine deaminase (AID), which acts on Switch (S) regions located upstream of all *IGHC* genes (Figure 1.6) (Dunnick *et al.*, 2009). AID induces double-stranded breaks in the DNA, which are repaired, and the intervening DNA excised (Stavnezer and Schrader, 2014). The order in which each subclass is secreted is based on the chromosomal arrangement of the *IGHC* genes (Oxelius and

Pandey, 2013). IgM/IgD antibodies are produced first, followed by IgG3, IgG1, IgA1, IgG2, IgG4, IgE and IgA2 – although CSR does not always occur consecutively (Kitaura *et al.*, 2017).

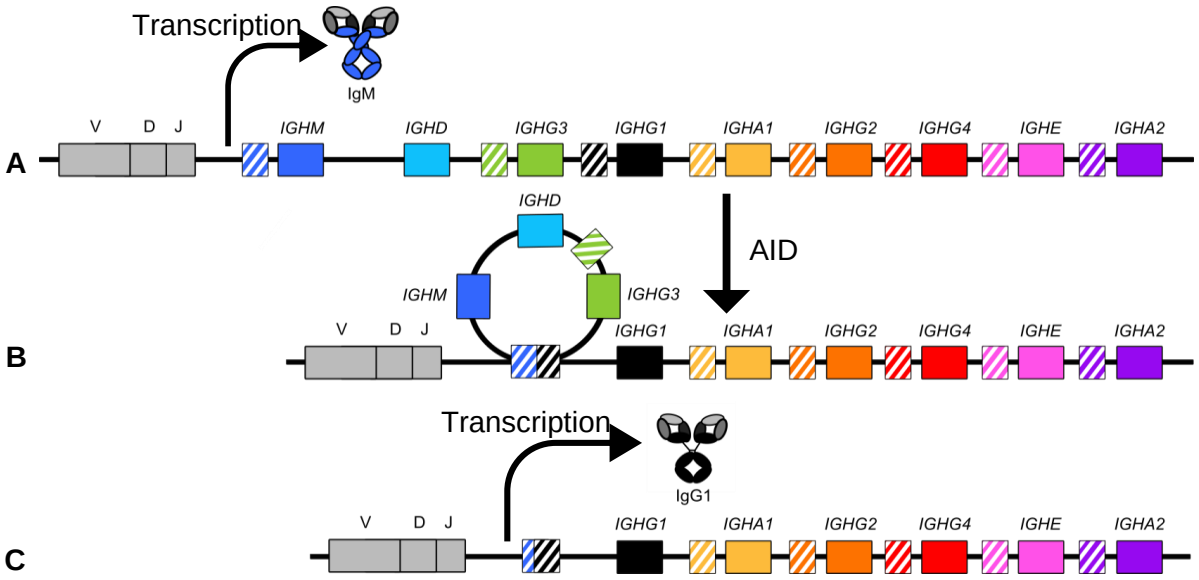


Figure 1.6. Class switch recombination within the *IGHC* locus. A) The chromosomal arrangement of the *IGHC* locus of a B cell in the peripheral tissue. Switch regions are represented as patterned blocks. B) The looping of the intervening DNA during CSR, mediated by AID. C) The intervening DNA is irreversibly excised, and the antibody is secreted as a different isotype with the same V region (Valenzuela, Hickey and Reed, 2016).

CSR is influenced by the type of antigen (protein or polysaccharide), the cytokines secreted by T follicular helper cells, and the pattern-recognition receptors on the surface of other lymphocytes (Moens and Tangye, 2014). For example, IgG1 and IgG3 antibodies are often secreted in response to T-cell presented protein antigens - such as viruses (Vidarsson, Dekkers and Rispens, 2014).

Antibody isotypes have conserved functional profiles. The half-life, tissue localization and FcR-binding capacity of each isotype and subclass is a result of amino acid differences in the FcR-binding sites (Dambrun *et al.*, 2017). Membrane-bound IgD and IgM antibodies form B-cell receptors (BCRs). Secreted IgD antibodies are found in the tonsils – although their function remains unclear (Gutzeit, Chen and Cerutti, 2018). Secreted IgM antibodies aggregate as pentamers and form immune complexes on initial antigen exposure (the primary immune response). IgA antibodies form both monomers and dimers that are found in the blood and the mucosae, respectively. IgE antibodies are key in mediating allergic reactions. IgG antibodies play a major role in humoral immunity, and make up >75% of circulating immunoglobulins (Murphy and Weaver, 2017). Each IgG subclass was named according to the amount present in

plasma: IgG1 makes up 60-70%, IgG2 20–30%, IgG3 5–8%, and IgG4 1–3% (Damelang *et al.*, 2019). IgG antibodies are widely distributed throughout both mucosal and humoral compartments – and as such, play an important role in infectious disease prevention (Dambrun *et al.*, 2017).

Furthermore, of the IgG subclass, IgG3 antibodies are secreted first following HIV exposure, and they are the most polyfunctional (Table 1.1) (Yates *et al.*, 2011; Damelang *et al.*, 2019; Richardson *et al.*, 2019).

Table 1.1. The structure and polyfunctionality of IgG subclasses. The shape of each subclass is represented above their column. The relative strength of each function is indicated by the number of "+", and absence of the function as "-".



Function	IgG1	IgG2	IgG3	IgG4
ADCP	++	+	+++	+
ADCC	++	-	+++	-
ADCD	++	+	++	-
Neutralization	++	++	++	++

The extended length of the hinge of IgG3 antibodies - which is nearly four times longer than that of other antibodies - allows for increased flexibility between the Fab and Fc, which can enhance antigen binding (Vidarsson, Dekkers and Rispens, 2014). It has also been shown to affect neutralization, with IgG3 antibodies neutralizing HIV more potently than IgG1 versions - although this appears to be epitope specific (Molinos-Albert *et al.*, 2017; Richardson *et al.*, 2019, 2021; Scheepers *et al.*, 2020). Furthermore, the extended hinge of IgG3 antibodies was shown to enhance ADCP, regardless of antibody specificity (Haynes *et al.*, 2012; Chung *et al.*, 2015; Tay *et al.*, 2016; Musich *et al.*, 2017; Richardson *et al.*, 2019; Chu, Patz and Ackerman, 2021). Finally, as a result of amino acid differences in the Fc region improving FcγR-binding, IgG3 antibodies have also been shown to induce ADCC, ADCD and ADCT more potently than IgG1 antibodies (Michaelsen *et al.*, 1992; Thommesen *et al.*, 2000; Damelang *et al.*, 2019; Richardson *et al.*, 2019; de Taeye *et al.*, 2020).

1.9. IgG3 antibodies and their therapeutic potential

Currently, there are over 80 therapeutic antibodies under marketing approval for use in various diseases – the majority of which are IgG1 (Kaplon and Reichert, 2019). Despite their impressive polyfunctionality, IgG3 antibodies have been largely overlooked as therapeutic antibodies due to enhanced degradation *in vitro*, challenges in large-scale production, and their reduced half-life (Chu, Patz and Ackerman, 2021). However, recent studies have suggested solutions to these barriers. Glycoengineering may prevent IgG3 degradation through protective O-linked glycosylation in the hinge (Jennewein and Alter, 2017; Kretschmer *et al.*, 2017). Saito *et al.* (2019) mutated three key amino acids in IgG3 antibodies to generate a stable engineered antibody that is resistant to aggregation and which is amenable to large-scale production like IgG1. Finally, studies investigating the genetic diversity within *IGHG3* (the gene encoding IgG3) have identified alleles in non-Caucasian populations that have half-lives equivalent to that of IgG1 (Dard *et al.*, 2001; Stapleton *et al.*, 2011).

1.10. *IGHG3* Allelic diversity

Recent advances in sequencing technology have allowed the germline sequencing of the constant heavy chain genes, revealing significant allelic diversity in the *IGHC* locus (Warrender and Kelton, 2020). Of the *IGHC* genes, the *IGHG3* gene – which encodes IgG3 antibodies – contains the most allelic diversity, with 29 documented alleles to date in IMGT (the Immunogenetics Database - Giudicelli, Chaume and Lefranc (2004)). In comparison, *IGHG1, IGHG2* and *IGHG4* each only contain 14, 17 and 8 alleles, respectively.

The functional impact of this allelic diversity is poorly understood (Vidarsson, Dekkers and Rispens, 2014). However, a handful of studies have shown that *IGHG3* allelic variants have different half-lives, FcγR-binding affinities, Fc effector functions and neutralization ability as a result of hinge length differences and single amino acid changes (Stapleton *et al.*, 2011; Richardson *et al.*, 2019; de Taeye *et al.*, 2020).

1.11. Genetic diversity in African populations

In addition to functional differences between alleles, *IGHC* allele frequency varies between populations (Calonga-Solís *et al.*, 2019; Khatri *et al.*, 2021). The majority of samples in international genetic databases are from Caucasian individuals (Popejoy and Fullerton, 2016; Bentley, Callier and Rotimi, 2020). As Caucasians represent a small segment of the human race, this doesn't accurately reflect the global genetic

diversity. Recently, Khatri *et al.* (2021) studied the immunoglobulin loci in 2,504 individuals across 26 populations, and identified 125 previously undocumented *IGHC* alleles across African populations alone. However, neither this study nor IMGT included any sequencing from Southern African ethnolinguistic groups. As African populations are amongst the most diverse globally, the diversity identified in specific sub-populations is not representative of others (Retshabile *et al.*, 2018; Fan *et al.*, 2019). Indeed, Scheepers *et al.* (2015) investigated the genetic diversity in the *IGHV* genes in South African individuals, and identified novel alleles in nearly half of the alleles sequenced. Additionally, Richardson *et al.* (2019) identified and characterized a novel *IGHG3* allele from an antibody in a South African individual that had improved neutralization and Fc effector functions compared to IgG3*17. This highlights the necessity of identifying allelic diversity in underrepresented populations, and linking this genetic diversity to functional diversity.

1.12. Study objectives

The overall aim of this project was to examine the genetic variability of *IGHG3* in African individuals and to determine its impact on Fc effector function and neutralization. This encompassed two main objectives:

1.12.1. Sequencing *IGHG3* in 10 CAPRISA participants

IGHG3 is a challenging template, and is thus generally sequenced in fragments – precluding haplotype identification (Warrender and Kelton, 2020). A full-length Polymerase Chain Reaction (PCR) protocol was developed to amplify the *IGHG3* gene in one fragment, using primers that bound either side of the CH1 and CH3. DNA was extracted from 10 participants from the Centre for the AIDS Programme of Research in South Africa (CAPRISA) 002 Acute Infection cohort (van Loggerenberg *et al.*, 2008), from whom monoclonal antibodies against HIV had been previously isolated (Gray *et al.*, 2011; Morris *et al.*, 2011; Doria-Rose *et al.*, 2016; Wibmer *et al.*, 2016, 2017; van Eeden *et al.*, 2018). The *IGHG3* gene was then amplified, cloned and sequenced using Sanger sequencing and PacBio next generation sequencing. The sequences generated were compared to existing *IGHG3* alleles in the IMGT database to identify any novel genes.

1.12.2. To characterize the impact of *IGHG3* alleles in this population on phagocytosis, Fc-receptor-binding, antibody cleavage and neutralization

We aimed to assess the functional impact of naturally occurring *IGHG3* allelic variation identified in 9 individuals (from aim 1) on HIV-specific antibodies isolated from the same individuals. All alleles determined for these individuals were used to make participant-matched HIV-specific antibodies. The phagocytic activity, FcγRIIA-binding affinity, neutralization potency and resistance to IgG-specific digestion of these new antibodies was then compared to *IGHG3*01* (the wildtype *IGHG3* allele), and *IGHG1*01* antibody versions.

2. Materials and methods

2.1. Ethics and the CAPRISA cohort

This project was approved by the Human Research Ethics Committee (Medical) of the University of the Witwatersrand (Clearance Certificate no. M190564). Additionally, this project fell under the ethics approval of the CAPRISA 002 study (Clearance Certificate no. MM040202), where participants consented to stored samples being used for additional studies.

The 10 individuals studied in this project form part of the CAPRISA 002 Acute Infection cohort. This cohort was established in order to investigate HIV-1 infection in this region (van Loggerenberg *et al.*, 2008). It comprised Zulu-speaking South African women from Vulindlela and Durban, in KwaZulu-Natal. HIV-specific monoclonal antibodies from each of these women had been previously isolated using antigen-specific B-cell sorting (Gray *et al.*, 2011; Morris *et al.*, 2011; Doria-Rose *et al.*, 2016; Wibmer *et al.*, 2016, 2017; van Eeden *et al.*, 2018). The binding specificity and the neutralization breadth of these antibodies had been previously characterized (Table 2.1).

Table 2.1. CAPRISA participant and monoclonal antibody (mAb) characteristics.

CAPRISA participant	mAb isolated	Isotype isolated	Epitope	bNAb or NAb	References
CAP85†	CAP85-14.8	IgG4	MPER	NAb	Gray *et al.* (2011)
CAP88	CAP88-CH06	IgA1	V2/apex	NAb	Gray *et al.* (2011)
CAP177	CAP177-24G	IgG1	N332 glycan	NAb	Gray *et al.* (2011)
CAP206†	CAP206-CH12	IgG1	MPER	bNAb	Morris *et al.* (2011)
CAP228*	CAP228-16H	IgG1	V2/apex	NAb	van Eeden *et al.* (2018)
CAP248	CAP248-2B	IgG1	Interface	bNAb	Wibmer *et al.* (2017)
CAP255	CAP255.C5	IgG1	N332 glycan	bNAb	Gray *et al.* (2011)
	CAP255.G3	IgG1	N332 glycan	bNAb	
CAP256	CAP256-VRC26.30	IgG3	V2/apex	bNAb	Doria-Rose *et al.* (2016)
CAP257	CAP257-RH1	IgG1	CD4bs	NAb	Wibmer *et al.* (2016)

The clinical progression of each participant is denoted as *controller and †rapid progressor. All others are intermediate progressors. The isotype that the antibody was made into, or isolated as based in sequencing is described in the "isotype isolated" column. The remaining three columns describe the epitope, whether the antibody is a bNAb or an NAb, and the publication from which this information was taken.

2.2. *IGHG3* sequencing protocol

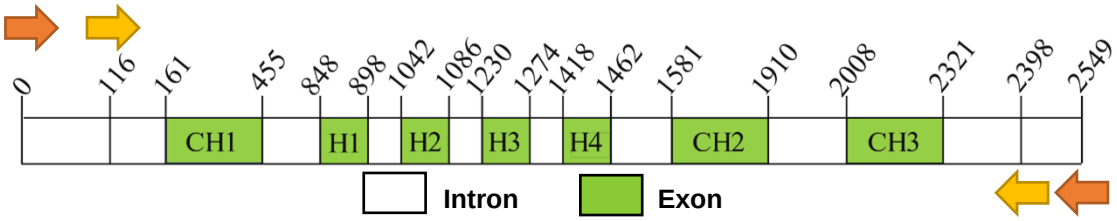
2.2.1. Sample DNA extraction

In order to amplify and then sequence the *IGHG3* in these samples, DNA was extracted from peripheral blood mononuclear cells (PBMCs) using the Wizard® Genomic DNA Purification Kit (Promega; Wisconsin, USA) as per manufacturer's protocol.

2.2.2. Polymerase Chain Reaction

A Polymerase Chain Reaction (PCR) was performed on the DNA extracted from PBMCs from 10 CAPRISA participants to amplify *IGHG3.* The Invitrogen™ Platinum™ SuperFI™ DNA Polymerase kit (Invitrogen™; Carlsbad, USA) was used: a 50 µL reaction was made containing 10 µL 5x SuperFi™ Buffer; 10 µL 5x SuperFI™ GC Enhancer; 1 µL 10 mM dNTP mix (Roche; Basel, Switzerland); 2.5 µL Forward primer (10 µM); 2.5 µL Reverse primer (10 µM); 0.5 µL Platinum™ SuperFi™ DNA Polymerase; 19.5 µL dH_2O and 4 µL 10 ng/µL sample DNA. Two sets of primers were used to overcome diversity between samples. The binding sites and sequences of the primers, and the thermocycler conditions are shown in Figure 2.1.

A



B

Primer position	Primer name	Primer sequence
Forward	N2F1 PreCH1	5'-CGYGGATAGACAAGAACCRAGGGG-3'
	F1 PreCH1	5'-GCTCTGTCCCACACCGCAGTCA-3'
Reverse	NR2 PostCH3	5'-TGTGGGGACAGTGGGACCCRC-3'
	R2 PostCH3	5'-GGGGTACGTGCCAAGCATCCTC-3'

C

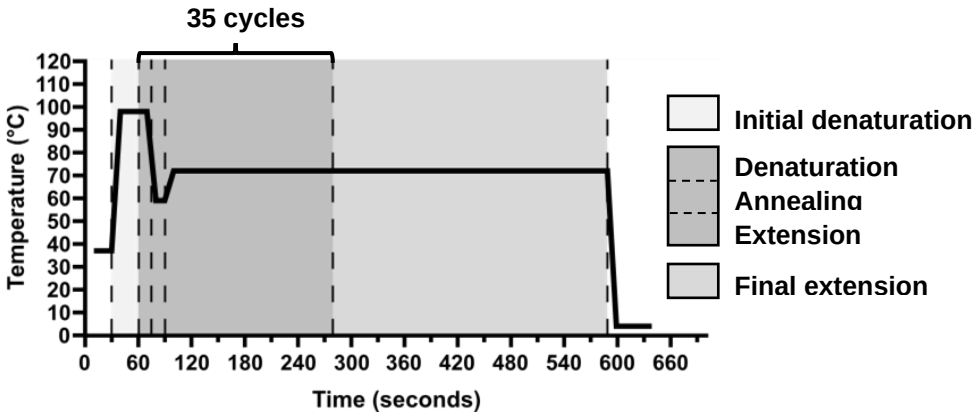


Figure 2.1. PCR conditions used to amplify *IGHG3*. A) The primer binding sites and intron/exon nucleotide numbering within *IGHG3*. B) The primer sequences. C) The thermocycler conditions used to amplify *IGHG3*.

2.2.3. Gel imaging and amplicon DNA extraction

The PCR product was electrophoresed on a 1% agarose gel (diluted 6:1 in Gel Loading Dye, Purple (6X) (New England BioLabs®; Ipswich, USA)) alongside 7 µL Quick-Load® Purple 1kb DNA Ladder (New England BioLabs®; Ipswich, USA). Images were obtained using the ChemiDoc™ imaging system (Bio-Rad; Hercules, USA). The DNA band corresponding to the ~2,300 nt *IGHG3* gene was extracted from the gel using the

QIAquick Gel Extraction kit (Qiagen; Hilden, Germany) according to the manufacturer's protocol.

2.2.4. Separation of alleles through bacterial cloning

Haplotypes in heterozygous individuals cannot be resolved using Sanger sequencing alone as amplicons contain both alleles. Thus, alleles were isolated using bacterial cloning prior to sequencing. The sample DNA was cloned into pJET1.2/blunt cloning vectors using the CloneJET PCR Cloning Kit and manufacturer's protocol (Thermo Fisher Scientific; Waltham, USA). The ligated pJET1.2/blunt cloning vector was transformed into Z-Competent™ JM109 cells (Zymo Research; Irvine, USA) as per the manufacturer's protocol, and plated on Luria-Bertani (LB) plates (Sigma-Aldrich; St. Louis, USA) containing 100 µg/mL Carbenicillin for incubation at 37°C overnight.

2.2.5. Screening of colonies for *IGHG3* inserts

A colony PCR was done to identify colonies containing *IGHG3* amplicons. Using the DreamTaq™ Green PCR Master Mix (2X) (Thermo Fisher Scientific; Waltham, USA) cells were inoculated into 5 µL DreamTaq™ Green PCR Master Mix (2X); 0,16 µL in-house pJET1.2 Forward Primer (25 µM); 0,16 µL in-house pJET1.2 reverse primer (25 µM); and 4,68 µL dH_2O. The primer sequences and the PCR conditions are shown in Figure 2.2. The size of the amplified inserts was visualized on a 1% agarose gel.

A

Primer name	Primer sequence
PJET F	5'-CGACTCACTATAGGGAGAGCGGC-3'
PJET R	5'-AAGAACATCGATTTTCCATGGCAG-3'

B

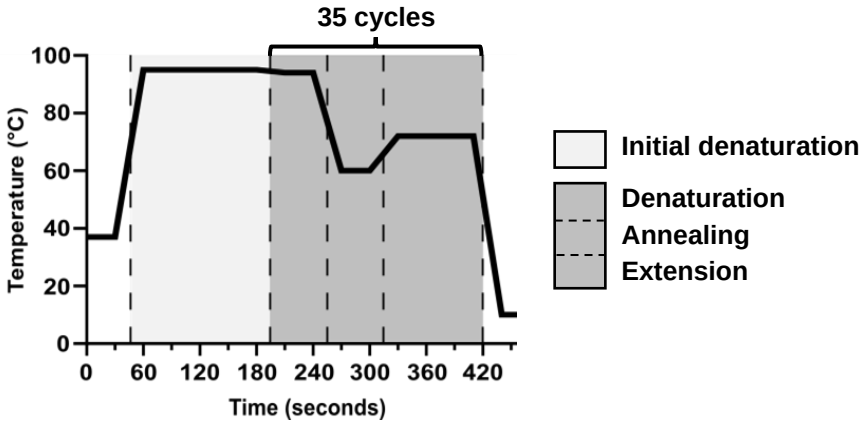


Figure 2.2. The primers and the thermocycler conditions used in the colony PCR. A) The names and sequences of the primers used to amplify the pJET1.2 plasmid. B) The thermocycler conditions used.

2.2.6. Plasmid DNA extraction and isolation (MiniPrep)

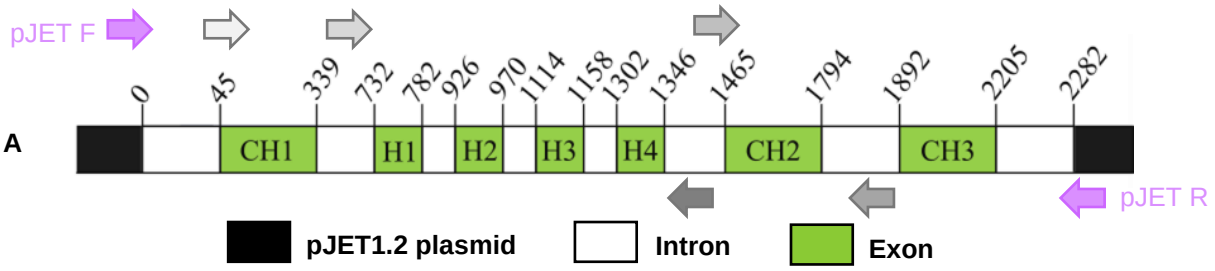
Colonies containing ~2,300 nt inserts were inoculated into 15 mL LB Broth (Sigma-Aldrich; St. Louis, USA) containing 100 µg/mL Carbenicillin, and incubated at 37°C

overnight with shaking (150 rpm). DNA was then extracted from the Z-Competent™ JM109 *E. coli* cells using the QIAprep® Spin Miniprep Kit (Qiagen; Hilden, Germany) according to the manufacturer's protocols, with the modification that DNA was eluted by centrifugation at 9,000 rpm for 2 minutes.

2.2.7. Sanger sequencing

Each *IGHG3* miniprep was sequenced using the BigDye™ Terminator v3.1 Cycle Sequencing Kit (Thermo Fisher Scientific; Waltham, USA). As *IGHG3* is ~2300 nt long, multiple overlapping primers were used to obtain full coverage of the gene (Figure 2.3A). One µL template DNA (or 1.5 µL where DNA concentration was < 100 ng/µL) was added to 1 µL BigDye ™ Terminator 3.1 Ready Reaction Mix; 1.5 µL 5X BigDye Buffer; 3.5 µL dH_2O; and 3 µL of a sequencing primer (Figure 2.3B). The sequencing reaction conditions were as in Figure 2.3C.

A



B

Primer position	Primer name	Primer sequence
CH1	VF02	5'–CCCAGCAACACCAAGGTGGACAAG–3'
CH1-H1 intron	F3Ext	5'–AGGAGGACCCTGCCCCTGACC–3'
CH2	CH2F	5'–GGACAGGTCCCAGTCGGG–3'
H4-CH2 intron	R1	5'–TAGAGTGGCCTGCATCCAGGG–3'
CH2-CH3 intron	R5	5'–ATGGACAGAGGCCAGCTTGACC–3'

C

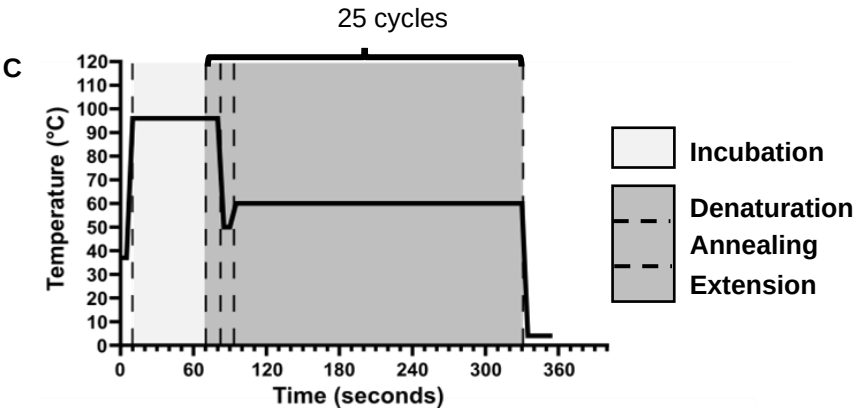


Figure 2.3. BigDye™ Terminator v3.1 Cycle Sequencing conditions. A) The binding sites of each sequencing primer within *IGHG3.* B) The primer sequences. C) The thermocycler conditions used.

Sequencing reactions were cleaned using a Sodium Acetate reaction clean-up (Kieleczawa, 2006). Samples were then sequenced on a 3500XL Genetic Analyzer (Applied Biosystems; Foster City, USA). Chromatograms were exported as .AB1 files.

2.2.8. PacBio Sequencing

PacBio is a next generation sequencing technique that can sequence templates of up to 30 kb, at a greater depth than Sanger sequencing (Slatko, Gardner and Ausubel, 2018). The *IGHG3* primers F1 and R2 were adapted for sequencing on the PacBio Sequel I (Pacific Biosciences; Menlo Park, USA) by adding 5' end-blocked universal sequences (Table 2.2). These PacBio-adapted primers were ordered from Whitehead Scientific (Pty) Ltd (Johannesburg, South Africa).

Table 2.2. First round PacBio PCR primer names and sequences. The underlined segment is the *IGHG3*-specific segment of the primers.

Primer name	Primer sequence
F1 PacBio	5'-GCAGTCGAACATGTAGCTGACTCAGGTCAC<u>GCTCTGTCCCACACCGCAGTCA</u>-3'
R2 PacBio	5'-TGGATCACTTGTGCAAGCATCACATCGTAG<u>GGGGTACGTGCCAAGCATCCTC</u>-3'

Two PCRs were required: the first used the PacBio-adapted F1 and R2 primers to incorporate the universal sequences, which provided standardized binding sites for the second round PCR primers. The second round PCR incorporated Unique Barcode Primers (UBPs) so that amplicons from each sample could be identified. Finally, Circular adaptor sequences were incorporated in the library preparation to allow cycling of the polymerase in the wells of the sequencing plate (Figure 2.4).

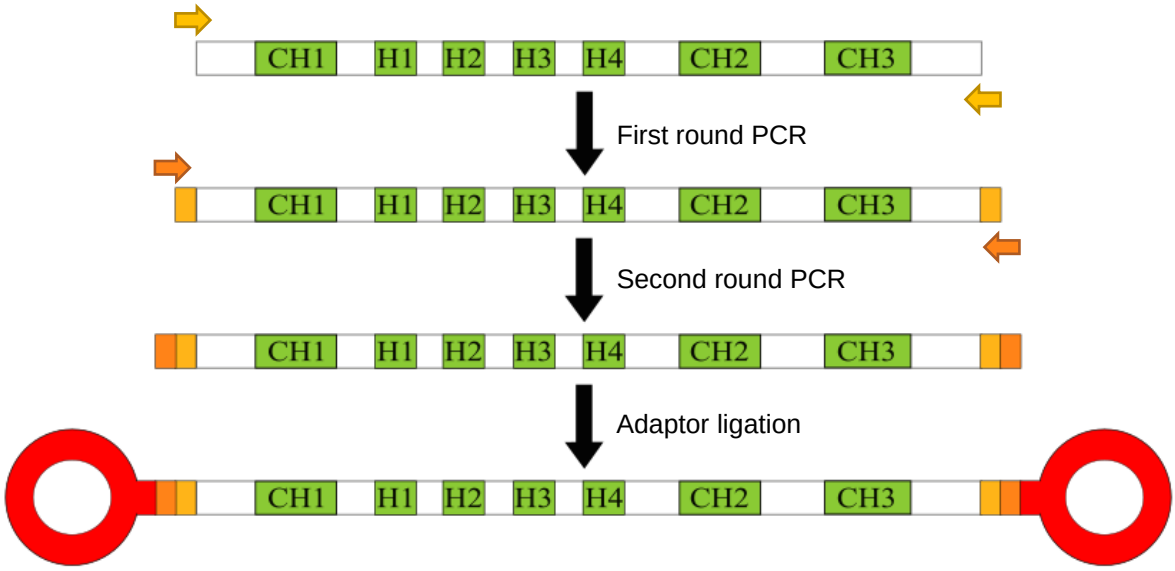


Figure 2.4. The library preparation process for PacBio sequencing. The binding sites of the first round PCR gene specific primers (F1 PacBio and R2 PacBio) with universal sequences at the 5' end shown in the first row. The binding sites of the participant specific Forward and Reverse Unique Barcode Primers (F UBP and R UBP) which incorporate unique participant identifiers in the second round PCR are in the second row. Finally, circular adaptor sequences were incorporated in the third step.

The first round PCR used the Invitrogen™ Platinum™ SuperFI™ DNA Polymerase kit (Thermo Fisher Scientific; USA): 10 µL 5x SuperFi™ Buffer; 10 µL 5x SuperFI™ GC Enhancer; 1 µL 10 mM dNTP mix (Roche; Basel, Switzerland); 0.5 µL Platinum™ SuperFi™ DNA Polymerase; and dH_2O was added to make a reaction volume of 50 µL. Genomic DNA (4 µL of 10 ng/µL) was added with 2.5 µL of 10 µM F1PacBio forward primer and 2.5 µL of 10 µM R2PacBio reverse primer. The thermocycler conditions are described in Figure 2.5.

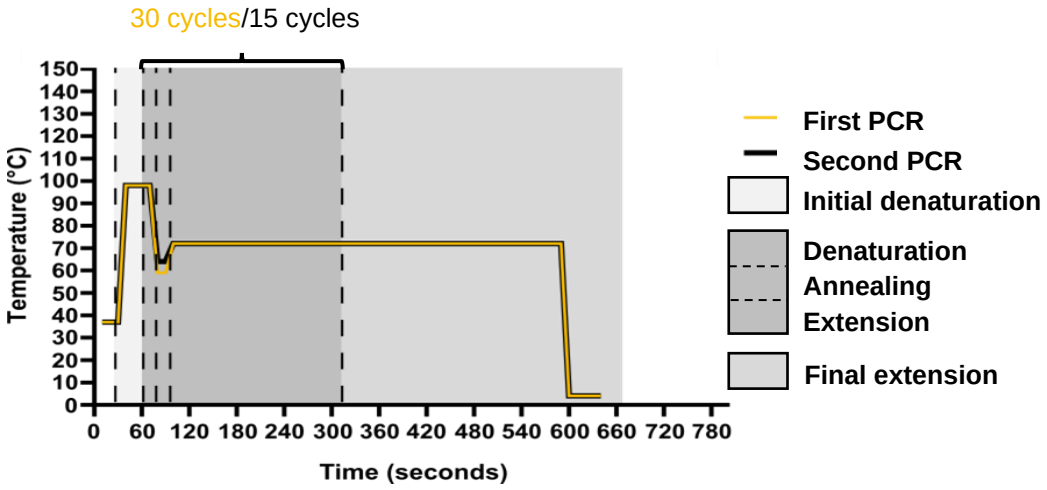


Figure 2.5. The thermocycler conditions for both the first (orange) and second (black) round PacBio PCRs. The first round PCR (orange) had an annealing temperature of 59°C and 30 cycles. The second round PCR (black) had an annealing temperature of 64°C and 15 cycles.

A PCR clean-up was done with SPRIselect beads (Beckman Coulter; Brea, USA), according to the manufacturer's protocol. To concentrate the PCR product, the three replicates for each participant were pooled. SPRIbeads were added to each sample's DNA at a ratio of 6:10 beads to DNA volume, to ensure binding of DNA amplicons of the correct size (~2300 nt). DNA concentration was measured by Qubit Fluorometric Quantification (Thermo Fisher Scientific; Waltham, USA).

The second round PCR was also done using the Invitrogen™ Platinum™ SuperFI™ DNA Polymerase kit (Thermo Fisher Scientific; USA). The template added was the bead-cleaned first round PCR product (1 µL 100 ng/µL) and the primers used were the PacBio Unique Barcoded F/R Primer (Pacific Biosciences; Menlo Park, USA) (2.5 µL). The thermocycler conditions are shown in Figure 2.5.

A second bead clean-up was done using AMPure PacBio beads (Pacific Biosciences; Menlo Park, USA) in a 7:10 part Beads to DNA volume, using the same protocol as the SPRIselect beads.

The size of the resulting PCR product was imaged using automated electrophoresis on a 4200 TapeStation System (Agilent Technologies; Santa Clara, USA). Samples were submitted to the National Institute for Communicable Diseases Sequencing Core for adaptor ligation and sequencing.

2.2.9. Sequencing analysis

2.2.9.1 Sanger sequencing pre-processing

The Sanger sequencing results (from each primer used to sequence a single allele within each participant) were exported as separate .AB1 files. These were then imported into Sequencher® version 5.4.6 DNA sequence analysis software (Gene Codes Corporation; Ann Arbor, USA). The overlapping sequences from multiple primers used on a single allele for each individual participant were aligned to form a contiguous read covering the entire *IGHG3* gene. The chromatograms for each contig were inspected to ensure good quality. The consensus contig of a single allele from each participant was exported as a .fasta file. Multiple .fasta files were exported where different colonies contained the same allele.

2.2.9.2 PacBio sequencing pre-processing and first round analysis

The PacBio sequencing was output as CCS reads, in FASTQ format. Sequence orientation was checked using a custom Python script that identified the forward primer sequence. Reverse complement sequences were reoriented using the RevSeq tool (Williams, 1999). The primer sequences in the reads were then trimmed using CutAdapt (Martin, 2011). They were then converted to .fasta files using the FASTX-Toolkit (Hannon, 2010). Next generation sequencing involves resequencing of the same template multiple times, therefore identical reads from the same allele were collapsed into a single read and the number of times it was sequenced noted. This "dereplication" was done using VSEARCH (Rognes *et al.*, 2016). Following dereplication, sequences only seen once (singletons) were removed from the results as they were likely PCR or sequencing errors. However, for one participant (CAP206), with particularly poor coverage, singletons were retained and data compared to previous sequencing analyses. The pre-processed data was then saved as .fasta files. These sequences were individually compared to a custom-made database including 14 *IGHG1* alleles, 15 *IGHG2* alleles, 29 *IGHG3* alleles and 4 *IGHG4* alleles sourced from IMGT®. This was made to identify chimaeras and exclude genes other than *IGHG3* from our downstream analyses. The database was made using the command line Makeblastdb tool (Camacho *et al.*, 2009) - part of the BLASTN suite (Altschul *et*

al., 1990). The output of the blast search was then parsed through an in-house R script to identify the best match for the sequence, to eliminate sequences that are chimaeras or artefacts (identified as those with more than 10 mismatches from the closest reference), and truncated sequences, and finally to rename the sequences according to their closest matching allele. These data were output in a tab delimited format including the following information: participant ID, sequence ID, the number of mismatches from the closest matching allele, the length of the sequence, the difference in length between the reference allele and the queried allele, the number of mismatches between the reference and the queried allele, the number of gaps, the nucleotide position that the queried allele started and ended at, the length of the queried allele, and a value representing the number of hits that could match by chance (evalue). This was done in RStudio (RStudio: Integrated Development for R. RStudio, Boston; USA), using the SeqinR library (Charif and Lobry, 2007). The output of this script was a single .fasta file containing the top sequences from each participant, aligned to their closest matching reference alleles.

2.2.9.2 Sanger and PacBio combined analysis

The results of the Sanger and PacBio were then combined, and run through the same custom R script. The output alignment was visually inspected in AliView (Larsson, 2014) to confirm the alleles present in each participant.

2.3. Assessing the impact of allelic variation on antibody function

2.3.1. Antibody subclass/allelic variant engineering and expression

Prior to making participant-specific *IGHG3* antibody plasmids, the antibody sequence and expression vector of the in-house heavy (HC) and light chain (LC) plasmid for each participant was confirmed by Sanger sequencing with the BigDye™ Terminator v3.1 Cycle Sequencing Kit (Thermo Fisher Scientific; Waltham, USA) according to the manufacturer's protocol. Half a microlitre of plasmid DNA was added to 1 µL BigDye ™ Terminator 3.1 Ready Reaction Mix; 1.5 µL 5X BigDye Buffer; 3.5 µL dH_2O; and 3 µL of one of the sequencing primers as previously described. The sequence of the primers used and their binding sites are described in Figure 2.6.

A

Which plasmids the primers were used on	Primer name	Primer sequence
HC plasmid primers	VHdRe	5'-GCTGTCCTACAGTCCTCAGG-3'
	VHCHF01	5'-CACCTCTGGGGGCACAGC-3'
	CH3F	5'-CAGCCCCGAGAACCACAGGTG-3'
	G3CH1rev	5'-CAGCAACACCAAGGTGGACAAGAG-3'
	R6	5'-CCAAGGATACCCTTATGATTTCCCG-3'
Both HC and LC plasmid	CMVR F	5'-CTAGTTAACGGTGGAGGGCAGTGT-3'
	SEQR	5'-CTTGACCCTGGAAGGTGCC-3'
Kappa LC plasmid	CK-ext	5'-GAGGCAGTTCCAGATTTCAA-3'
	CK-int	5'-GGGAAGATGAAGACAGATGGT-3'
Lambda LC plasmid	CL-int	5'-GGGYGGGAACAGAGTGACC-3'

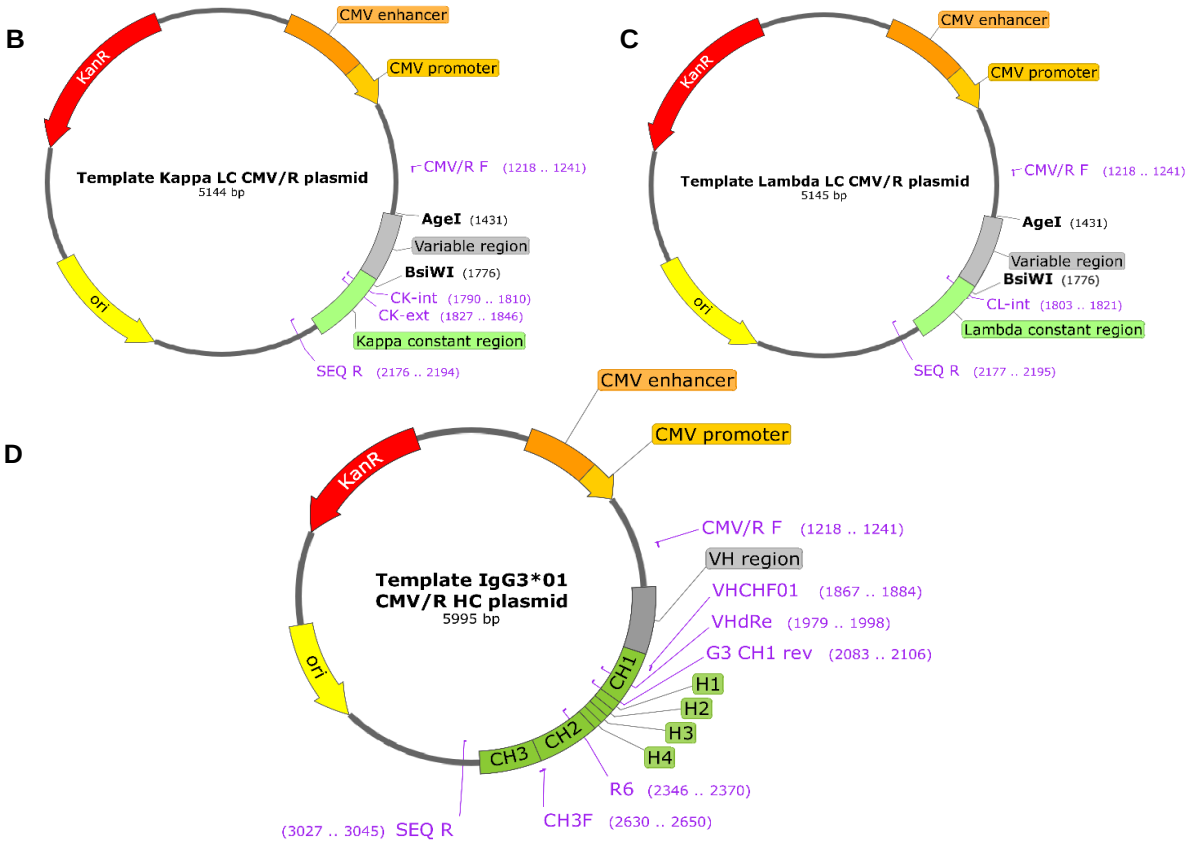


Figure 2.6. The sequences and binding sites of the primers used to confirm both HC and LC plasmid identities. A) The sequencing primer names, nucleotides and the plasmids for which they were used. All 7 "HC" and "Both HC and LC" primers were used to sequence both IgG1 and IgG3 antibodies. Primers CMVR F and SEQR were used to sequence all plasmids as they bind within the CMV/R backbone. B) The kappa LC CMV/R plasmid. C) The lambda LC CMV/R plasmid. D) The HC CMV/R plasmid.

The majority of the antibody plasmids were the standard in-house expression vector – CMV/R. This vector was obtained through the NIH HIV Reagent Program, Division of AIDS, NIAID, NIH: Human Immunodeficiency Virus 1 (HIV-1). The in-house CMV/R HC IgG1*01, IgG3*01, IgG3*17 and IgG3*01m, and CMV/R Lambda LC CAP256-VRC26.25 plasmid was used as a donor backbone for all of the HC and Lambda antibodies made (Figure 2.7). The CMV/R Kappa LC CAP206-CH12 was used as a backbone for the Kappa LC antibodies. Three plasmids were not in CMV/R vectors.

Both the HC and LC plasmids for CAP177-24G were in an SEK backbone designed by Dr Hua-Xin Liao (Liao *et al.*, 2009), while CAP248-2B HC was in a pLM2 backbone (Smith *et al.*, 2009) modified by Dr Constantinos Wibmer (Wibmer, 2016). The methods used to excise these from their respective plasmids into CMV/R plasmids are described in section 2.3.1.2 PCR cloning to insert V-regions from SEK and pLM2 plasmids into CMV/R plasmid.

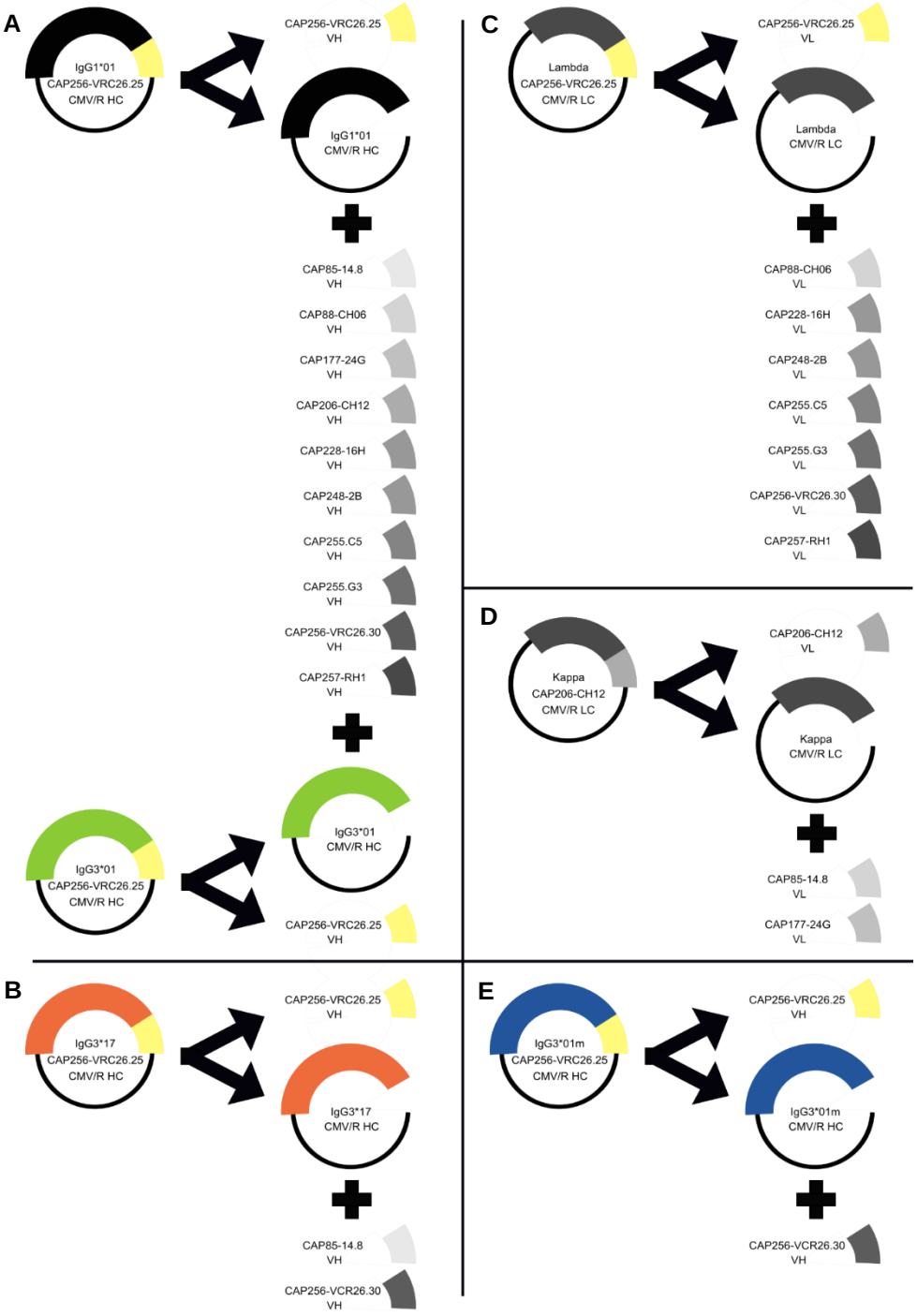


Figure 2.7. The digestion and ligations to make HC and LC plasmids for this project. A) Making IgG1*01 and IgG3*01 HC CMV/R plasmids for all participants. B) Making IgG3*17 HC plasmids for two participants from the CAP256-VRC26.25 IgG3*17 backbone. C) Making the Lambda LC plasmids using the CAP256-VRC26.25 CMV/R LC backbone. D) Making the two Kappa LC plasmids from the CAP206-CH12 LC backbone. E) Making the CAP256-VRC26.30 IgG3*01m HC plasmid, using the CAP256-VRC26.25 IgG3*01m CMV/R HC backbone.

2.3.1.1 CMV/R plasmid digestion and V-region swaps

To make different HC versions of each antibody, the V-regions from each participant's antibody plasmid were excised using restriction enzyme digestion and ligated into the CMV/R backbone. There are two restriction enzyme sites on either side of the V-region DNA: *SalI* and *AgeI* (Figure 2.8).

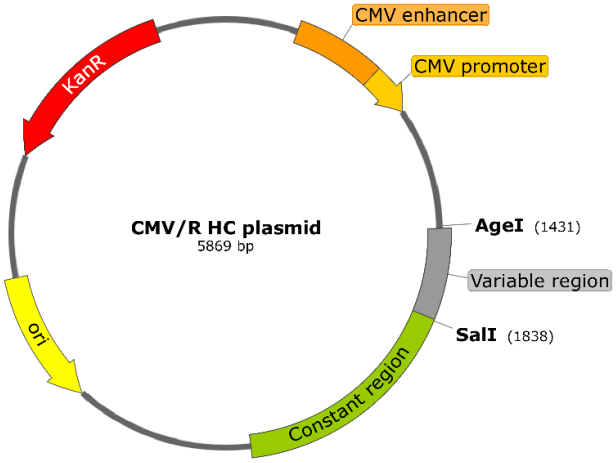


Figure 2.8. CMV/R heavy chain plasmid structure and elements. In CMV/R plasmids, the RE sites used to insert DNA are *AgeI* and *SalI* in the HC.

The V-region in both the V-donor plasmid and the backbone plasmid was digested using the Fast Digest® kit and enzymes (Thermo Fisher Scientific; Waltham, USA). Digestion reactions were set up using 5 µL Fast Digest® buffer; 1.5 µL of plasmid (3 µg); 2.5 µL Fast Digest® *BshTI*; 2.5 µL Fast Digest® *SalI*; and 38.5 µL dH_2O. In the case of the IgG3*17 and IgG3*01m CAP256-VRC26.25 backbone plasmids, there were two *BshTI* restriction sites, thus, these two plasmids with the VH donor plasmids (CAP256-VRC26.30 and CAP85-14.8) were digested with *XbaI* in place of *BshTI*. All reactions were digested according to manufacturer's protocols. The presence of the desired product was confirmed by a 1% agarose gel. The digested V-regions were ligated into the desired IgG3, IgG3 variant or IgG3 novel backbone (Figure 2.7) using the Rapid DNA Ligation Kit and protocol (Roche Holding AG; Basel, Switzerland). Each ligation mix contained 2 µL 5X DNA Dilution Buffer; 10 µL 2X T4 DNA Ligation Buffer; and 1 µL T4 DNA Ligase. The insert and backbone were added in a 3:1 molar ratio. dH_2O was added to make the reaction volume up to 20 µL.

2.3.1.2 PCR cloning to insert V-regions from SEK and pLM2 plasmids into CMV/R plasmid

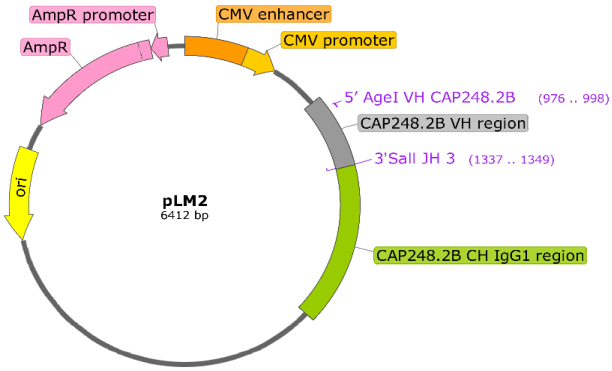
In order to standardize the antibodies produced for this project, all the plasmids were made into the same CMV/R backbone. As CAP177-24G (HC and LC) and CAP248-2B LC plasmids were not in CMV/R, the V-regions from each plasmid were transferred.

Neither the SEK nor the pLM2 plasmids contained the same restriction enzyme sites on either side of the V-region as the CMV/R constructs. To incorporate these, the V-regions from both SEK and pLM2 plasmids were amplified via PCR using primers that added the CMV/R restriction enzyme sites (*BshTI* and *SalI* for the HC, or *AgeI* and *BswiWI* for the LC) as shown in Figure 2.9.

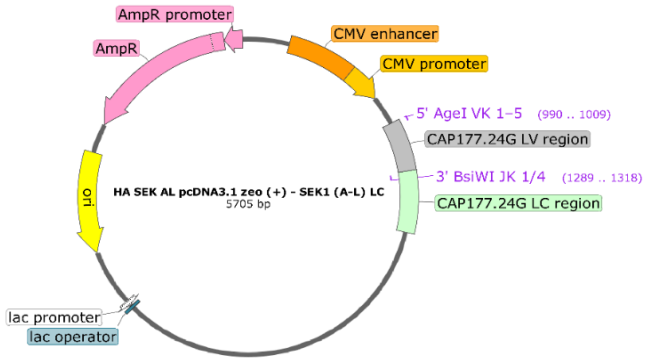
A

Plasmid	Primer name	Primer sequence
SEK HC	5'AgeI VH 1–24	5'-CTGCAACCGGTGTACATTCCCAGGTCCAGCTGGTACAG-3'
	3'SalI JH 6	5'-CACGGTCACCGTCTCCTCAGCGTCGACTTCGCA-3'
SEK LC	5'AgeI VK 1–5	5'-CTGCAACCGGTGTACATTCTGACATCCAGATGACCCAGTC-3'
	3'BsiWI JK 1/4	5'-GACCAAGGTGGARATCAAACGTACGGTGGC-3'
pLM2 HC	5' AgeI VH CAP248.2B	5'-CTGCAACCGGTGTACATTCCCAGGTGCAGCTCCAGCAGAG-3'
	3'SalI JH 3	5'-CAATGGTCACCGTCTCTTCAGCGTCGACTTCGCA-3'

B



C



D

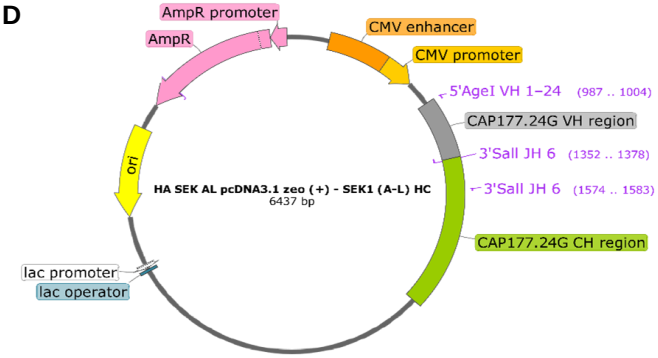


Figure 2.9. The SEK and pLM2 mutagenesis primers and the SEK and pLM2 plasmid structures with the primer binding sites. A) The sequences of the primers used to amplify the V-region of the non-CMV/R plasmids with the restriction enzyme sites underlined. B) the pLM2 HC plasmid. C) the SEK LC. D) the SEK HC plasmid structure. All primer binding sites are shown in purple. The CMV/R LC is shown here as CAP177-24G LC was cloned from an SEK plasmid into this construct.

The AccuPrime™ *Pfx* DNA Polymerase kit (Invitrogen™; Carlsbad, USA) was used to amplify in the RE sites. A 50 µL reaction mix was made containing 5 µL 10X AccuPrime™ Reaction Mix; 0.5 µL AccuPrime™ *Pfx* DNA Polymerase; 41.9 µL dH_2O; 0.8 µL Forward Primer; 0.8 µL Reverse Primer; and 1 µL (2 ng/µL) plasmid DNA for each participant. The thermocycler conditions used are shown in Figure 2.10.

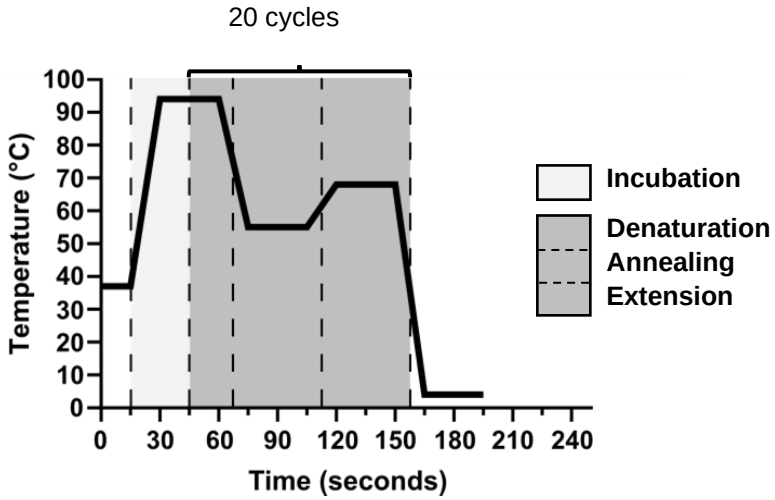


Figure 2.10. Thermocycler conditions used to amplify in CMV/R restriction enzyme sites.

Both CAP177-24G and CAP248-2B PCR products were visualized on a 1% agarose gel using the 6X Orange G loading dye (Thermo Fisher Scientific; Waltham, USA). The V-region PCR product from both samples was extracted from the gel using the QIAquick Gel Extraction kit (Qiagen; Hilden, Germany) and protocol. DNA concentration was nanodropped, and the V-region DNA digested and ligated into the backbone plasmids as previously described in section 2.3.1.1. CMV/R plasmid digestion and V-region swaps.

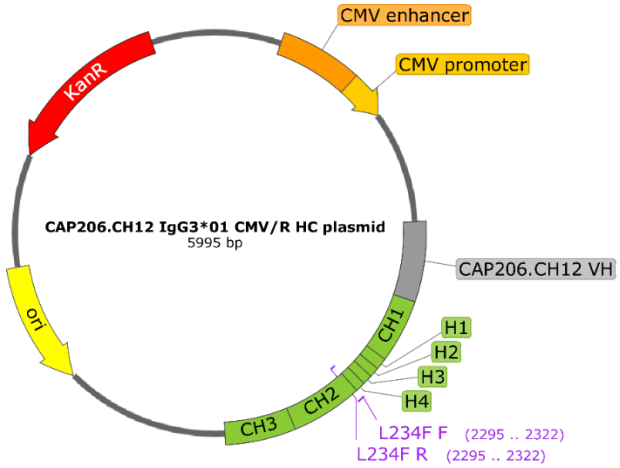
2.3.1.3 Site-directed mutagenesis

Three plasmids only required site-directed mutagenesis, rather than sub-cloning, to convert them from one allele to another. One IgG3*01 was mutated to include a novel L234F SNP, and another mutated to include a Y296F mutation to form *IGHG3*11*. IgG3*01m was made into an IgG3*13 antibody by introducing a N392K mutation using the QuikChange Lightning Site-Directed Mutagenesis Kit (Agilent Technologies; Santa Clara, USA) as per manufacturer's protocol. Forward and reverse primers were designed for each mutation Figure 2.10.

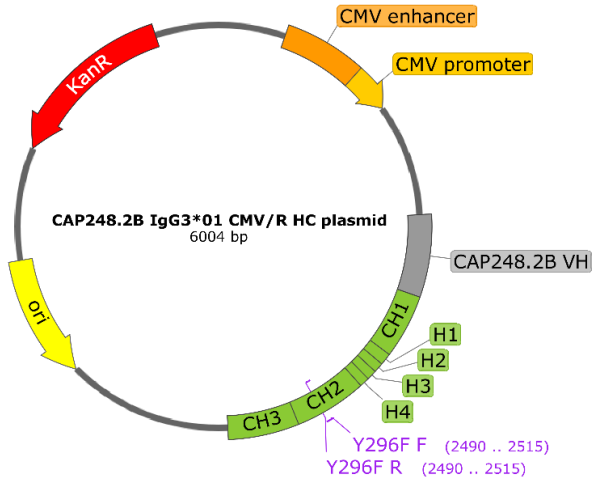
A

Plasmid to be mutated	Primer name	Primer sequence
IgG3*01	L234F F	5'CTGCCAGGAGGGTCCTTGAGTCCACGAC-3'
	L234F R	5'-GACGGTCCTCCCAGGAACTCAGGTGCTG-3'
IgG3*01	Y296 F	5'-CTTGCACGACAACTTGACGAGGAGGG-3'
	Y296 R	5'-GAACGTGCTGTTGAACTGCTCCTCCC-3'
IgG3*01m	N392K F	5'-CAGCCGGAGAACAACTACAAGACCACGCCTC-3'

B



C



D

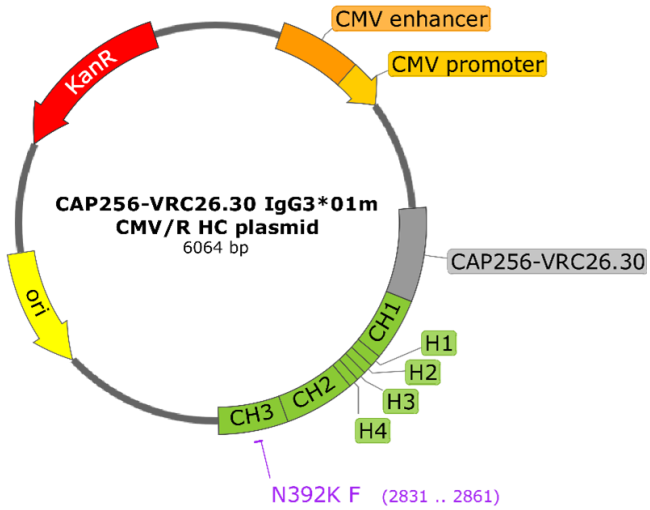


Figure 2.10. The *IGHG3* mutations introduced to generate novel and variant alleles using Site-Directed Mutagenesis. A) The names and sequences of the primers used, and the plasmid they were used to mutate. B, C and D) The structure and primer binding sites of each of the plasmids mutated. The primer used to mutate CAP256-VRC26.30 was designed for use with the multi-site-directed mutagenesis kit, so only one primer was used.

A 50 µL reaction mix was made containing 5 µL of 10X reaction buffer; 1 µL of 10-100 ng plasmid template; 1 µL 125 ng forward primer; 1 µL 125 ng reverse primer; 1 µL

dNTP mix; 1.5 µL QuikSolution reagent; 39.5 µL dH_2O; and 1 µL QuikChange Lightning Enzyme. Thermocycler conditions are shown in Figure 2.11.

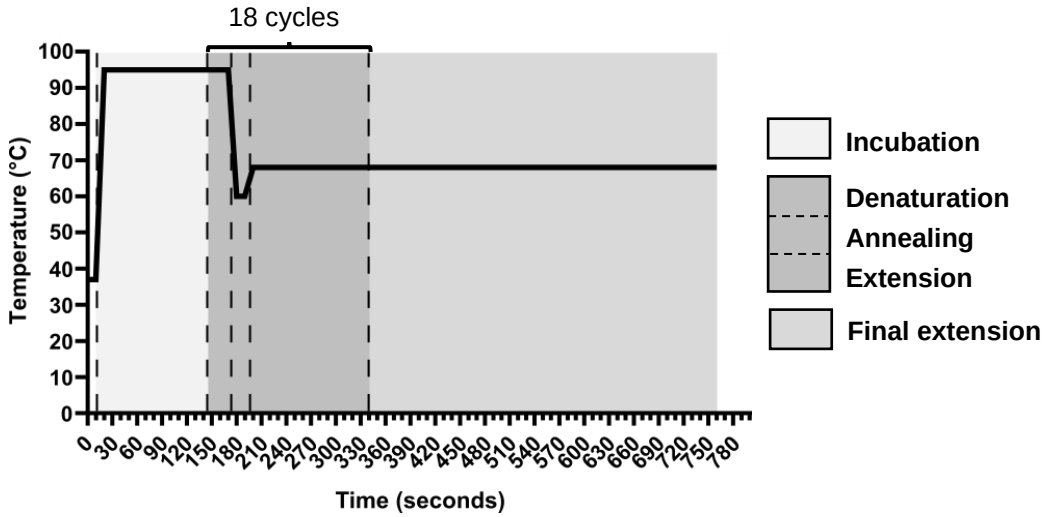


Figure 2.11. The thermocycler conditions used in Site-Directed Mutagenesis.

2.3.1.5 Plasmid DNA isolation and sequencing

Following digestion and ligation or mutagenesis, all plasmids were transformed, cultured and miniprepped as described in section 2.2.6 Plasmid DNA extraction and isolation (MiniPrep). To confirm the success of the V-region swaps and the mutagenesis, plasmid DNA was Sanger sequenced using plasmid specific primers (Figure 2.6) and the BigDye™ Terminator v3.1 Cycle Sequencing Kit (Thermo Fisher Scientific; Waltham, USA) and protocol. Sequenced plasmids were transformed into Z-Competent™ JM109 cells (Zymo Research; Irvine, USA) according to the manufacturer's protocol. A single colony was picked and inoculated into 100 µg/mL Kanamycin LB broth (Sigma-Aldrich; St. Louis, USA and incubated with shaking (150 rpm) overnight. Plasmid DNA was isolated using the ZymoPURE™ II Plasmid MaxiPrep Kit (Zymo Research; Irvine, USA).

2.3.2. Antibody plasmid transfection and protein expression

To express the antibodies, the HC and LC plasmids were co-transfected into FreeStyle™ 293-F cells (Thermo Fisher Scientific; Waltham, USA). Cells were cultured in FreeStyle™ 293 Expression Medium (Thermo Fisher Scientific; Waltham, USA) in a shaking incubator (125 rpm) at 37°C, 5% CO_2 and 70% humidity.

Briefly, 1.2 mL PEI-MAX 40,000, a transfection reagent (Polysciences, Inc.; Warrington, USA) and both HC and LC plasmids (200 µg of each) were added to 20 mL Gibco Opti-MEM I Reduced Serum Media (Thermo Fisher Scientific; Waltham, USA), and filtered through a 0.22 µM Minisart filter (Sartorius; Göttingen, Germany).

The transfection was combined with 400 mL HEK293-F cells (2x10^6 million per mL), and incubated for 6 days as previously described by van Eeden *et al.* (2018).

2.3.3. Antibody purification

The supernatant was harvested and filtered through Vacuum Filtration "rapid"-Filtermax flasks (TPP; Trasadingen, Switzerland). IgG1 antibodies were purified using Protein A columns (BioVision; Milpitas, USA) while all IgG3 antibodies were purified using Protein G columns as described by Richardson *et al.* (2019) (Thermo Fisher Scientific; Waltham, USA). The antibodies were eluted from the column with 12.6 mL Elution Buffer (pH 2.5: 0.1 M glycine; 0.15 M NaCl) into 1.4 mL Neutralization Buffer (12 g UltraPure TRIS; 80 mL dH_2O; 1 M HCl; pH 8), and dialysed overnight. The antibody was filtered through a 0.2 µM filter (Merck; Darmstadt, Germany) and the concentration measured. An antibody-specific extinction coefficient for each sequence was calculated using the ExPASy ProtParam online tool (https://web.expasy.org/protparam/) to ensure comparable antibody concentrations for downstream assays. Antibodies were concentrated using Vivaspin® 15 Turbo Centrifugal Concentrators (if necessary), aliquoted and stored at -70°C.

2.3.4. ADCP assay

The ADCP assay described by Ackerman *et al.* (2011) was used to assess the ability of mAbs to mediate engulfment of antigen-coated fluorescent neutravidin beads by a monocytic cell line. THP-1 cells are a monocytic leukaemia cell line (Tsuchiya *et al.*, 1980) obtained from the AIDS Reagent Program (Division of AIDS, NIAID, NIH contributed by Dr Li Wu and Vineet N. KewalRamani). They were maintained at <400,000 cells/mL (to prevent differentiation) in 10% FBS-RPMI with 1% Penicillin Streptomycin (R10 media) (Thermo Fisher Scientific; Waltham, USA) and β-mercaptoethanol (0,05 mM - Stratagene California; San Diego, USA) at 37°C, 5% CO_2. The antigen used for each set of mAbs is described in Table 2.3.

Table 2.3. The antigens used for each participant in the ADCP assay.

mAb	Antigen
CAP85-14.8	MPR.03
CAP206-CH12	
CAP228-16H	CE1086
CAP256-VRC26.30	BG505 SOSIP.664 trimer
CAP88-CH06	gp120 ConC
CAP177-24G	
CAP255.C5	
CAP255.G3	
CAP248-2B	BG505.CAP45 trimer

The antigen of interest was biotinylated using the EZ-Link NHS-Biotin kit (Thermo Fisher Scientific, Waltham, USA) in a 50 Molar excess, as per manufacturer's protocol. Ten µL fluorescent neutravidin beads (Molecular Probes Inc; Eugene, USA) were coated with biotinylated antigen (1 mg/mL). All mAbs were serially diluted 1:3 over 4 or 6 titrations in R10 media from a starting concentration of 50 µg/mL in a Corning® 96-well Clear Round Bottom Microplate (Sigma-Aldrich; St. Louis, USA). In house antigens were used for each assay - MPR.03 (CPC Scientific Inc; San Jose, USA), CE1086 trimer (van Eeden *et al.*, 2018), BG505 SOSIP.664 trimer (Sanders *et al.*, 2013), gp120 Consensus C (NIH HIV Reagent Program, Division of AIDS, NIAID, NIH: Human Immunodeficiency Virus 1 (HIV-1)) and BG505.CAP45 trimer (Wibmer *et al.*, 2017). Ten µL of coated beads were added to each well containing antibodies. Excess beads were washed by centrifugation in R10 media. Finally, 100,000 THP-1 cells were added to each well, and incubated overnight. All plates were centrifuged, 150 µL supernatant removed, and the samples fixed in 50 µL 4% PFA. Two antibody controls were included in each ADCP assay. Synagis (a respiratory syncytial virus antibody (MedImmune; Gaithersburg, USA)) was used as a negative control, while HIVIG B (polyclonal anti-HIV immunoglobulin from pooled inactivated human sera) was used as a positive control (obtained from the NIH AIDS Research and Reference Reagent Program, Division of AIDS, NIAID, NIH).

2.3.5. ADCP analysis

The results of the ADCP assays were read using a FACSAriaII flow cytometer (BD Biosciences; Franklin Lakes, USA. FCS files obtained from the FACSAriaII were imported into FlowJo™ 10 Software. Cells were gated on using forward vs side scatter, and single cells gated on by size (forward scatter height vs forward scatter area) (Figure 2.12). This population of cells was then represented as a histogram, and a gate drawn on the subset of FITC-A+ cells – indicating those containing beads.

The proportion of THP-1 cells that had taken up neutravidin beads (FITC-A+ population) was calculated, as well as the geometric mean (the average number of beads taken up by each cell). These values were exported into Microsoft Excel. ADCP scores for each sample were calculated as the number of THP-1 cells containing beads multiplied by the geometric mean of these cells, with the background signal of the assay subtracted. The background signal was calculated as the average signal of the no mAb control (wells with only beads and THP-1 cells) (Equation 1).

$$\frac{(Frequency\ of\ parent\ \times\ Geometric\ mean) - no\ mAb\ average}{x}$$

Equation 1. The equation used to calculate the phagocytosis score for each sample. The no mAb average was used to eliminate background. "x" was a factor which was kept constant used to reduce each ADCP score from in the hundreds of thousands to single- or double-digit scores.

The ADCP score was then exported to GraphPad Prism version 8.0.0 for Windows (GraphPad Software; San Diego, USA, www.graphpad.com).

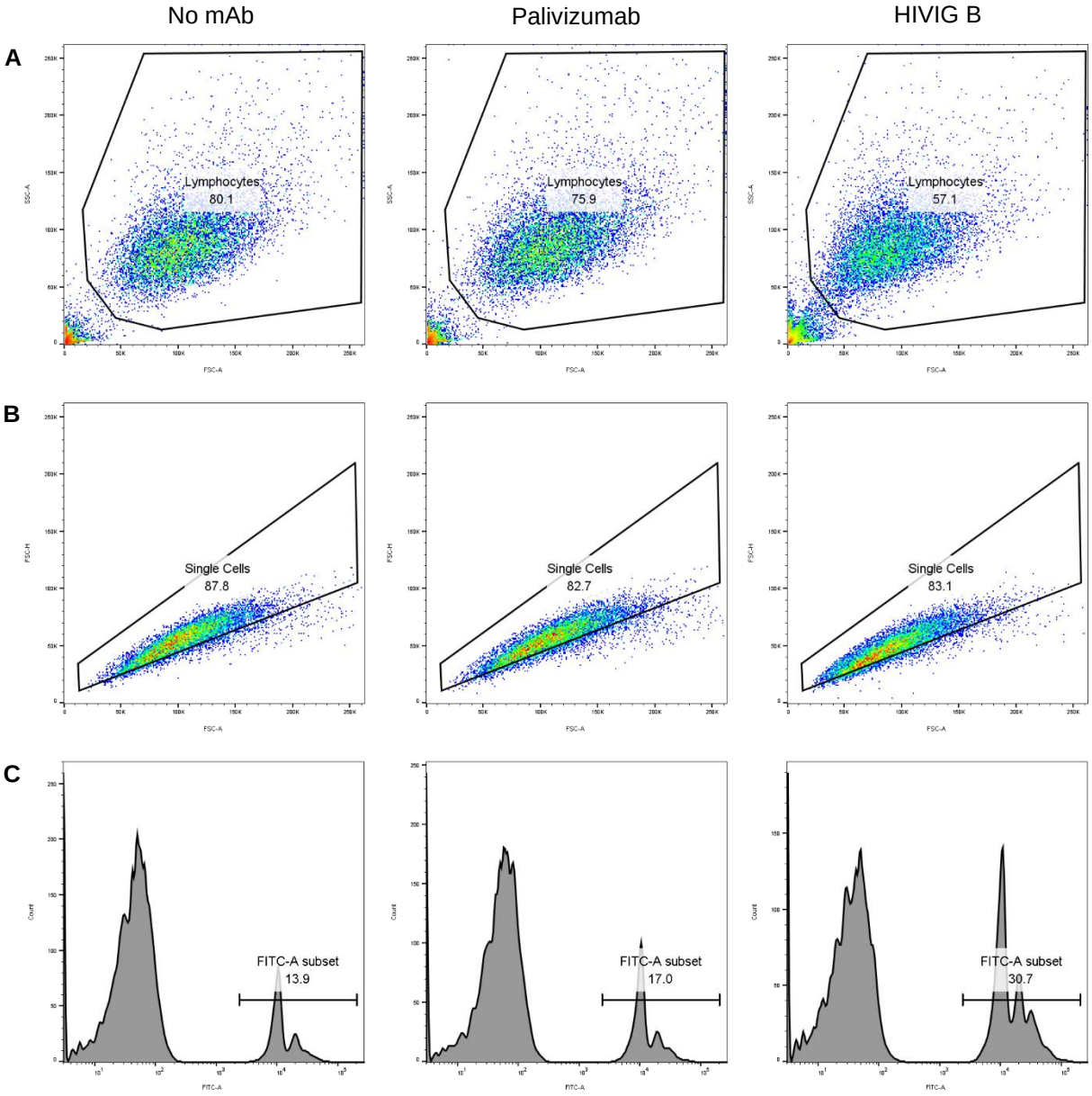


Figure 2.12. The gating used to analyse the ADCP assay in FlowJo™ 10 Software. Each column shows the gating strategy for a different control. No mAb and Palivizumab were negative controls. HIVIG B was a positive control. Row A shows the gating to isolate lymphocytes (SSC-A – Side Scatter Area; FSC-A – Forward Scatter Area). Row B shows the gating to isolate single cells (SSC-H – Side Scatter Height). And row C shows a histogram to gate on cells containing fluorescent beads (FITC-A - Fluorescein isothiocyanate Area).

2.3.6. ADCP assay statistics

In GraphPad Prism, a Spearman's nonparametric correlation was performed between all 3 repeats of each ADCP assay to assess the reproducibility of the results. If correlations were >0.6, repeats were normalized to a positive control to account for fluorescence variation between experiments. The area under the titrated curve was calculated for each of the mAbs, and the significance of the differences between antibody subclasses and alleles was calculated using Friedman's test with Dunn's correction.

2.3.7. TZM-bl neutralization assay and analysis

The TZM-bl neutralization assay was performed as described by Montefiori (2004). This assay measures the reduction in luminescence in Relative Light Units (RLU) from pseudovirus infected TZM-bl cells incubated in the presence of antibodies, relative to the RLU of cells incubated without antibodies (Wei *et al.*, 2002; Montefiori, 2004). TZM-bl cells contain a luciferase reporter gene under the control of the HIV-1 LTR promoter. Following HIV infection, Tat binds to the LTR and the LTR-controlled firefly luciferase gene (*Luc*) is expressed (Wei *et al.*, 2002). The cells were cultured in 10% FBS-DMEM with 50 µg/ml gentamycin (Sigma-Aldrich; St. Louis, USA) and 12,5 mL HEPES Buffer Solution (1M - Invitrogen; Waltham, USA). At 80% confluency (approximately every 2-3 days), cells were disrupted with 0.25% trypsin-EDTA (1 mM - Sigma-Aldrich; St. Louis, USA). The pseudoviruses used were taken from in-house stocks made using the transfection protocol described by Li *et al.* (2005). Each pseudovirus consisted of the HIV Env of interest cloned into a pcDNATM3.1D/V5-His-TOPO® vector (Invitrogen™; Carlsbad, USA), and a pSG3Δenv backbone plasmid (obtained from the NIH AIDS Research and Reference Reagent Program, Division of AIDS, NIAID, NIH). A 96-well sterile flat-bottom culture plate (Corning Costar no. 3595 – Sigma-Aldrich; St. Louis, USA) was used to set up 1:3 serial dilutions of mAbs. The IC_{50} was calculated using Equation 2.

$$\frac{(final\ mAb\ starting\ concentration\ mg/mL\ )}{mAb\ stock\ concentration * 37.5 * 2 * 2 * (the\ number\ of\ viruses + 1)}$$

Equation 2. The dilution calculation used in all neutralization assays. 37.5 is the volume of mAb required to maintain the starting concentration in the final reaction volume. This is multiplied by 2 as each series of dilutions is run in duplicate, and by 2 again as the addition of 25 µL virus dilutes the mAb by half.

MAB dilutions were added to the volume of pseudovirus that yielded an RLU of at least 40,000 (calculated by adding virus to cells prior to the TZM-bl assay). One-hundred thousand TZM-bl cells (with 0,146 µL Dextran) were then added to each well. After 24 hours, 100 µL media was removed and replaced with 100 µL Bright-Glo Reagent (Promega; Madison, USA). One-hundred and fifty µL of the reaction was then transferred to a black assay plate and the RLU measured using a PerkinElmer VICTOR XLight Luminometer (PerkinElmer; Waltham, USA). The antibody inhibitory concentration (IC) at which the RLU was reduced to 50% compared to the virus control in the absence of antibody was calculated. The IC_{50} for a minimum of three repeats was averaged for each antibody. Significant difference between antibody neutralization potency was calculated using Friedman's test with Dunn's correction.

2.3.8. FcγRIIA-binding ELISA

In order to compare the impact of IgG3 allelic variation on FcγRIIA-binding, an FcγRIIA-binding ELISA was run as described by Moldt *et al.* (2012). Antibody-FcγRIIA affinity was measured using Recombinant Human Fc gamma RIIA H131 (R&D Systems; Minneapolis, USA). FcγRIIA H131 is a high-affinity polymorphism allowing optimal binding in the ELISA (Caaveiro, Kiyoshi and Tsumoto, 2015). FcγRIIA H131 was diluted 1:10,000 to a final starting concentration of 2 µg, in a Pierce™ Nickel Coated Plate – 96-well (Thermo Fisher Scientific; Waltham, USA). Washing and blocking was done using a wash buffer (0,05% TWEEN; 99,95% PBS). One-in-four antibody dilutions were prepared in the wash buffer, at a starting concentration of 0,005 µg/mL. Fifty µL of Anti-Human IgG (Fc specific) secondary antibody (Merck; Darmstadt, Germany) was added to each well at a 1:10,000 dilution. The FcγRIIA-antibody binding was visualized by adding 100 µL 1-Step™ Ultra TMB-ELISA Substrate Solution (Thermo Fisher Scientific; Waltham, USA). The reaction was stopped after 5 minutes by adding 1M H_2SO_4. In-house variants of VRC01 were used as controls - the positive controls were an IgG1 Fc mutant (G236A/S239D/A330L/ I332E) with enhanced FcγR-binding (Ahmed *et al.*, 2016), an IgG1 VRC01 antibody (Lazar *et al.*, 2006), and the negative control was VRC01 N297Q (which abrogates FcγR-binding) (Shields *et al.*, 2001). The ELISA was measured using a SpectraMax® ABS Plus Microplate Reader (Molecular Devices; San Jose, USA).

2.3.9. Fc region enzyme digest

A mAb digest (as described by Deveuve *et al.* (2020)) was done to assess the effect of allelic variation on the IdeS (Immunoglobulin G-degrading enzyme of *Streptococcus*

pyogenes) antibody cleavage site. IdeS is secreted in natural *Streptococcus pyogenes* infection, and abrogates Fc effector function – thus variants resistant to cleavage are ideal as therapeutic mAbs. Lyophilized FabRICATOR® Enzyme (Genovis; Lund, Sweden) was reconstituted in 30 µL ddH_2O and stored at 4°C. Digestion mixes were made with 0,05 mg/mL of each mAb and the volume made up to 50 µL with 1 X PBS (Thermo Fisher Scientific; Waltham, USA). Seventy-five nL IdeS was added, and separate reactions incubated at 37°C for 5 minutes and 30 minutes. The reaction was stopped by adding 10 mM Iodoacetamide (Amersham Biosciences; Little Chalfont, United Kingdom). Six-point-five microlitres of Novex NuPAGE LDS Sample Buffer (4X) (Thermo Fisher Scientific; Waltham, USA) was added to 20 µL sample, and the samples denatured at 95°C for 5 minutes. Twelve microlitres of sample were loaded on a pre-cast NativePAGE 4-16% BisTris Gel (Thermo Fisher Scientific; Waltham, USA), with 5 µL Novex Sharp Pre-Stained Protein Standard (Invitrogen™; Carlsbad, USA) and run at 150 V for 120 minutes. Results were imaged using a ChemiDoc™ imaging system (Bio-Rad; Hercules, USA).

3. Results

The aim of this project was to identify genetic diversity in *IGHG3* in South African populations, and to investigate whether this diversity influenced neutralization and Fc effector function. *IGHG3* is GC-rich, contains four repetitive regions (the hinge), and shares over 95% sequence homology with the other *IGHG* genes (Warrender and Kelton, 2020). As such, it is generally sequenced in fragments excluding the hinge region, which prevents haplotype identification (Calonga-Solís *et al.*, 2019; Warrender and Kelton, 2020). During this project a sequencing strategy was developed and optimised enabling the identification of five previously undescribed alleles from full-length *IGHG3* sequences. Furthermore, these alleles were engineered into previously isolated monoclonal antibodies and their impact on neutralization and phagocytosis of HIV-1 was assessed.

3.1. Sanger sequencing results

IGHG3 is a challenging template to sequence. As such, two sets of primers were designed and used with a high-fidelity, proof-reading enzyme under conditions optimized for GC-rich templates. Full-length *IGHG3*-sized amplicons were observed in all ten of the participants using a combination of both sets of primers (Figure 3.1; Supplementary Figure 1). Although low-level laddering was observed in the agarose gels, a distinct band of ~2,200 or ~2,500 nt (the expected size of an *IGHG3* allele from each set of primers) was observed in each reaction (Green arrow, Figure 3.1 and Supplementary Figure 1).

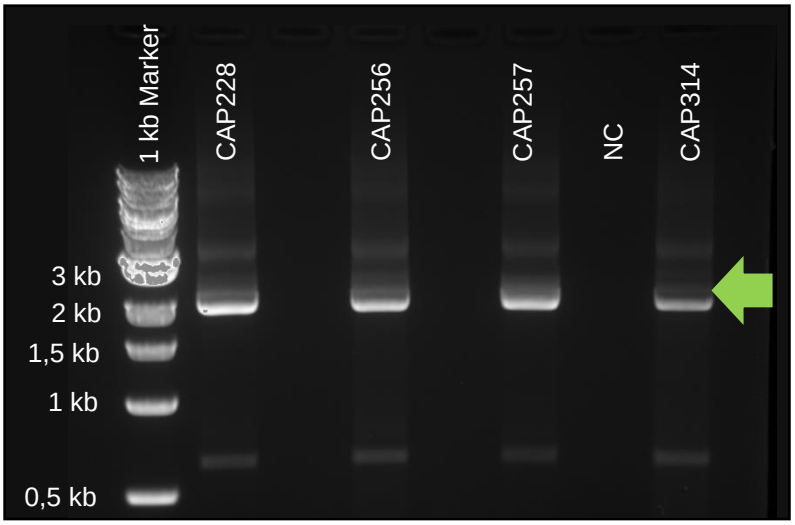


Figure 3.1. The results of the *IGHG3* PCR. A subset of the agarose gels imaged showing the results of the PCR reaction using forward primer N2F1 and reverse primer NR2. The band containing *IGHG3* is indicated by the green arrow. NC – Negative control.

After purifying and cloning this band, the colony PCR (as shown in Figure 3.2 for CAP206) revealed colonies containing the desired sized band. Plasmid preps were made from colonies with the appropriate size insert and were Sanger sequenced. Eight *IGHG3* alleles were identified in only six participants - despite bands corresponding to *IGHG3* on the gels in all ten participants. The colonies sequenced that did not contain *IGHG3* were a mixture of *IGHG1, IGHG2* and *IGHG4* genes, as well as chimaeras of all four *IGHG* genes, which were removed from downstream analyses.

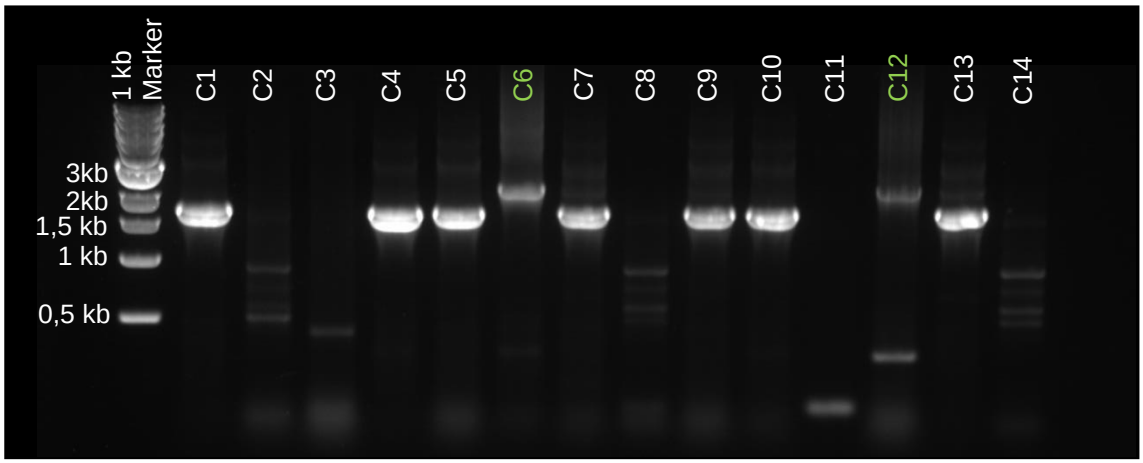


Figure 3.2. A subset of colony PCR results for CAP206. C denotes colony, followed by the number of the colony. The initial *IGHG3* PCR was done using primers F1 and R2, thus the expected *IGHG3* insert size is ~2,200 nt. The colonies labelled in green were sequenced. These were selected based on size. In this subset of colonies, only C6 contained an *IGHG3* insert. C12 contained an insert that could not be sequenced using the *IGHG3* sequencing primers.

3.2. PacBio sequencing results

Two PCRs were done for each participant in the PacBio protocol: the first round PCR was done to amplify *IGHG3* and incorporate the universal sequences that provide binding sites for the second round PCR primers. The second-round primers incorporate unique participant identifiers. All ten participants yielded amplicons of the correct size in the first round of PCR (Figure 3.3). Due to loss of DNA during PCR clean-up, and a low efficiency second round PCR, only two participants (CAP85 and CAP256) had ~2,200 nt sized bands visible on the 4200 TapeStation gel following the second round PCR. More sensitive 4200 TapeStation density plots demonstrated the presence of the desired amplicons in an additional four participants (CAP88, CAP177, CAP248 and CAP255) (Figure 3.4, highlighted in green). In order to increase the yield following PCR clean-up and second round PCR, both the first and second round PCR were repeated in replicate, and the bead-cleaned product pooled. Despite this, two samples (CAP248 and CAP314) did not reach the minimum DNA concentration (500-

1,000 ng) required to progress to sample library construction, and therefore did not undergo PacBio sequencing. Thus, eight samples were submitted to the National Institute for Communicable Diseases Sequencing Core for adaptor ligation and sequencing.

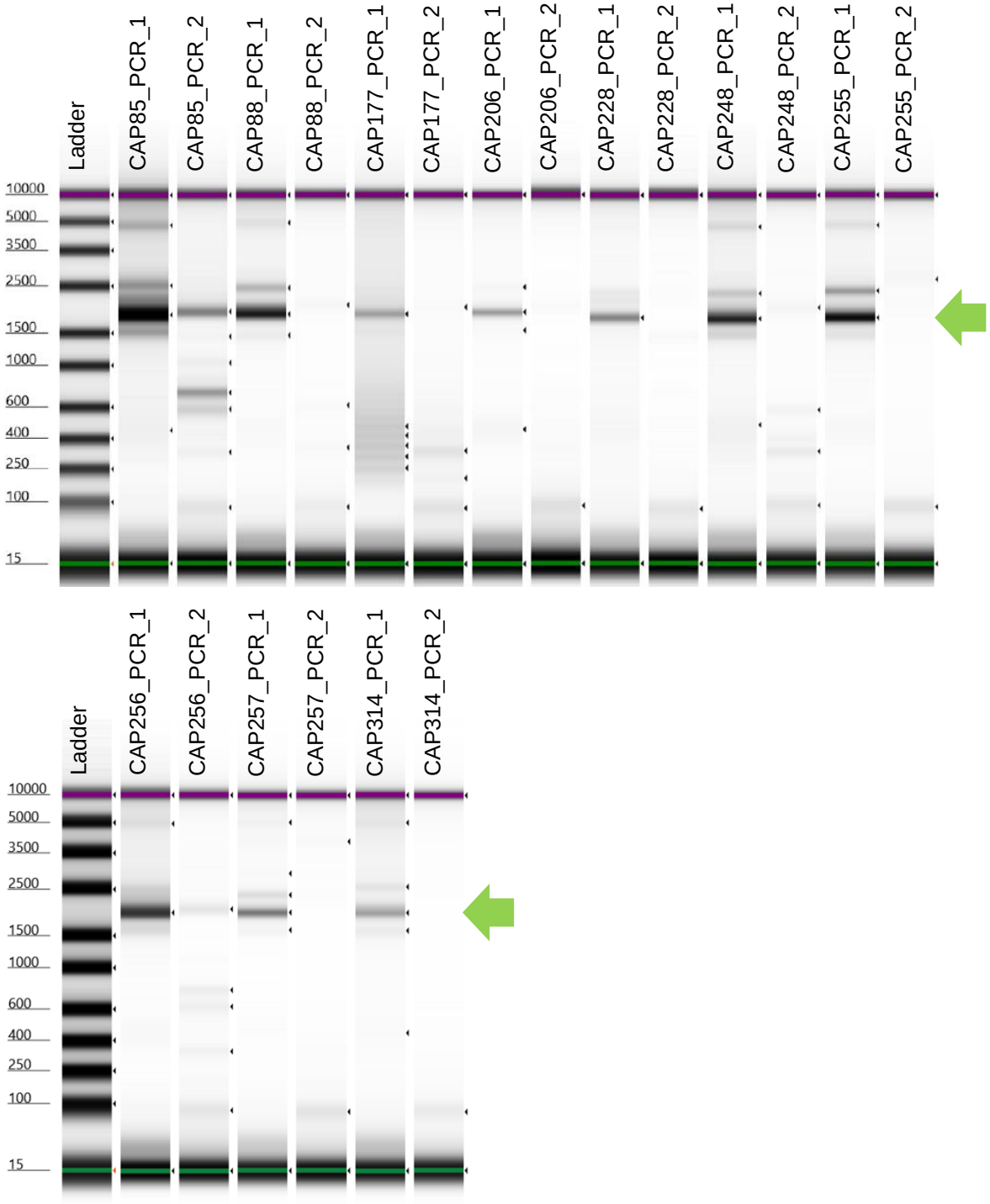


Figure 3.3. The size of the product generated in both first and second round PCRs in preparation for PacBio sequencing. Samples were imaged using a 4200 TapeStation. The expected size of *IGHG3* is denoted by the green arrow.

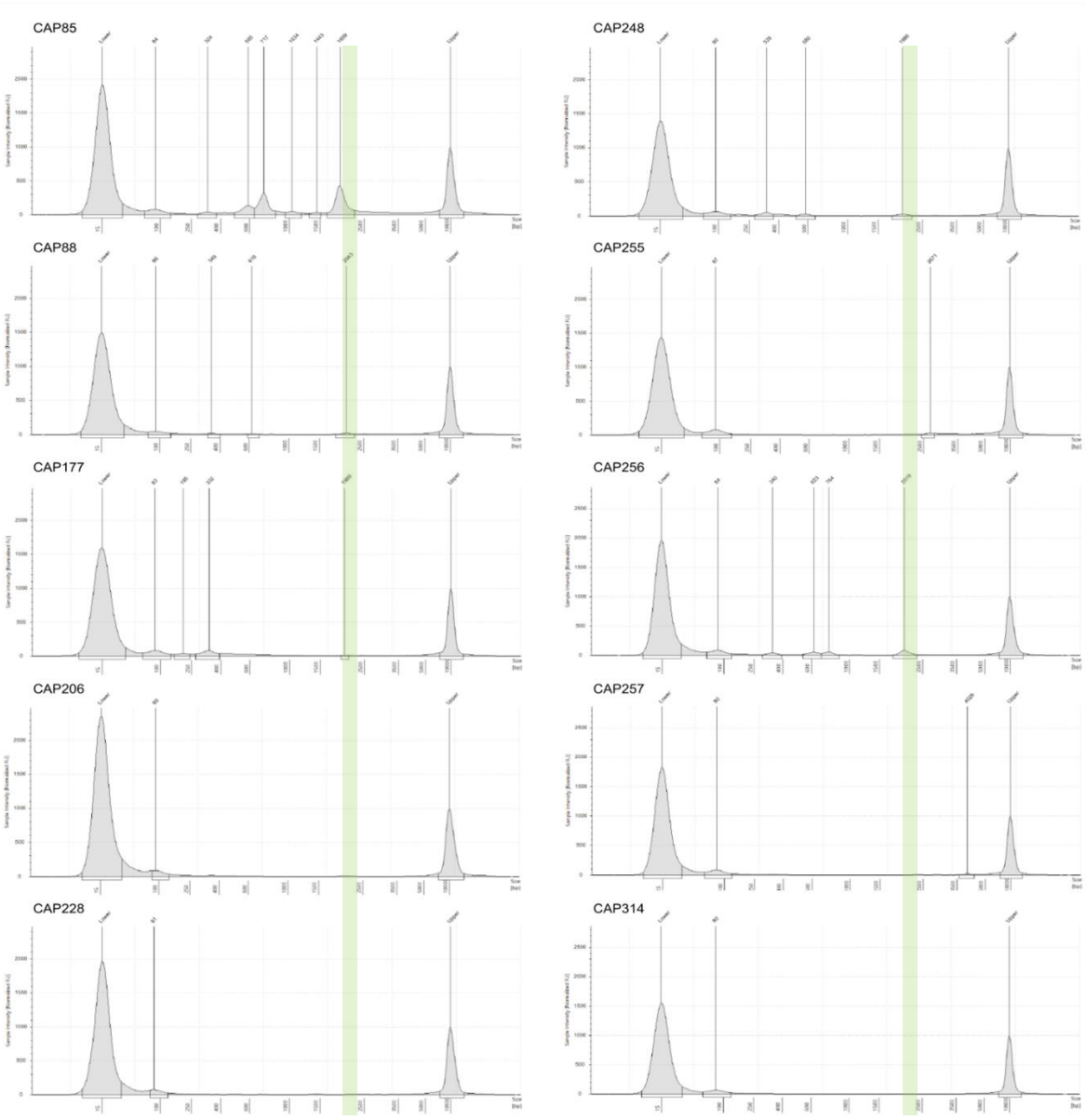


Figure 3.4. A density plot of the TapeStation results from each CAPRISA participant after the second round PacBio PCR. The size of the amplicons generated following the second round PCR is plotted on the x-axis and the fluorescence intensity on the y-axis. The fluorescence intensity of the amplicons corresponds to the concentration of the DNA. The expected location of the *IGHG3* amplicons is highlighted in the green box.

3.3. *IGHG3* haplotypes in CAPRISA participants

A total of fifteen *IGHG3* alleles were identified in nine participants using both PacBio and Sanger sequencing. Eight alleles were identified using only Sanger sequencing, and thirteen through only PacBio sequencing. Five alleles were identified using both techniques (Table 3.1). Furthermore, we have previously sequenced fragments of *IGHG3* in seven of the ten participants studied (excluding CAP256, CAP257 and CAP314). These data were combined with the full-length sequencing data generated in this project to confirm the genetic diversity observed and to identify sequencing

artefacts due to PCR error. There was one sample (CAP314) which did not yield any *IGHG3* sequences. This was despite extensive troubleshooting. Multiple clones were Sanger sequenced, and both Sanger and PacBio sequencing were done on different aliquots from separate bleeds and PBMC isolations to ensure the lack of *IGHG3* sequences was not due to degraded sample DNA.

Table 3.1. The technique used, and participant each allele was identified in.

Allele	Participant ID	Sequencing method identified	
		Sanger	PacBio
*IGHG3*01m*	CAP256		✓
*IGHG3*01m1*	CAP177	✓	
*IGHG3*03*	CAP177	✓	✓
	CAP228		✓
*IGHG3*03m*	CAP257		✓
*IGHG3*05*	CAP228		✓
*IGHG3*10*	CAP88	✓	✓
	CAP255	✓	✓
*IGHG3*11*	CAP248	✓	
*IGHG3*13*	CAP206		✓
*IGHG3*14*	CAP255	✓	
*IGHG3*17*	CAP85	✓	✓
	CAP256		✓
*IGHG3*11mm*	CAP85		✓
*IGHG3*11mm1*	CAP206	✓	✓

The frequency of the alleles identified is represented in Figure 3.5. Seven described alleles were sequenced (*IGHG3*03; IGHG3*05; IGHG3*10; IGHG3*11; IGHG3*13; IGHG3*14* and *IGHG3*17*), and five novel alleles (*IGHG3*01m; IGHG3*01m1; IGHG3*03m; IGHG3*11mm* and *IGHG3*11mm1*). The novel alleles represented a third of the total *IGHG3* alleles identified. Each novel allele was named according to the number of mismatches from their closest matching allele ("m" for a single mismatch, "mm" for multiple mismatches). Where there were multiple novel alleles that matched the same documented allele, the first allele identified was named according to its closest matching documented allele followed by "m" or "mm". Thereafter, alleles were differentiated by a number – e.g., *IGHG3*01m* and *IGHG3*01m1*. These names were merely used as identifiers until submitted and accepted to IMGT, upon which they will receive an official IMGT-based name. Described alleles *IGHG3*03*, *IGHG3*10* and

*IGHG3*17* were the most common alleles, identified in two individuals each. No two participants had the same genotype.

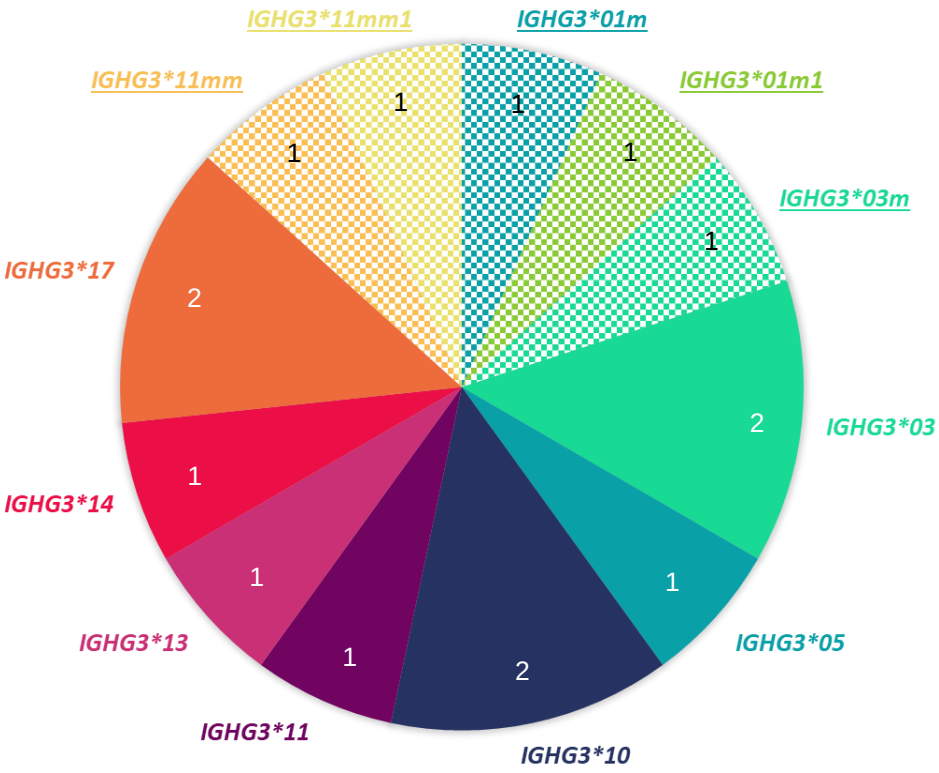


Figure 3.5. *IGHG3* alleles sequenced using both Sanger and PacBio techniques. Novel alleles are indicated by the chequered slices with underlined names. The number of sequences identified of each allele is denoted by the number in the chart.

Novel alleles *IGHG3*01m1* (identified in CAP177) and *IGHG3*03m* (identified in CAP257) differed from their closest matching documented *IGHG3* allele (*IGHG3*01* and *IGHG3*03*, respectively) by a single intronic SNP (Figure 3.6; Supplementary Figure 2 and 3). The novel *IGHG3*01m1* allele contained a G479C intronic SNP that is observed in all other *IGHG3* alleles. The novel *IGHG3*03m* also contained a single intronic SNP (G1434A), although this was unique to this allele. Both *IGHG3*11mm* and *IGHG3*11mm1* (identified in CAP85 and CAP206 respectively) differed from the closest matching *IGHG3*11* allele by six and seven SNPs, respectively (Supplementary Figure 4). They shared six SNPs, of which three were intronic, and three exonic that resulted in amino acid changes in the CH2 region. Two of these exonic SNPs were consecutive substitutions (A1543G and C1544TA) that resulted in a leucine to phenylalanine swap at position 234 (L234F). This substitution was not observed in any other *IGHG3* allele, but is found in *IGHG4* alleles – an isoallotypic change (an amino acid substitution specific to one or more subclass) (Vidarsson, Dekkers and Rispens, 2014). It is worth noting that position 234 is proximal to the

FcγRIIA and C1q binding sites - a region responsible for inducing phagocytosis and complement deposition, respectively. The third shared exonic SNP (T1731A) resulted in a phenylalanine to tyrosine substitution (F296Y). A tyrosine at position 296 is seen in all documented *IGHG3* alleles but four, including *IGHG3*01* – the first *IGHG3* allele identified, thus designated as the reference allele.

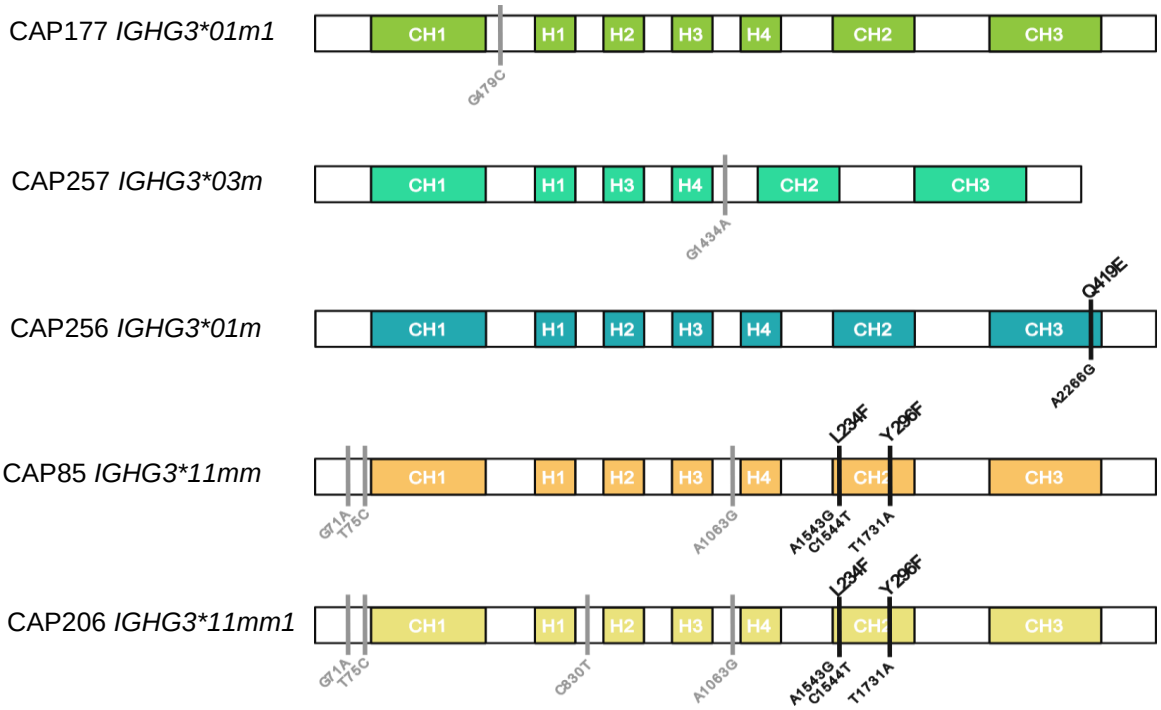


Figure 3.6. Schematic of the five novel alleles detected in nine CAPRISA participants. The location of each SNP is denoted by the vertical stripe, with the nucleotide position and substitution below. Intronic SNPs are shown in grey, while exonic SNPs are shown in black. Amino acid (AA) substitutions are shown above the vertical strip, also in black. *IGHG3*03* and novel *IGHG3*03m* are both 3 hinge alleles.

The fifth novel allele (*IGHG3*01m*) was documented by Richardson *et al.* (2019). However, it was identified from an expressed antibody, where only the exons were present. The *IGHG3*01m* sequence identified here therefore provides the full-length germline sequence for this allele. Interestingly, while the expressed IgG3*01m antibody differs from the reference IgG3*01 antibody by a single AA change – Q419E, the germline allele is more closely matched to *IGHG3*05* than *IGHG3*01.* There are 5 intronic SNPs between *IGHG3*01* and *IGHG3*05,* and only one SNP that differs between *IGHG3*05* and *IGHG3*01m* (nucleotide C2166G that results in an AA change Q419E) (Figure 3.7; Supplementary Figure 5). However, due to this allele already being documented in the literature, it will be referred to as *IGHG3*01m.* This data highlights the importance of sequencing the germline.

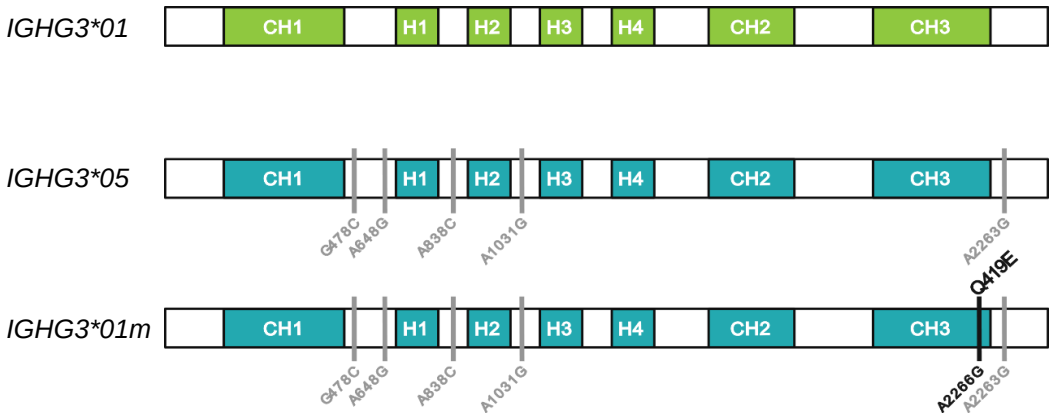


Figure 3.7. The allele structure and SNPs that differ between *IGHG3*01*, *IGHG3*05* and *IGHG3*01m*. Intronic SNPs are indicated in grey, while exonic SNPs are denoted in black. A2266G (Q419E) is the only SNP that differs between *IGHG3*05* and *IGHG3*01m*, while the 5 SNPs denoted in grey (all intronic) are the SNPs that are shared between *IGHG3*05* and *IGHG3*01m,* but which differ from *IGHG3*01*.

3.4. Characterizing *IGHG3* functional diversity

3.4.1. The impact of allelic diversity on protein structure

The SNPs that separate the twenty-nine documented *IGHG3* alleles in IMGT and the five novel alleles identified in this project are more commonly located in introns than exons. This results in some of alleles having identical protein sequences – such as *IGHG3*01,* which is the same antibody as *IGHG3*01m1*, *IGHG3*05* and *IGHG3*10* (Figure 3.8).

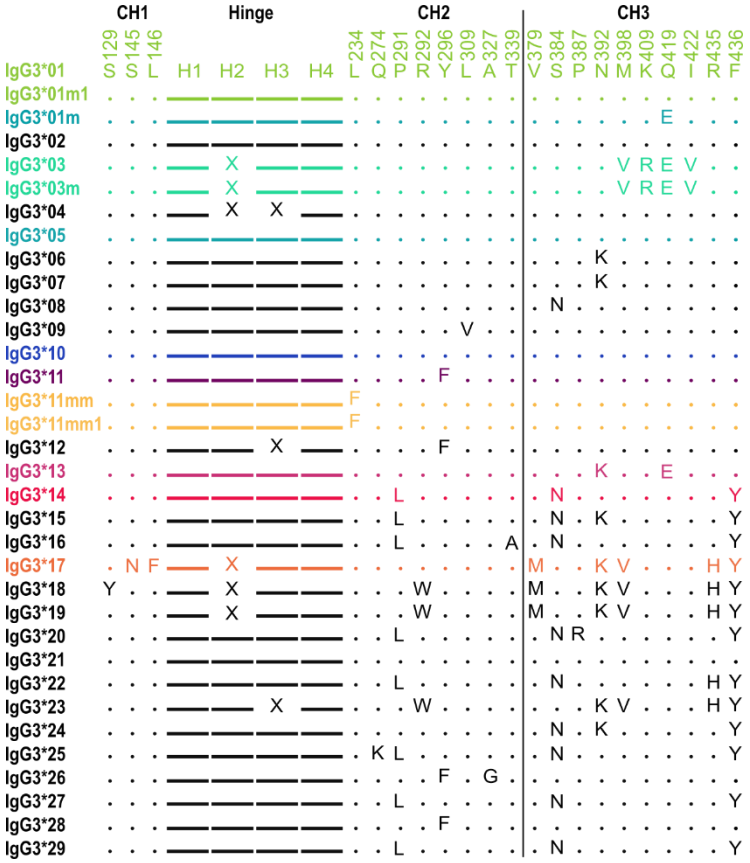


Figure 3.8. The amino acid differences between all 29 documented *IGHG3* alleles, and the five novel alleles. The coloured antibody names are those alleles identified in CAPRISA participants. The novel alleles identified are aligned below their closest matching documented allele – except for IgG3*01m, which was aligned to IgG3*01 instead of IgG3*05 as this is the allele it was named for. Amino acids are numbered at the top of the figure, according to Eu numbering (Lefranc, 2000). "X" in the hinge denotes alleles missing that hinge exon.

3.4.2. Converting alleles to participant-matched HIV-specific antibodies

We have previously isolated 10 HIV-specific antibodies from the same nine CAPRISA participants sequenced in this study (Gray *et al.*, 2011; Morris *et al.*, 2011; Doria-Rose *et al.*, 2016; Wibmer *et al.*, 2016, 2017; van Eeden *et al.*, 2018). The constant regions were engineered to incorporate the donor matched *IGHG3* alleles identified in section 3.3. Additionally, IgG1*01 and IgG3*01 antibodies were made for all participants as controls, as IgG1*01 is the most widely used subclass in therapeutic antibodies, and IgG3*01 serves here as the reference IgG3 allele (Figure 3.9).

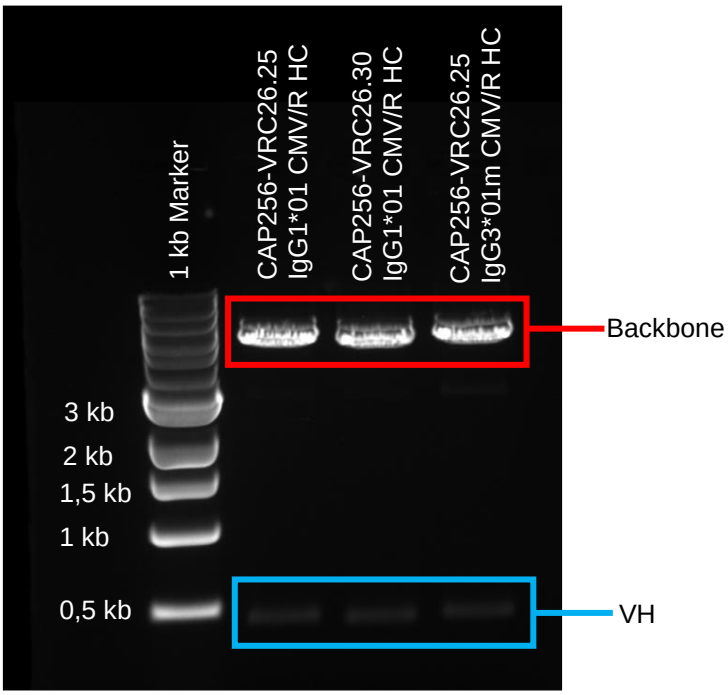


Figure 3.9. An example gel of the plasmid digestion fragments. The backbones from CAP256-VRC26.25 IgG1*01 and CAP256-VRC26.25 IgG3*01m were extracted from the gel, and ligated with the gel-extracted CAP256-VRC26.30 IgG1*01 VH.

The names of the antibodies from each participant, and the subclasses made are depicted in Figure 3.10.



Figure 3.10. The antibodies and the subclass variants made for each participant. The antibody names are shown in the grey boxes. The CH regions are coloured based on their alleles. Three hinge variants (IgG3*03 and IgG3*17) are shown with only 3 cysteine bonds in the hinge. The novel *IGHG3*11mm* and *IGHG3*11mm1* alleles code for the same antibody, thus both were coloured the same colour (mustard), and labelled “IgG3*11mm”.

3.4.3. The variable region differences between participants

The ten antibodies made in this project targeted a variety of epitopes. CAP85-14.8 and CAP206-CH12 both targeted MPER (Gray *et al.*, 2011; Morris *et al.*, 2011). Although CAP85 developed intermediate breadth in her sera, CAP85-14.8 is strain-specific (Gray *et al.*, 2011). CAP206-CH12 was neither broad (only accounting for 13% of the CAP206 plasma breadth), nor potent (Morris *et al.*, 2011). CAP88-CH06 is C3 directed, and strain-specific (Gray *et al.*, 2011). CAP177-24G, and CAP255.C5 and CAP255.G3 are all N332-glycan dependant. CAP177-24G is strain-specific, while

CAP255.C5 and CAP255.G3 are two clonally related bNAbs (Gray *et al.*, 2011; Kitchin, 2019 - unpublished). CAP228-16H and CAP256-VRC26.30 both target the V2/apex, although CAP228-16H is strain-specific, while CAP256-VRC26.30 is potent but not very broad (neutralizing 26% of a 46 virus panel) (Doria-Rose *et al.*, 2016; van Eeden *et al.*, 2018). CAP248-2B is a weak neutralizer at IC_{50} titres (neutralizing 22% of 45 pseudoviruses), but broader at IC_{20} titres (neutralizing 58% of the 45 pseudovirus panel) (Wibmer *et al.*, 2017). This bNAb targets the interface (Wibmer *et al.*, 2017). Finally, CAP257-RH1 is a strain-specific antibody that targets the CD4bs (Wibmer *et al.*, 2016). The epitopes and antibodies targeting each epitope are shown in Figure 3.11. The antigens used in the ADCP assay were based on the epitope and ability to bind those particular viruses, while the neutralization virus panel was selected based on previous neutralization data for each antibody.

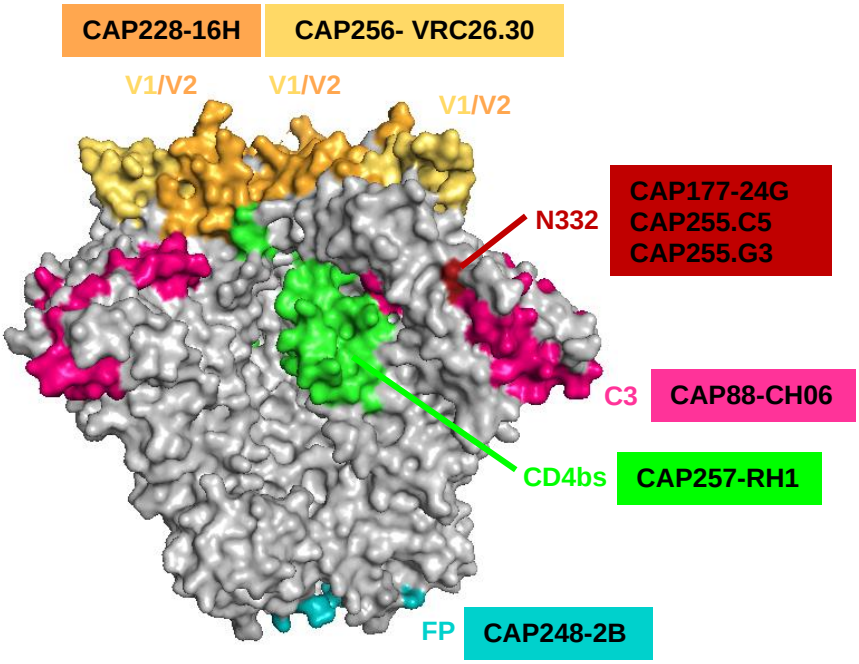


Figure 3.11. The HIV epitopes of the CAPRISA antibodies studied. The epitope is coloured on the trimer and labelled by coloured text, while the antibodies that bind the epitope are shown in coloured boxes. V1/V2 corresponds to the V2/apex. MPER is not present on the BG505 SOSIP.664 trimer (PDB accession code 4zmj).

3.4.4. The impact of *IGHG3* allelic variation on phagocytosis

The impact of subclass and allele on ADCP in nine of the HIV-specific antibodies studied in this project was assessed. CAP257-RH1 was excluded from this assay due to its lack of binding to available trimers (Wibmer *et al.*, 2016). In order to ensure reproducibility, repeat runs of each assay were correlated. Area under the curve (AUC)

- calculated for each mAb in serial dilution (Supplementary Figure 6) – was used to compare ADCP between antibodies (Supplementary Figure 7).

The majority of the antibodies (six out of nine) showed improved ADCP when engineered as IgG3 compared to IgG1*01. However only four of these showed statistically significant differences: CAP85-14.8 IgG3*11mm, CAP228-16H IgG3*03, CAP248-2B IgG3*01 and CAP256-VRC26.30 IgG3*01m (Figure 3.12). Additionally, CAP256-VRC26.30 IgG3*01m was significantly better at ADCP than IgG3*17.

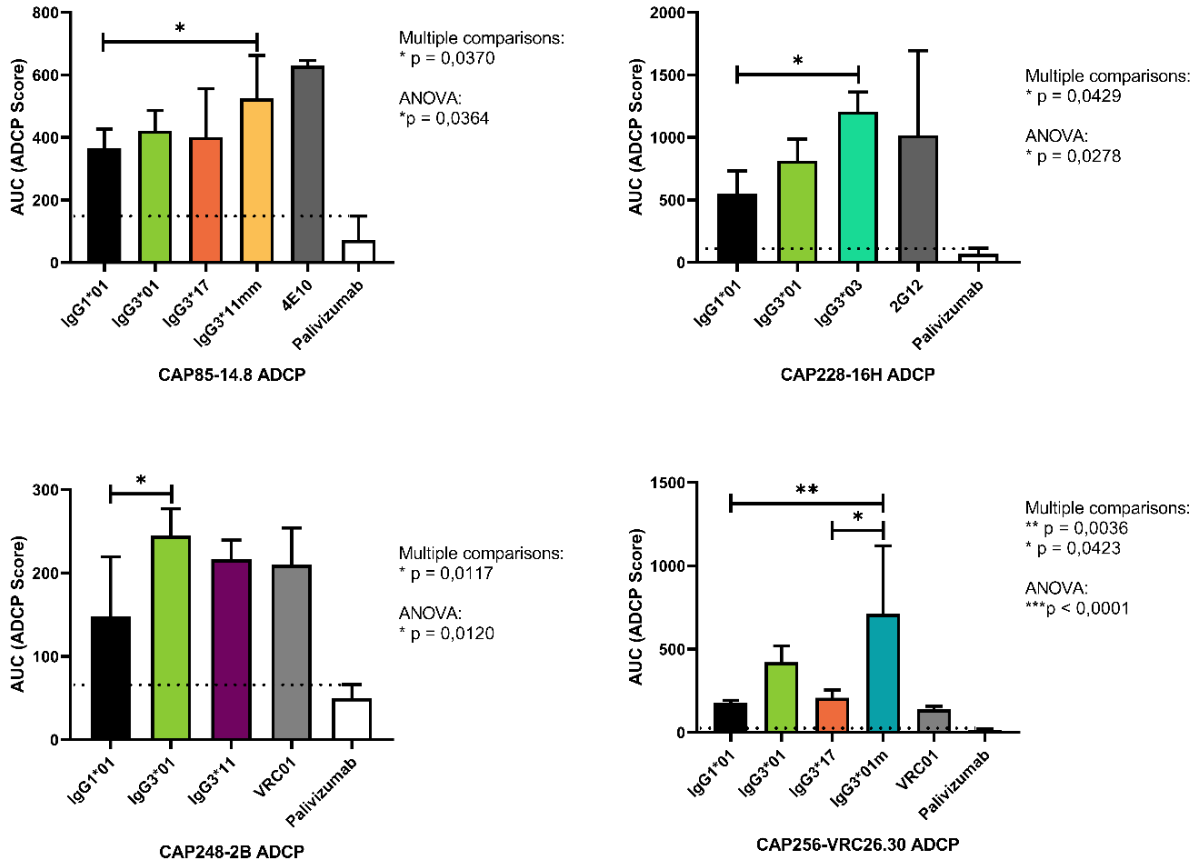


Figure 3.12. The AUC for each set of antibodies where differences between subclass/allele reached statistical significance. Each bar graph was calculated as the area under the titration curve, and is the average of three repeats. The negative control was Palivizumab (clear box). The positive control is represented in grey. The level of background signal was calculated using the AUC of Palivizumab, and shown as the dotted black line.

There were two samples where IgG3*01 was marginally worse than IgG1*01 - CAP88-CH06 and CAP177-24G, while there was no difference between the subclasses in CAP255.G3 (Supplementary Figure 8).

To compare results between ADCP assays, the average AUC for each antibody was calculated as fold change relative to IgG1*01 (Figure 3.13). Across the ADCP assays, the majority of the IgG3 alleles other than IgG3*01 (nine of eleven) were better at

ADCP than their IgG1*01 counterparts. Interestingly, IgG3*03 was worse than IgG1*01 as a CAP177-24G antibody, but better than IgG1*01 as a CAP228-16H antibody. A similar difference was also observed in the two IgG3*14 mAbs: IgG3*14 was better than IgG1*01 as a CAP255.C5 antibody, but worse than IgG1*01 as a CAP255.G3 antibody, suggesting the Fab region impacted ADCP.

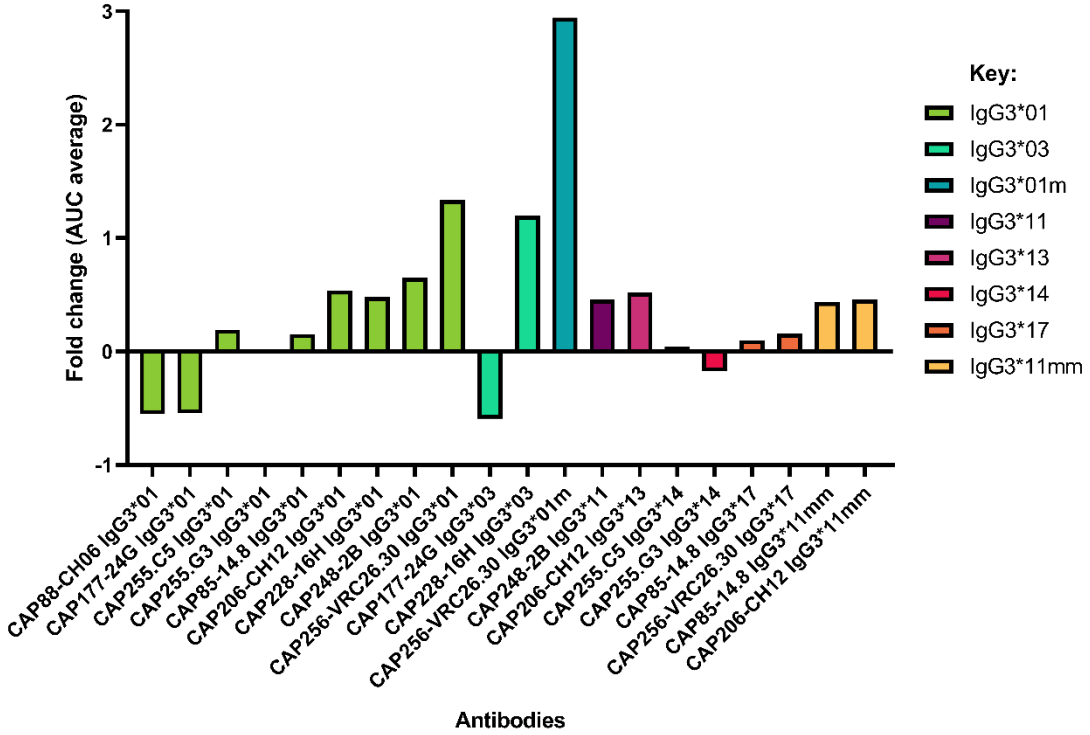


Figure 3.13. The fold change between IgG1*01 and all IgG3 antibodies. Each antibody is coloured according to its *IGHG3* allele, described by the Key on the right. IgG3*01 antibodies (green) are ordered along the x-axis according to the antigen they were tested against. IgG3 alleles (assorted colours) were ordered numerically. The fold change of each antibody was calculated compared to IgG1*01 of the same antibody. The distance from the 0 line indicates fold change.

3.4.5. The influence of Fc region variation on pseudovirus neutralization

Virus neutralization has been shown to be influenced by different isotypes (Tudor *et al.*, 2012; Richardson *et al.*, 2019, 2021; Scheepers *et al.*, 2020). To investigate whether IgG3 improved neutralization in a subset of samples (CAP85-14.8, CAP206-CH12, CAP255.C5 and CAP255.G3), the TZM-bl neutralization assay was run. The pseudoviruses used were selected based on in-house neutralization data (Gray *et al.*, 2011; Morris *et al.*, 2011; Kitchin, 2019 - unpublished; Sacks, 2019 - unpublished). The neutralization titration curves are shown in Supplementary Figure 8. Significant difference between antibodies was calculated using Friedman's test with Dunn's correction.

In nine of fourteen neutralization assays, IgG3 antibodies did not differ from IgG1*01 antibodies in potency (Figure 3.14). Five assays demonstrated different neutralization

profiles when subclass was changed. CAP85-14.8 was significantly more potent (p=0,0036) as an IgG3*01 antibody compared to IgG1*01, when tested against the CAP85.9 virus. Across all four viruses, CAP255.C5 IgG1*01 was less potent than the CAP255.C5 IgG3 antibodies (p=0,024). CAP255.C5 did not neutralize CE703010217.C4 nor Zm135M.PL10a as an IgG1*01 antibody, but potently neutralized these two viruses as IgG3 antibodies. There was no difference in neutralization profile between CAP255.C5 IgG3*01 and IgG3*14. CAP255.G3 had a strikingly different neutralization pattern to CAP255.C5, where all four viruses were potently neutralized by all three antibodies. In contrast to CAP255.C5, antibody subclass did not impact CAP255.G3 neutralization potency. These results suggest that the constant region does not significantly impact neutralization potency for these antibodies against this selection of viruses. Overall, this indicates that antibody subclass can affect neutralization in a virus and antibody specific manner, likely influenced by the angle of approach to the target.

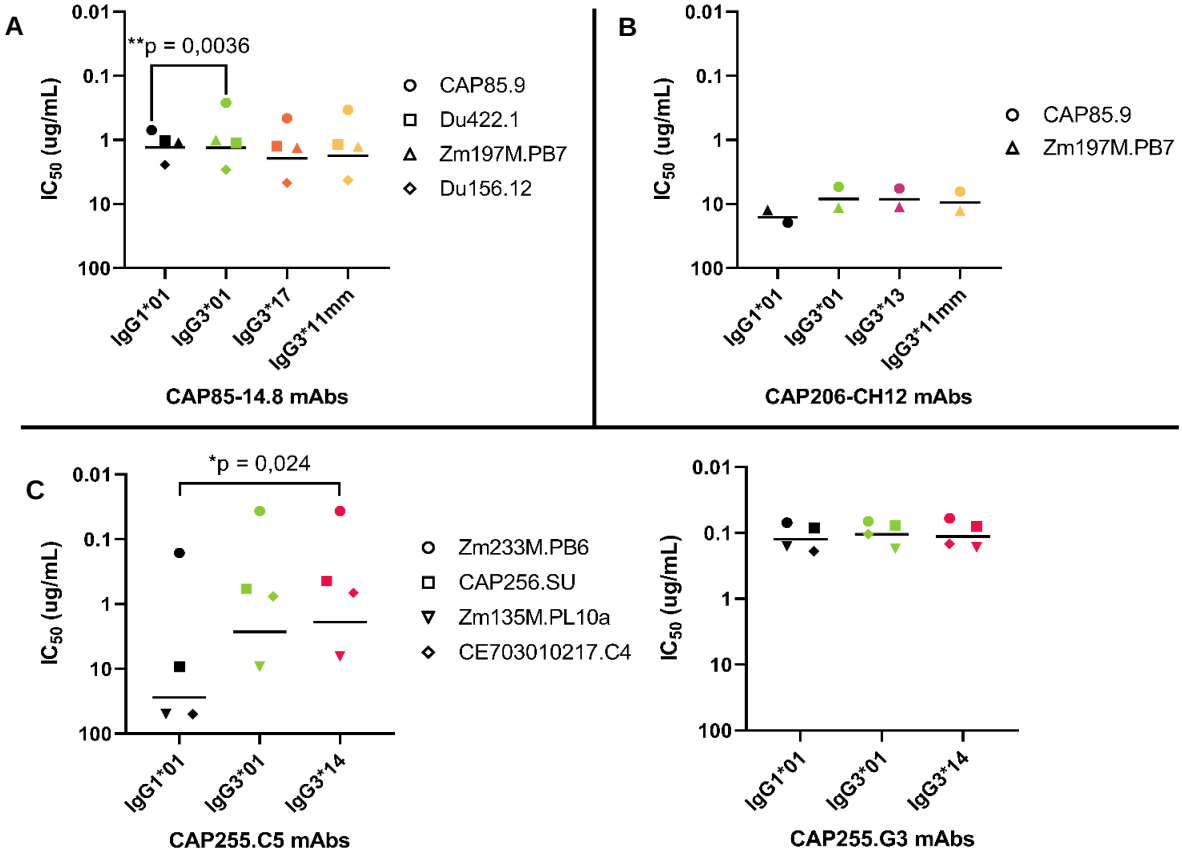


Figure 3.14. The neutralization titres of the four groups of antibodies tested. Each virus is denoted by a different shaped point, with the key on the right of figures A and B, and in the middle of figure C. A) The four CAP85-14.8 antibodies were tested against four subtype C viruses: CAP85.9 (tier 2), Du422.1 (tier 2), ZM197M.PB7 (tier 1B) and Du156.12 (tier 2). Only CAP85-14.8 IgG3*01 was significantly better at neutralizing the autologous virus than IgG1*01. B) The four CAP206-CH12 antibodies were tested against two subtype C viruses: CAP85.9 (tier 2) and ZM197M.PB7 (tier 1B). C) CAP255.C5 and CAP255.G3 were tested against the same set of four clade C viruses: Zm233M.PB6 (tier 2), CAP256.SU (unclassified), ZM135M.PL10a (tier 2), and CE703010217.C4 (tier 2). CAP255.C5 IgG3 antibodies were more potent than their IgG1 counterparts. P values were calculated using Friedman's test with Dunn's correction.

3.4.1. Reduced FcγRIIA-binding by novel *IGHG3* alleles containing an L234F mutation

Novel alleles *IGHG3*11mm* and *IGHG3*11mm1* contain an isoallotypic amino acid mutation, L234F, that is also observed in *IGHG4* (Deveuve *et al.*, 2020). IgG4 antibodies are responsible for downregulating the immune response (Vidarsson, Dekkers and Rispens, 2014). This is a result of the low affinity of IgG4 antibodies for FcγRIIA (and other activating FcγRs) (Caaveiro, Kiyoshi and Tsumoto, 2015). Thus, an FcγRIIA-binding ELISA (Moldt *et al.*, 2012) was done to determine the impact of the L234F SNP on IgG3 FcγR-binding.

As expected, both IgG3*11mm antibodies bound to FcγRIIA less efficiently than the other IgG3 antibodies (Figure 3.15; Supplementary Figure 9). Furthermore, consistent with previous studies (Bruhns *et al.*, 2009; Boesch *et al.*, 2017; de Taeye *et al.*, 2020), the overall trend observed across both sets of antibodies was that IgG3*01 bound best to FcγRIIA, while IgG1*01 had the least efficient binding. The two positive controls were an Fc region mutant with mutations G236A/S239D/A330L/I332E, and VRC01 IgG1*01 (Ahmed *et al.*, 2016). A VRC01 IgG1 with an N297Q mutation was a negative control (Bolt *et al.*, 1993).

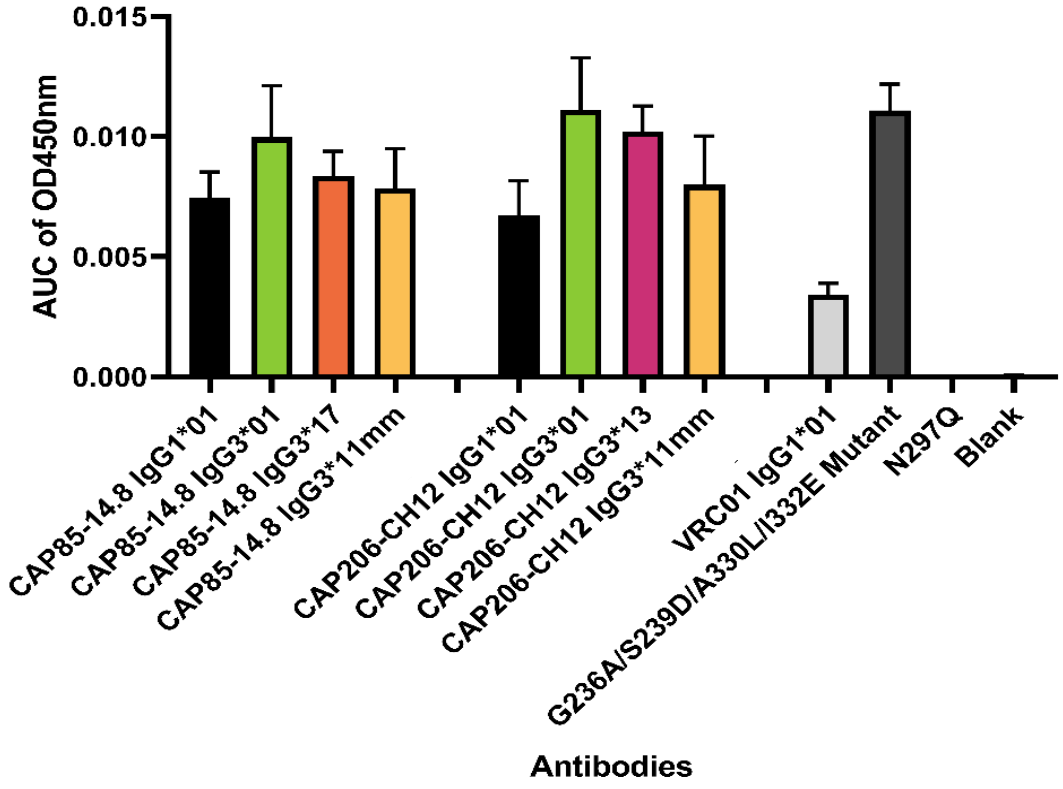


Figure 3.15. L234F SNP in *IGHG3*11mm* and *IGHG3*11mm1* influences FcγRIIA-binding. Two repeats of this assay were done, and the average AUC and error bars from both results plotted.

3.4.2. Investigating the impact of allelic diversity on IdeS cleavage

IdeS is an IgG-specific protease secreted by *Streptococcus pyogenes*. It cleaves IgG antibodies at the start of the CH2 region, in the motif PAPELLGˇGP (Vincents *et al.*, 2004). Antibodies resistant to IdeS and matrix metalloprotease (MMP) enzymes (digestive enzymes produced by cancer cells which cleave at the same binding site as IdeS), are ideal as therapeutic mAbs as cleavage abrogates FcγR-binding and thus Fc effector function (Fan *et al.*, 2012; Hsiao *et al.*, 2018). The two novel alleles identified in CAP85 and CAP206 (*IGHG3*11mm* and *IGHG3*11mm1*) contain an amino acid substitution (L234F) within the IdeS binding motif. To investigate whether this SNP affected IdeS activity, the IgG3 antibodies from each of these two participants were digested at different time points (Figure 3.16).

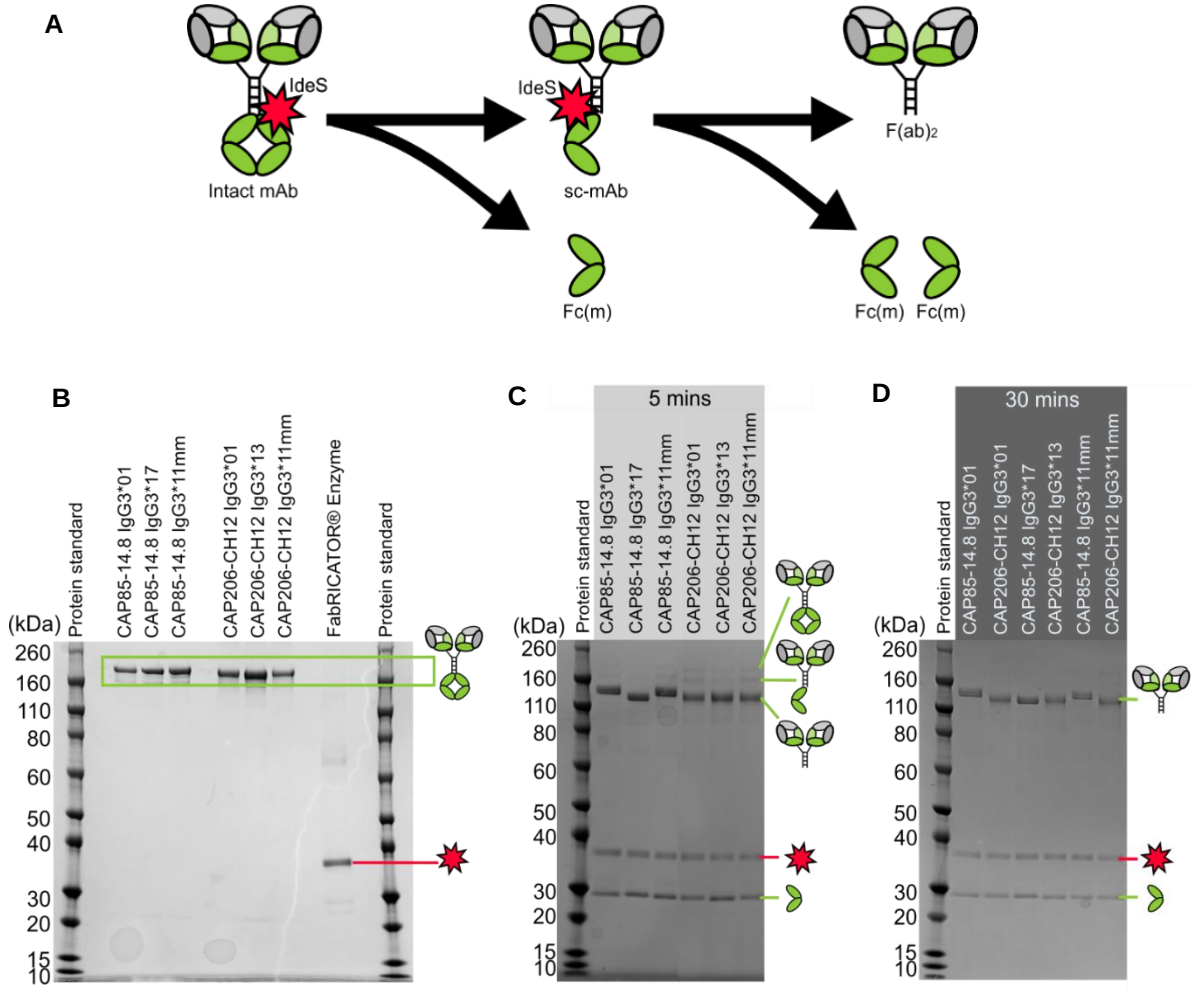


Figure 3.16. The mechanism of IdeS mAb digestion followed by the SDS-PAGE results. A) IdeS cleaves each HC separately, first generating a single chain-mAb (sc-mAb) and an Fc monomer (Fc(m)). The second cleavage generates a F(ab)2 fragment and two Fc(m) fragments. B) The undigested controls alongside the IdeS (FabRICATOR®) enzyme – represented in the figure as a red star. C) The results of the digestion stopped after 5 minutes. D) The results of the digestion stopped after 30 minutes.

After exposure to IdeS for 5 minutes, there was a mix of undigested antibody, partially digested and fully digested antibody across all samples. By 30 minutes all of the

samples had been completely digested. Overall, based on the similar cleavage pattern between all IgG3 alleles at all time points, the novel mutation observed in the IgG3*11mm antibodies did not appear to confer resistance to IdeS digestion. However, it was worth noting that the molecular weights of the antibodies tested differed from their expected molecular weight by ~20 kDa. This is most likely due to N- and O-linked glycosylation (Krapp *et al.*, 2003; Kretschmer *et al.*, 2017). Overall, the outcome of this digest contributed to the characterization of the novel IgG3*11mm allele in confirming that it did not confer therapeutically relevant resistance to IdeS.

4. Discussion

IgG3 antibodies have the widest range of Fc effector functions and were associated with reduced risk of infection in the RV144 vaccine trial (Chung *et al.*, 2014; Yates *et al.*, 2014). Additionally, the gene encoding *IGHG3* is the most genetically diverse subclass with 29 documented alleles to date. The functional differences between these alleles are poorly characterized, and none of the sequences in IMGT are from Southern African individuals (Warrender and Kelton, 2020). We therefore sequenced *IGHG3* in nine Zulu-speaking HIV-infected women from the CAPRISA cohort in South Africa, and identified five novel alleles. The effect of this diversity on ADCP, neutralization, FcγRIIA-binding and IdeS protease cleavage was tested. Overall, the majority of IgG3 antibodies demonstrated superior ADCP compared to IgG1. In addition, IgG3 either enhanced or maintained neutralization potency. Allelic differences between the IgG3 antibodies did not significantly affect function. Additionally, two novel alleles contained an isoallotypic amino acid change in the FcγRIIA-binding site (L234F), that was shown to reduce FcγRIIA-binding in a binding ELISA. Despite this amino acid change also occurring in the IdeS cleavage motif, the two novel alleles did not demonstrate IdeS cleavage resistance compared to other IgG3 alleles of the same antibodies.

The first aim of this project was to optimize a PCR that enabled sequencing of *IGHG3* in a single fragment. This was achieved, and despite a small sample size of nine individuals, five novel alleles were identified. In total, fifteen alleles were sequenced, and twelve allele variants identified, indicating a high level of genetic diversity in these individuals. This is in agreement with other data documenting increased genetic diversity in African individuals as a result of greater population admixture over a longer period of time compared to other populations (Campbell and Tishkoff, 2008; Scheepers *et al.*, 2015).

To sequence *IGHG3* in a larger portion of this population, the PCR protocol will need to be further optimized, as the current protocol – while successful - was inefficient. The low efficiency observed was due to the repetitive nature of *IGHG3* and its similarity to other *IGHG* genes, which interferes with PCRs. Spontaneous reannealing of double-stranded DNA (ds-DNA) during the primer annealing phase can occur in repetitive, highly similar sequences of DNA. When the DNA reanneals incorrectly, it is termed “out of register reannealing” (Hommelsheim *et al.*, 2014). This can cause displacement

of the polymerase – which results in truncated PCR products that serve as mega-primers (Smyth *et al.*, 2010; Hommelsheim *et al.*, 2014). Mega-primers can bind to similar sequences in the genomic DNA. A mega-primer binding to the same allele it was generated from, will result in an amplicon indistinguishable from one generated by the PCR primers. However, should the mega-primer bind to a different gene or allele, a chimaera is produced. Chimaeras were observed in both Sanger and PacBio sequence results. The second issue occurs in the event that the polymerase isn't displaced, and instead skips over the reannealed segment, generating an amplicon that is missing a section of the gene (Hommelsheim *et al.*, 2014). The ladder-like banding pattern observed following the PCR is a result of this. The lower and brightest band was approximately 1800 nt long, which is shorter than any of the other three IGH genes - indicating amplicons missing some of their DNA.

Solutions to overcoming out of register reannealing to be explored in the future include shifting the primers further out into the intergenic DNA. This has been shown to reduce out of register reannealing in other repetitive gene sequencing (Hommelsheim *et al.*, 2014). The greater the distance between the primer binding site and the repetitive region, the less likely the polymerase is to dissociate when it encounters ds-DNA. Increasing the length of the amplicon would eliminate Sanger sequencing as a technique for sequencing *IGHG3*, however PacBio is not constrained by template length and can thus be used. Alternatively, out of register reannealing can be overcome by digestion and separation of the DNA prior to amplification. Enzymatic cleavage of the genomic DNA at the switch regions, and subsequent separation of the fragments using droplet emulsion prior to PCR could prevent chimaera formation (Nakano *et al.*, 2003).

In addition to out of register reannealing, it is possible that there is genetic diversity at the primer binding sites. Although two sets of primers with different binding sites and degenerate bases – bases that can bind to more than one nucleotide (Linhart and Shamir, 2005) - were tested on these samples, *IGHG3* was still not sequenced in one participant. These primers were designed to incorporate all known *IGHG3* SNPs in the primer binding site, to overcome potential diversity. However, few samples in international databases are from Southern African individuals. As such, we cannot discount undocumented genetic variation at the primer binding site as cause for unsuccessful sequencing. Furthermore, there was also preferential primer bias in all the samples for IgG1. As a result, the low efficiency of the PCR meant that the depth

of sequencing may have been insufficient. Renewed attempts at designing primers that are more specific for IgG3 would eliminate this bias and subsequently improve sequencing depth. Alternatively, it is possible that some of these samples contain a germline *IGHG3* deletion. African individuals have a greater proportion of structural genomic insertions and deletions than other populations (Dunston *et al.*, 2019). Whether the deletion is gene specific or over a larger part of the chromosome in this participant remains to be determined. To investigate chromosome structure, a hybridization bead capture method where large fragments of the IGH locus are isolated, sequenced using PacBio and the locus reconstructed (developed by our collaborator, Dr Corey Watson), could be employed (Rodriguez *et al.*, 2020). However, in the case of CAP314, antibody repertoire sequencing from this donor has revealed the presence of IgG3 antibodies, thus the lack of amplification of germline *IGHG3* in this donor is not due to an *IGHG3* deletion.

Despite the low PCR efficiency, this project achieved the aim of sequencing the full-length *IGHG3* gene, identifying sequence diversity that would have been overlooked using other methods such as allotyping. Gamma marker (Gm) allotypes are a way of classifying *IGHG1*, *IGHG2* and *IGHG3* (G1m, G2m and G3m respectively) genes by serological typing of particular amino acids (Yacoubi Loveslati *et al.*, 2001). Due to linkage disequilibrium, the combination of genes is inherited in specific combinations - called Gm-haplotypes. Traditionally, the benefit of allotypes is the ease with which they can be tested, rendering them useful in population genetics and forensic science (Warrender and Kelton, 2020). However, allotypes overlook both intronic diversity and amino acid substitutions between alleles. There are sixteen G3m allotypes, compared to the 29 documented *IGHG3* alleles (Warrender and Kelton, 2020). Furthermore, while some alleles match their designated allotype exactly (*IGHG3*14* and G3m21), generally these allotypes include other alleles which differ from each other by a number of amino acids (G3m21 also includes *IGHG3*15* and *IGHG3*16*). Our study highlights the importance of delineating alleles based on genomic sequence over allotypic methods as novel alleles such as *IGHG3*11mm* and *IGHG3*11mm1* (which may impact disease outcomes due to reduced FcγRIIA-binding, and contribute to population studies), would be overlooked using allotyping.

To investigate the functional impact of *IGHG3* diversity, the alleles identified in the nine participants were made into HIV-specific IgG3 antibodies. The extended hinge of IgG3 antibodies generally improves ADCP (Giuntini and Granoff, 2016; Tay *et al.*, 2016;

Richardson *et al.*, 2019; Chu *et al.*, 2020; Pollara *et al.*, 2021). The longer, more flexible hinge enhances immune complex multimer formation, promoting FcγR-cross-linking (Richardson *et al.*, 2019; Chu *et al.*, 2020). This is critical to FcγR activation, and thus ADCP (Patel, Roberts and Barb, 2019). In this study, the extended hinge in IgG3 antibodies either improved ADCP or maintained function compared to IgG1*01. The impact of hinge length within IgG3 alleles on ADCP varied between antibodies, suggesting that the hinge may not be the only influence on the antibody/epitope interaction. This could be due to the different Fab regions of the antibodies which have unique angles of approach.

The extended hinge of IgG3 antibodies has also been shown to improve neutralization potency through altered Fab-antigen binding affinity, and through improved flexibility (Tudor *et al.*, 2012). In HIV, Richardson *et al.* (2019) observed improved neutralization by IgG3 versions of V2/apex specific antibodies compared to IgG1 versions, while Scheepers *et al.* (2020) observed the same in C3-specific antibodies (Moyo-Gwete, 2021 - unpublished). However, neither Chu *et al.* (2020) nor Molinos-Albert *et al.* (2017) observed significant difference in neutralization between IgG1 and IgG3 CD4bs and MPER bNAbs (respectively). This indicates that hinge length affects neutralization based on antibody specificity and virus characteristics (Chu *et al.*, 2020). Similar to ADCP, in this project, neutralization was either unaffected or improved by an antibody subclass with a longer hinge. Interestingly, while three of the assays where IgG3 was improved were in an N332-directed antibody, the fourth instance was in an MPER-directed antibody. Furthermore, the other N332-directed antibody that was tested was unaffected by subclass change. This may suggest that the impact of subclass change on neutralization potency is antibody-specific, rather than epitope-specific. In future, this could be investigated by making different alleles of the same antibody, thus eliminating the difference of both the Fab and the antigen. Additionally, the impact of the subclass and the V-region on neutralization could be isolated and assessed by using chimaeras where each region across both the Fab and the Fc is substituted.

As with the TZM-bl neutralization assay, the varied epitopes of these antibodies necessitated different antigens in the ADCP assay. Both size and differences in antigen conformation appeared to impact the results of the ADCP assay. Across three of the four monomeric gp120 ConC assays (CAP88-CH06, CAP177-24G and CAP255.G3), IgG3 antibodies were less efficient at inducing ADCP than IgG1*01. In the fourth gp120 ConC assay (CAP255.C5), IgG3*01 was only marginally better at

ADCP compared to IgG1. In contrast, all three of the ADCP assays tested against trimers demonstrated statistically significantly improved ADCP in at least one of the IgG3 antibodies tested. It is possible that the nature of the gp120 ConC monomer compared to that of a trimer negatively affected the ability of IgG3 antibodies to cross-link. FcγRIIA is a low-affinity FcR, and thus binds preferentially to multivalent immune complexes (Tay *et al.*, 2016). Reduced antibody cross-linking due to antigen may lower IgG3 ADCP scores in that assay. This could be supported by investigating the role of inter-trimer crosslinking in this assay. To limit the impact of different antigens, future work could investigate the impact of IgG3 alleles in a single antibody, tested on the same antigen. An additional limitation of this ADCP assay is that it is bead-based, which is a simplification of the process of ADCP (Richards and Endres, 2014), and which may not capture the complexity of ADCP *in vivo*. Future work could include the use of an infectious-virus ADCP assay, and ultimately animal models.

It is interesting to note that several of the differences we saw in neutralization (for example the notable improvement in neutralization as an IgG3 in CAP255.C5) did not translate to improved ADCP in the same antibodies. It is possible that the difference between the results seen for these assays is because of the format of antigen presented. ADCP is measured by binding of soluble protein on the surface of beads, and measures the ability to engulf particles, while neutralization is measured using pseudovirions and measures an antibody's ability to block infection. In order to determine the effect of different antigen formats, in future, an ADCP assay that measures the internalization of viral particles could be used.

CAP85-14.8 IgG3*11mm demonstrated significantly improved ADCP compared to IgG1*01, but had a similar affinity for FcγRIIA as IgG1*01 in the Fc-binding ELISA. The lack of concordance between these assays may be because the ADCP assay tested the antibody as a whole, including both Fab and Fc regions, while the Fc-binding ELISA tested only the Fc region's affinity to FcγRIIA. It is possible that the binding of the Fab region to an antigen induces conformational changes to the Fc region, improving the ability of CAP85-14.8 IgG3*11mm to induce ADCP (Janda and Casadevall, 2010). These results could be further investigated using surface plasmon resonance (SPR) to determine the binding affinity of FcγRIIA to free antibody, compared to the binding affinity of FcγRIIA to antigen-bound antibody (Kiyoshi *et al.*, 2015). Finally, while the FcγRIIA-binding ELISA performed used the high-affinity FcγRIIA H131 variant, the difference between variants was unlikely to influence the outcome of the results as the

order of strength of affinity between IgG1 and IgG3 is unchanged between FcγRIIA H131 and R131 (Caaveiro, Kiyoshi and Tsumoto, 2015).

There are a number of amino acid differences between IgG3 alleles that resulted in marginal differences in ADCP and FcγRIIA-binding (de Taeye *et al.*, 2020), but did not affect neutralization or IdeS cleavage. IgG3*11 differs from IgG3*01 by a single amino acid, Y296F which occurs in one of two subsites (amino acids 234-238 and 296-298) important for FcγR-binding (Caaveiro, Kiyoshi and Tsumoto, 2015). Neighbouring N297 is a glycosylation site that is conserved across all IgG antibodies (Krapp *et al.*, 2003). Águila *et al.* (2014) demonstrated that an aromatic amino acid (phenylalanine) two positions before an N-linked glycosylation site improved the glycosylation efficiency of the antithrombin protein. While Y296F is only one position before the N297 glycosylation site, and both phenylalanine and tyrosine are aromatic amino acids, this substitution could potentially be impacting the efficiency of glycosylation in the IgG3*11 antibody. The type of glycan at position 297 affects FcγR-binding (Shields *et al.*, 2001; Ferrara *et al.*, 2011; Washburn *et al.*, 2015). While all antibodies were produced in the same cell lines in this study, it is possible that they had slightly different glycosylation that may have impacted their function. Identifying the glycan at this position in different alleles using High-performance liquid chromatography would confirm this hypothesis (Wang *et al.*, 2019). The impact of different glycans at this position could be investigated using glycoengineering to test different isoforms, while ensuring that glycosylation of each subclass is homogenous (Mimura *et al.*, 2018).

IgG3*14 had marginally lower ADCP scores than IgG3*01 in both CAP255.C5 and CAP255.G3. IgG3*14 differs from IgG3*01 by three aa: P291L in the CH2, S384N and F436Y – both in the CH3. While none of these amino acids are associated with glycosylation or FcγR-binding sites, de Taeye *et al.* (2020) observed that P291L reduced the overall FcγRIIA-binding affinity in the context of antigen-bound antibody. They hypothesize that this mutation negatively affects the conformation of the CH2 region, although the mechanism underlying this shift has yet to be elucidated.

IgG3*17 differs from IgG3*01 by two amino acids in the CH1, and 5 amino acids in the CH3. One of these CH3 substitutions (R435H) has been shown to increase the half-life of IgG3*17 from approximately 7 days to 21 days (equivalent to that of IgG1 antibodies) through improved pH-dependent binding to FcRn (Stapleton *et al.*, 2011). While this was an exciting discovery for proponents of IgG3 antibodies as therapeutic mAbs, the K392N mutation also seen in IgG3*17 results in the loss of a glycan, which

subsequently destabilizes the CH3-CH3 interaction. This has been shown to negatively affect FcγRIIIA-binding, and ADCC (Rispens *et al.*, 2014; Richardson *et al.*, 2019). However, an unstable CH3-CH3 bond does not affect FcγRIIA-binding (de Taeye *et al.*, 2020). IgG3*17 was marginally less potent at ADCP than IgG3*01 most likely due to its shorter hinge.

The benefit of studying these antibodies was that they were isolated from HIV-infected individuals, and could be matched to that particular participant's *IGHG3* genotype. However, not all of the antibodies studied were isolated as IgG antibodies, resulting in some of these IgG3 antibodies being artificial. Synthetic antibodies have been shown to have limited Fab-Fc allostery (Al Qaraghuli *et al.*, 2020), which could potentially impact Fc effector function – in addition to hinge length, the antigen used (monomer, peptide or trimer) and the epitope targeted, and amino acid differences between subclasses and alleles.

5. Conclusion

The aim of this project was to determine the genetic variability of *IGHG3* in ten South African individuals from the CAPRISA cohort, and to assess its impact on Fc effector function and neutralization. *IGHG3* was sequenced in nine individuals, and fifteen alleles identified – five of which were novel, demonstrating a high level of genetic diversity in a small sample size. Uncovering genetic diversity within underrepresented populations can yield important insights into potential response to disease, as different alleles have altered effector functions (de Taeye, Rispens and Vidarsson, 2019; Khatri *et al.*, 2021). Despite amino acid substitutions and variation in hinge length, the functional differences between *IGHG3* alleles in this project were marginal, and likely influenced by the Fab and the antigen used. Altogether, IgG3 antibodies either maintained or improved neutralization and ADCP compared to IgG1 antibodies. These results were in line with the growing body of evidence suggesting that IgG3 antibodies should be considered for use as therapeutic antibodies. Ultimately, these data have provided insights into the functional impact of genetic diversity in an underrepresented population, and how this can be exploited to improve antibody function, with implications for passive immunization for HIV prevention.

References

Abdool Karim, S. S., Abdool Karim, Q. and Baxter, C. (2015) 'Antibodies for HIV prevention in young women', *Curr. Opin. HIV AIDS*, 10(3), pp. 183–189. doi: 10.1097/COH.0000000000000147.

Ackerman, M. E. *et al.* (2011) 'A robust, high-throughput assay to determine the phagocytic activity of clinical antibody samples', *J. Immunol. Methods*, 366(1–2), pp. 8–19. doi: 10.1016/j.jim.2010.12.016.

Ackerman, M. E. *et al.* (2013) 'Enhanced phagocytic activity of HIV-specific antibodies correlates with natural production of immunoglobulins with skewed affinity for FcyR2a and FcyR2b', *J. virol*, 87(10), pp. 5468–5476. doi: 10.1128/jvi.03403-12.

Ackerman, M. E. *et al.* (2016) 'Polyfunctional HIV-specific antibody responses are associated with spontaneous HIV control', *PLoS Pathog*, 12(1), pp. 1–14. doi: 10.1371/journal.ppat.1005315.

Ackerman, M. E. *et al.* (2018) 'Route of immunization defines multiple mechanisms of vaccine-mediated protection against SIV', *Nat Med*, 24(10), pp. 1590–1598. doi: 10.1038/s41591-018-0161-0.Route.

Ackerman, M. E. and Nimmerjahn, F. (2013) 'Antibody-dependent cellular cytotoxicity (ADCC)', in *Antibody Fc: Linking Adaptive and Innate Immunity*. First. Academic Press, pp. 1–27. doi: 10.1016/B978-0-12-394802-1.00001-7.

Águila, S. *et al.* (2014) 'Increased N-glycosylation efficiency by generation of an aromatic sequon on N135 of antithrombin', *PLoS ONE*, 9(12), pp. 1–14. doi: 10.1371/journal.pone.0114454.

Ahmed, A. A. *et al.* (2016) 'Structural characterization of GASDALIE Fc Bound to the activating Fc receptor FcyRIIIa', *J Struct Biol*, 194(1), pp. 78–89. doi: 10.1016/j.jsb.2016.02.001.Structural.

Altschul, S. F. *et al.* (1990) 'Basic local alignment search tool', *J. Mol. Bio.*, 215(3), pp. 403–410. doi: 10.1016/S0022-2836(05)80360-2.

Andrabi, R. *et al.* (2015) 'Identification of common features in prototype broadly neutralizing antibodies to HIV envelope V2 apex to facilitate vaccine design', *Immunity*, 43(5), pp. 959–973. doi: 10.1016/j.immuni.2015.10.014.

Awi, N. J. and Teow, S. (2018) 'Antibody-mediated therapy against HIV/AIDS: where are we standing now?', *J. Pathog.*, 2018, pp. 1–9. doi: 10.1155/2018/8724549.

Bar, K. J. *et al.* (2016) 'Effect of HIV antibody VRC01 on viral rebound after treatment interruption', *N. Engl. J. Med.*, 375(21), pp. 2037–2050. doi: 10.1056/nejmoa1608243.

Barouch, D. H. *et al.* (2013) 'Protective efficacy of a global HIV-1 mosaic vaccine against heterologous SHIV challenges in rhesus monkeys', *Cell*, 155(3), p. 531. doi: 10.1016/j.cell.2013.09.061.

Bentley, A. R., Callier, S. L. and Rotimi, C. N. (2020) 'Evaluating the promise of inclusion of African ancestry populations in genomics', *npj Genom. Med.*, 5(1), pp. 1–9. doi: 10.1038/s41525-019-0111-x.

Bettadapur, A., Miller, H. W. and Ralston, K. S. (2020) 'Biting off what can be chewed: trogocytosis in health, infection, and disease', *Infect. Immun.*, 88(7). doi: 10.1128/IAI.00930-19.

Boesch, A. W. *et al.* (2017) 'IgG Fc variant cross-reactivity between human and rhesus macaque FcγRs', *mAbs*, 9(3), pp. 455–465. doi: 10.1080/19420862.2016.1274845.

Bolt, S. *et al.* (1993) 'The generation of a humanized, non-mitogenic CD3 monoclonal antibody which retains in vitro immunosuppressive properties', *Eur. J. Immunol.*, 23(2), pp. 403–411. doi: 10.1002/eji.1830230216.

Bournazos, S., Klein, F., *et al.* (2014) 'Broadly neutralizing anti-HIV-1 antibodies require Fc effector functions for in vivo activity', *Cell*, 158, pp. 1243–1253. doi: 10.1016/j.cell.2014.08.023.

Bournazos, S., Chow, S. K., *et al.* (2014) 'Human IgG Fc domain engineering enhances antitoxin neutralizing antibody activity', *J. Clin. Investig.*, 124(2), pp. 725–729. doi: 10.1172/JCI72676.

Bruhns, P. *et al.* (2009) 'Specificity and affinity of human Fcy receptors and their polymorphic variants for human IgG subclasses', *Blood*, 113(16), pp. 3716–3726. doi: 10.1182/blood-2008-09-179754.The.

Bruhns, P. and Jönsson, F. (2015) 'Mouse and human FcR effector functions', *Immunol. Rev*, 268(1), pp. 25–51. doi: 10.1111/imr.12350.

Burton, D. R. (2019) 'Advancing an HIV vaccine; advancing vaccinology', *Nat. Rev. Immunol.*, 19(2), pp. 77–78. doi: 10.1038/s41577-018-0103-6.

Caaveiro, J. M. M., Kiyoshi, M. and Tsumoto, K. (2015) 'Structural analysis of Fc/FcγR

complexes: A blueprint for antibody design', *Immunol. Rev*, 268(1), pp. 201–221. doi: 10.1111/imr.12365.

Calonga-Solís, V. *et al.* (2019) 'Unveiling the diversity of Immunoglobulin Heavy Constant Gamma (IGHG) gene segments in Brazilian populations reveals 28 novel alleles and evidence of gene conversion and natural selection', *Front. Immunol.*, 10. doi: 10.3389/fimmu.2019.01161.

Camacho, C. *et al.* (2009) 'BLAST+: architecture and applications', *BMC Bioinform.*, 10, pp. 1–9. doi: 10.1186/1471-2105-10-421.

Campbell, M. C. and Tishkoff, S. A. (2008) 'African genetic diversity: implications for human demographic history, modern human origins, and complex disease mapping', *Annu. Rev. Genom. Hum. Genet.*, 9, pp. 403–433. doi: 10.1146/annurev.genom.9.081307.164258.

Caskey, M. *et al.* (2015) 'Viraemia suppressed in HIV-1-infected humans by broadly neutralizing antibody 3BNC117', *Nature*, 522(7557), pp. 487–491. doi: 10.1038/nature14411.

Charif, D. and Lobry, J. (2007) *SeqinR 1.0-2: a contributed package to the R project for statistical computing devoted to biological sequences retrieval and analysis*, *Structural Approaches to Sequence Evolution: Molecules, Networks, Populations*. Edited by U. Bastolla et al. New York: Springer Verlag.

Chu, T. H. *et al.* (2020) 'Hinge length contributes to the phagocytic activity of HIV-specific IgG1 and IgG3 antibodies', *PLoS Pathog.*, 16(2), pp. 1–25. doi: 10.1371/journal.ppat.1008083.

Chu, T. H., Patz, E. F. and Ackerman, M. E. (2021) 'Coming together at the hinges: therapeutic prospects of IgG3', *mAbs*, 13(1). doi: 10.1080/19420862.2021.1882028.

Chung, A. W. *et al.* (2011) 'Activation of NK cells by ADCC antibodies and HIV disease progression', *J. Acquir. Immune Defic. Syndr.*, 58(2), pp. 127–131. doi: 10.1097/QAI.0b013e31822c62b9.

Chung, A. W. *et al.* (2014) 'Polyfunctional Fc-effector profiles mediated by IgG subclass selection distinguish RV144 and VAX003 vaccines', *Sci. Transl. Med.*, 6(228), pp. 1–11. doi: 10.1126/scitranslmed.3007736.

Chung, A. W. *et al.* (2015) 'Dissecting polyclonal vaccine-induced humoral immunity against HIV using systems serology', *Cell*, 163(4), pp. 988–998. doi:

10.1016/j.cell.2015.10.027.

Chung, A. W. *et al.* (2018) 'Viral control in chronic HIV-1 subtype C infection is associated with enrichment of p24 IgG1 with Fc effector activity', *AIDS*, 32(10), pp. 1207–1217. doi: 10.1097/QAD.0000000000001812.Viral.

ClinicalTrials.gov (2018) *A phase I trial to evaluate the safety and immunogenicity of eOD-GT8 60mer vaccine, adjuvanted*. Available at: https://clinicaltrials.gov/ct2/show/NCT03547245?term=NCT03547245&draw=2&rank=1 (Accessed: 16 February 2021).

Corey, L. *et al.* (2021) 'Two randomized trials of neutralizing antibodies to prevent HIV-1 acquisition', *N. Engl. J. Med.*, 384, pp. 1003–1014. doi: 10.1056/NEJMoa2031738.

Crowley, A. R. and Ackerman, M. E. (2019) 'Mind the gap: How Interspecies Variability in IgG and Its Receptors May Complicate Comparisons of Human and Non-human Primate Effector Function', *Frontiers in Immunology*, 10(APR), pp. 1–19. doi: 10.3389/fimmu.2019.00697.

Dambrun, M. *et al.* (2017) 'Human immunoglobulin heavy gamma chain polymorphisms: molecular confirmation of proteomic assessment', *Mol. Cell. Proteom.*, 16(5), pp. 824–839. doi: 10.1074/mcp.M116.064733.

Damelang, T. *et al.* (2019) 'Role of IgG3 in infectious diseases', *Trends Immunol.*, 40(3), pp. 197–211. doi: 10.1016/j.it.2019.01.005.

Dard, P. *et al.* (2001) 'DNA sequence variability of IGHG3 alleles associated to the main G3m haplotypes in human populations', *Eur. J. Hum. Genet.*, 9(10), pp. 765–772. doi: 10.1038/sj.ejhg.5200700.

Deveuve, Q. *et al.* (2020) 'The proteolytic cleavage of therapeutic monoclonal antibody hinge region: more than a matter of subclass', *Front. Immunol.*, 11, p. 168. doi: 10.3389/fimmu.2020.00168.

Doria-rose, N. A. *et al.* (2014) 'Developmental pathway for potent V1V2-directed HIV-neutralizing antibodies', *Nature*, 509(7498), pp. 55–62. doi: 10.1038/nature13036.Developmental.

Doria-Rose, N. A. *et al.* (2016) 'A new member of the V1V2-directed CAP256-VRC26 lineage that shows increased breadth and exceptional potency', *J. Virol.*, 90(1), pp. 76–91. doi: 10.1128/jvi.01791-15.

Dunnick, W. *et al.* (2009) 'Switch recombination and somatic hypermutation are

controlled by the heavy chain 3′ enhancer region', *J. Exp. Med.*, 206(12), pp. 2613–2623. doi: 10.1084/jem.20091280.

Dunston, G. M. *et al.* (2019) 'Assembly of a pan-genome from deep sequencing of 910 humans of African descent', *Nat. Genet.*, 51(1), pp. 30–35. doi: 10.1038/s41588-018-0273-y.

van Eeden, C. *et al.* (2018) 'V2-Directed vaccine-like antibodies from HIV-1 infection identify an additional K169-binding light chain motif with broad ADCC activity', *Cell Rep.*, 25(11), pp. 3123-3135.e6. doi: 10.1016/j.celrep.2018.11.058.

Fan, S. *et al.* (2019) 'African evolutionary history inferred from whole genome sequence data of 44 indigenous African populations', *Genome Biol.*, 20(1), pp. 1–14. doi: 10.1186/s13059-019-1821-1.

Fan, X. *et al.* (2012) 'A single proteolytic cleavage within the lower hinge of trastuzumab reduces immune effector function and in vivo efficacy', *Breast Cancer Res.*, 14(4), p. R116. doi: 10.1186/bcr3240.

Ferrara, C. *et al.* (2011) 'Unique carbohydrate-carbohydrate interactions are required for high affinity binding between FcγRIII and antibodies lacking core fucose', *Proc. Natl. Acad. Sci. U.S.A.*, 108(31), pp. 12669–12674. doi: 10.1073/pnas.1108455108.

Forthal, D. N. *et al.* (2007) 'FcγRIIa genotype predicts progression of HIV infection', *J. Immunol. Res.*, 179(11), pp. 7916–7923. doi: 10.4049/jimmunol.179.11.7916.

Forthal, D. N., Landucci, G. and Daar, E. S. (2001) 'Antibody from patients with Acute Human Immunodeficiency Virus (HIV) infection inhibits primary strains of HIV type 1 in the presence of natural-killer effector cells', *J. Virol.*, 75(15), pp. 6953–6961. doi: 10.1128/JVI.75.15.6953.

Gautam, R. *et al.* (2018) 'A single injection of crystallizable fragment domain-modified antibodies elicits durable protection from SHIV infection', *Nat. Med.*, 24(5), pp. 610–616. doi: 10.1038/s41591-018-0001-2.

Giudicelli, V., Chaume, D. and Lefranc, M. (2004) 'IMGT/GENE-DB: A comprehensive database for human and mouse immunoglobulin and T cell receptor genes', *Nucleic Acids Res.*, 33, pp. 256–261. doi: 10.1093/nar/gki010.

Giuntini, S. and Granoff, D. M. (2016) 'Different protection capabilities against meningococci depending on the target antigen and epitope specificity', *Clin. Vaccine Immunol.*, 23(8), pp. 698–706. doi: 10.1128/CVI.00193-16.Editor.

Goldberg, B. S. and Ackerman, M. E. (2020) 'Antibody-mediated complement activation in pathology and protection', *Immunol. Cell Biol.*, 98(4), pp. 305–317. doi: 10.1111/imcb.12324.

Gray, E. S. *et al.* (2007) 'Neutralizing antibody responses in acute Human Immunodeficiency Tirus type 1 subtype C infection', *J. Virol.*, 81(12), pp. 6187–6196. doi: 10.1128/jvi.00239-07.

Gray, E. S. *et al.* (2011) 'The neutralization breadth of HIV-1 develops incrementally over four years and is associated with CD4+T cell decline and high viral load during acute infection', *J. Virol.*, 85(10), pp. 4828–4840. doi: 10.1128/JVI.00198-11.

Gutzeit, C., Chen, K. and Cerutti, A. (2018) 'The enigmatic function of IgD: some answers at last', *Eur. J. Immunol.*, 48(7), pp. 1101–1113. doi: 10.1002/eji.201646547.

Halper-stromberg, A. *et al.* (2014) 'Broadly neutralizing antibodies and viral inducers decrease rebound from HIV-1 latent reservoirs in humanized mice', *Cell*, 158(5), pp. 989–999. doi: 10.1016/j.cell.2014.07.043.

Hannon, G. J. (2010) 'FASTX-Toolkit'.

Havenar-daughton, C. *et al.* (2018) 'The human naive B cell repertoire contains distinct subclasses for a germline-targeting HIV-1 vaccine immunogen', *Sci. Transl. Med.*, 10. doi: 10.1126/scitranslmed.aat0381.

Haynes, B. F. *et al.* (2012) 'Immune-correlates analysis of an HIV-1 vaccine efficacy trial', *N Engl J Med*, 366(14), pp. 1275–1286. doi: 10.1056/NEJMoa1113425.

Hessell, A. J. *et al.* (2007) 'Fc receptor but not complement binding is important in antibody protection against HIV', *Nature*, 449(7158), pp. 101–104. doi: 10.1038/nature06106.

Hoffmann, C. and Rockstroh, J. (2011) *HIV*. Available at: https://www.hivbook.com/category/part-2-antiretroviral-therapy/ (Accessed: 6 November 2020).

Hommelsheim, C. M. *et al.* (2014) 'PCR amplification of repetitive DNA: A limitation to genome editing technologies and many other applications', *Sci. Rep.*, 4(5052), pp. 1–13. doi: 10.1038/srep05052.

Hsiao, H. *et al.* (2018) 'Proteolytic single hinge cleavage of pertuzumab impairs its Fc effector function and antitumor activity in vitro and in vivo', *Breast Cancer Res.*, 20(1), pp. 1–12. doi: 10.1186/s13058-018-0972-4.

Huang, D. *et al.* (2020) ‘B cells expressing authentic naive human VRC01-class BCRs can be recruited to germinal centers and affinity mature in multiple independent mouse models’, *Proc. Natl. Acad. Sci. U.S.A.*, 117(37). doi: 10.1073/pnas.2004489117.

Janda, A. and Casadevall, A. (2010) ‘Circular Dichroism Reveals Evidence of Coupling Between Immunoglobulin Constant and Variable Region Secondary Structure’, *Mol Immunol*, 47(7–8), pp. 1421–1425. doi: 10.1038/jid.2014.371.

Jardine, J. *et al.* (2013) ‘Rational HIV immunogen design to target specific germline B cell receptors’, *Science*, 340(6133), pp. 711–716. doi: 10.1126/science.1234150.

Jennewein, M. F. and Alter, G. (2017) ‘The immunoregulatory roles of antibody glycosylation’, *Trends Immunol.*, 38(5), pp. 358–372. doi: 10.1016/j.it.2017.02.004.

Joly, E. and Hudrisier, D. (2003) ‘What is trogocytosis and what is its purpose?’, *Nat. Immunol.*, 4(9), p. 5998. doi: 10.1038/ni0903-815.

Kaplon, H. and Reichert, J. M. (2019) ‘Antibodies to watch in 2019’, *mAbs*, 11(2), pp. 219–238. doi: 10.1080/19420862.2018.1556465.

Khatri, I. *et al.* (2021) ‘Population matched (pm) germline allelic variants of immunoglobulin (IG) loci: Relevance in infectious diseases and vaccination studies in human populations’, *Genes Immun.*, 22, pp. 172–186. doi: 10.1101/2020.04.09.033530.

Kieleczawa, J. (2006) ‘Fundamentals of sequencing of difficult templates - an overview’, *J. Biomol. Tech.*, 17(3), pp. 207–217. Available at: https://www.ncbi.nlm.nih.gov/pmc/articles/PMC2291785/.

Kitaura, K. *et al.* (2017) ‘Different somatic hypermutation levels among antibody subclasses disclosed by a new next-generation sequencing-based antibody repertoire analysis’, *Front. Immunol.*, 8, pp. 1–11. doi: 10.3389/fimmu.2017.00389.

Kitchin, D. (2019) *CAP255.C5 and CAP255.G3 Neutralization Data*.

Kiyoshi, M. *et al.* (2015) ‘Structural basis for binding of human IgG1 to its high-affinity human receptor FcγRI’, *Nat. Commun.* Nature Publishing Group, 6, pp. 4–6. doi: 10.1038/ncomms7866.

Kong, R. *et al.* (2015) ‘Improving neutralization potency and breadth by combining broadly reactive HIV-1 antibodies targeting major neutralization epitopes’, *J. Virol.*, 89(5), pp. 2659–2671. doi: 10.1128/jvi.03136-14.

Krapp, S. *et al.* (2003) ‘Structural analysis of human IgG-Fc glycoforms reveals a

correlation between glycosylation and structural integrity', *J. Mol. Biol.*, 325(5), pp. 979–989. doi: 10.1016/S0022-2836(02)01250-0.

Krebs, S. J. *et al.* (2019) 'Longitudinal analysis reveals early development of three MPER-directed neutralizing antibody lineages from an HIV-1-infected individual', *Immunity*, 50(3), pp. 677-691.e13. doi: 10.1016/j.immuni.2019.02.008.

Kretschmer, A. *et al.* (2017) 'Antibody isotypes for tumor immunotherapy', *Transfus. Med. Hemother.*, 44(5), pp. 320–326. doi: 10.1159/000479240.

Kwong, P. D. and Mascola, J. R. (2018) 'HIV-1 vaccines based on antibody identification, B cell ontogeny, and epitope structure', *Immunity*, 48(5), pp. 855–871. doi: 10.1016/j.immuni.2018.04.029.

Lambotte, O. *et al.* (2009) 'Heterogeneous neutralizing antibody and antibody-dependent cell cytotoxicity responses in HIV-1 elite controllers', *AIDS*, 23(8), pp. 897–906. doi: 10.1097/QAD.0b013e328329f97d.

Larsson, A. (2014) 'AliView: a fast and lightweight alignment editor for large data sets', pp. 3276–3278. Available at: http://dx.doi.org/10.1093/bioinformatics/btu531.

Lazar, G. A. *et al.* (2006) 'Engineered antibody Fc variants with enhanced effector function', *Proc. Natl. Acad. Sci. U.S.A.*, 103(11), pp. 4005–4010. doi: 10.1073/pnas.0508123103.

Lefranc, M. (2000) 'Nomenclature of the human immunoglobulin genes', *Curr. Protoc. Immunol.*, pp. 1–37. doi: 10.1002/0471142735.ima01ps40.

Li, M. *et al.* (2005) 'Human Immunodeficiency Virus type 1 env clones from acute and early subtype B infections for standardized assessments of vaccine-elicited neutralizing antibodies', *J. Virol.*, 79(16), pp. 10108–10125. doi: 10.1128/jvi.79.16.10108-10125.2005.

Liao, H. *et al.* (2009) 'High-throughput isolation of immunoglobulin genes from single human B cells and expression as monoclonal antibodies', *J. Virol. Methods.*, 158(1), pp. 1–7. doi: 10.1016/j.jviromet.2009.02.014.High-throughput.

Linhart, C. and Shamir, R. (2005) 'The degenerate primer design problem: Theory and applications', *Comput. Biol.*, 12(4), pp. 431–456. doi: 10.1089/cmb.2005.12.431.

Lofano, G. *et al.* (2018) 'Antigen-specific antibody Fc glycosylation enhances humoral immunity via the recruitment of complement', *Sci. Immunol.*, 3(26), pp. 24–27. doi: 10.1126/sciimmunol.aat7796.

van Loggerenberg, F. *et al.* (2008) 'Establishing a cohort at high risk of HIV infection in South Africa: Challenges and experiences of the CAPRISA 002 acute infection study', *PLoS ONE*, 3(4), pp. 1–8. doi: 10.1371/journal.pone.0001954.

Lu, C. *et al.* (2016) 'Enhanced clearance of HIV-1-infected cells by broadly neutralizing antibodies against HIV-1 in vivo', *Science*, 352(6288), pp. 1001–1005. doi: 10.1126/science.aaf1279.

Lynch, R. M. *et al.* (2015) 'Virologic effects of broadly neutralizing antibody VRC01 administration during chronic HIV-1 infection', *Sci. Transl. Med.*, 7(319). doi: 10.1126/scitranslmed.aad5752.

Mahomed, S. *et al.* (2021) 'Clinical trials of broadly neutralizing monoclonal antibodies for HIV prevention: A Review', *J. Infect. Dis.*, 223(3), pp. 370–380. doi: 10.1093/infdis/jiaa377.

Marasco, W. A. and Sui, J. (2007) 'The growth and potential of human antiviral monoclonal antibody therapeutics', *Nat. Biotechnol.*, 25(12), pp. 1421–1434. doi: 10.1038/nbt1363.

Martin, M. (2011) 'Cutadapt removes adaptor sequences from high-throughput sequencing reads', *EMBnet*, 7(10), pp. 2803–2809. doi: 10.14806/ej.17.1.200.

McMichael, A. J. *et al.* (2010) 'The immune response during acute HIV-1 infection: Clues for vaccine development', *Nat. Rev. Immunol.*, 10(1), pp. 11–23. doi: 10.1038/nri2674.

Michaelsen, T. E. *et al.* (1992) 'Antibody dependent cell-mediated cytotoxicity induced by chimeric mouse-human IgG subclasses and IgG3 antibodies with altered hinge region', *Mol. Immunol.*, 29(3), pp. 319–326. doi: 10.1016/0161-5890(92)90018-S.

Mimura, Y. *et al.* (2018) 'Glycosylation engineering of therapeutic IgG antibodies: challenges for the safety, functionality and efficacy', *Protein Cell*. Higher Education Press, 9(1), pp. 47–62. doi: 10.1007/s13238-017-0433-3.

Mkaddem, S. B., Benhamou, M. and Monteiro, R. C. (2019) 'Understanding Fc receptor involvement in inflammatory diseases: From mechanisms to new therapeutic tools', *Front. Immunol.*, 10. doi: 10.3389/fimmu.2019.00811.

Moens, L. and Tangye, S. G. (2014) 'Cytokine-mediated regulation of plasma cell generation: IL-21 takes center stage', *Front. Immunol.*, 5, pp. 1–13. doi: 10.3389/fimmu.2014.00065.

Moldt, B. *et al.* (2012) 'A nonfucosylated variant of the anti-HIV-1 monoclonal antibody b12 has enhanced FcyRIIIA-mediated antiviral activity in vitro but does not improve protection against mucosal SHIV challenge in macaques', *J. Virol.*, 86(11), pp. 6189–6196. doi: 10.1128/jvi.00491-12.

Molinos-Albert, L. M. *et al.* (2017) 'Immunologic insights on the membrane proximal external region: A major human immunodeficiency virus type-1 vaccine target', *Front. Immunol.*, 8, pp. 1–12. doi: 10.3389/fimmu.2017.01154.

Montefiori, D. C. (2004) 'Evaluating neutralizing antibodies against HIV, SIV, and SHIV in luciferase reporter gene assays', *Curr. Protoc. Immunol.*, 64, pp. 1–17. doi: 10.1002/0471142735.im1211s64.

Moore, P. L. *et al.* (2009) 'Limited neutralizing antibody specificities drive neutralization escape in early HIV-1 subtype C infection', *PLoS Pathog.*, 5(9). doi: 10.1371/journal.ppat.1000598.

Morris, L. *et al.* (2011) 'Isolation of a human anti-HIV gp41 membrane proximal region neutralizing antibody by antigen-specific single B cell sorting', *PLoS ONE*, 6(9). doi: 10.1371/journal.pone.0023532.

Moyo-Gwete, T. (2021) *The mechanism behind the neutralization potency of HIV neutralizing antibodies with identical variable regions but different isotypes*.

Moyo, T., Kitchin, D. and Moore, P. L. (2020) 'Targeting the N332-supersite of the HIV-1 envelope for vaccine design', *Expert Opin. Ther. Targets*, 24(6), pp. 499–509. doi: 10.1080/14728222.2020.1752183.

Murphy, K. and Weaver, C. (2017) *Janeway's Immunobiology*. 9th edn. New York: Garland Science.

Musich, T. *et al.* (2017) 'Monoclonal antibodies specific for the V2, V3, CD4-binding site, and gp41 of HIV-1 mediate phagocytosis in a dose-dependent manner', *J. Virol.*, 91(8), pp. 1–13. doi: 10.1128/JVI.02325-16.

Nakano, M. *et al.* (2003) 'Single-molecule PCR using water-in-oil emulsion', *J. Biotechnol.*, 102(2), pp. 117–124. doi: 10.1016/S0168-1656(03)00023-3.

Oxelius, V. A. and Pandey, J. P. (2013) 'Human immunoglobulin constant heavy G chain (IGHG) (Fcy) (GM) genes, defining innate variants of IgG molecules and B cells, have impact on disease and therapy', *J. Clin. Immunol.*, 149, pp. 475–486. doi: 10.1016/j.clim.2013.10.003.

Patel, K. R., Roberts, J. T. and Barb, A. W. (2019) ‘Multiple variables at the leukocyte cell surface impact Fcy receptor-dependent mechanisms’, *Front. Immunol.*, 10, p. 223. doi: 10.3389/fimmu.2019.00223.

Perez, L. G. *et al.* (2017) ‘V1V2-specific complement activating serum IgG as a correlate of reduced HIV-1 infection risk in RV144’, *PLoS ONE*, 12(7), pp. 1–17. doi: 10.1371/journal.pone.0180720.

Pincetic, A. *et al.* (2014) ‘Type-I and Type-II Fc receptors regulate innate and adaptive immunity’, *Nat. Immunol.*, 15(8), pp. 707–716. doi: 10.1038/ni.2939.Type-I.

Pollara, J. *et al.* (2021) ‘Functional homology for antibody-dependent phagocytosis across humans and rhesus macaques’, *Front. Immunol.*, 12, pp. 1–17. doi: 10.3389/fimmu.2021.678511.

Popejoy, A. B. and Fullerton, S. M. (2016) ‘Genomics is failing on diversity’, *Nature*, 538(7624), pp. 161–164. doi: 10.1109/EMBC.2016.7590696.Upper.

Al Qaraghuli, M. M. *et al.* (2020) ‘Antibody-protein binding and conformational changes: identifying allosteric signalling pathways to engineer a better effector response’, *Sci. Rep.*, 10(1), pp. 1–10. doi: 10.1038/s41598-020-70680-0.

Raghavan, M. and Bjorkman, P. J. (1996) ‘Fc receptors and their interactions with immunoglobulins’, *Annu. Rev. Cell Dev. Biol.*, 12, pp. 181–220. doi: 10.1146/annurev.cellbio.12.1.181.

Rerks-Ngarm, S. *et al.* (2009) ‘Vaccination with ALVAC and AIDSVAX to prevent HIV-1 infection in Thailand’, *New Eng. J. Med.*, 361(23), pp. 2163–2173. doi: 10.1056/NEJMoa0904327.

Retshabile, G. *et al.* (2018) ‘Whole-exome sequencing reveals uncaptured variation and distinct ancestry in the Southern African population of Botswana’, *Am. J. Hum. Genet.*, 102(5), pp. 731–743. doi: 10.1016/j.ajhg.2018.03.010.

Richards, D. M. and Endres, R. G. (2014) ‘The mechanism of phagocytosis: Two stages of engulfment’, *Biophys. J.*, 107(7), pp. 1542–1553. doi: 10.1016/j.bpj.2014.07.070.

Richardson, S. I., Chung, A. W., *et al.* (2018) ‘HIV-specific Fc effector function early in infection predicts the development of broadly neutralizing antibodies’, *PLoS Pathog.*, 14(4), pp. 1–25. doi: 10.1371/journal.ppat.1006987.

Richardson, S. I., Crowther, C., *et al.* (2018) ‘Measuring the ability of HIV-specific

antibodies to mediate trogocytosis', *J. Immunol. Methods*, 463, pp. 71–83. doi: 10.1016/j.jim.2018.09.009.

Richardson, S. I. *et al.* (2019) 'IgG3 enhances neutralization potency and Fc effector function of an HIV V2-specific broadly neutralizing antibody', *PLoS Pathog.*, 15(12). doi: 10.1371/journal.ppat.1008064.

Richardson, S. I. *et al.* (2021) 'HIV broadly neutralizing antibodies expressed as IgG3 preserve neutralization potency and show improved Fc effector function', *Front. Immunol.* doi: 10.3389/fimmu.2021.733958.

Rispens, T. *et al.* (2014) 'Dynamics of inter-heavy chain interactions in human immunoglobulin G (IgG) subclasses studied by kinetic fab arm exchange', *J. Biol. Chem*, 289(9), pp. 6098–6109. doi: 10.1074/jbc.M113.541813.

Rodriguez, O. L. *et al.* (2020) 'A novel framework for characterizing genomic haplotype diversity in the human immunoglobulin heavy chain locus', *Front. Immunol.*, 11, pp. 1–16. doi: 10.3389/fimmu.2020.02136.

Rognes, T. *et al.* (2016) 'VSEARCH: A versatile open source tool for metagenomics', *PeerJ*, 2016(10), pp. 1–22. doi: 10.7717/peerj.2584.

Ruiz, M. J. *et al.* (2017) 'Evaluation of different parameters of humoral and cellular immune responses in HIV serodiscordant heterosexual couples: humoral response potentially implicated in modulating transmission rates', *EBioMedicine*, 26, pp. 25–37. doi: 10.1016/j.ebiom.2017.11.001.

Sacks, D. (2019) *CAP85-14.8 Neutralization Data*.

Saito, S. *et al.* (2019) 'A stable engineered human IgG3 antibody with decreased aggregation during antibody expression and low pH stress', *Protein Sci.*, 28(5), pp. 900–909. doi: 10.1002/pro.3598.

Sanders, R. W. *et al.* (2013) 'A next-generation cleaved, soluble HIV-1 Env trimer, BG505 SOSIP.664 gp140, expresses multiple epitopes for broadly neutralizing but not non-neutralizing antibodies', *PLoS Pathog.*, 9(9). doi: 10.1371/journal.ppat.1003618.

Santra, S. *et al.* (2015) 'Human non-neutralizing HIV-1 envelope monoclonal antibodies limit the number of founder viruses during SHIV mucosal infection in rhesus macaques', *PLoS Pathog.*, 11(8), pp. 1–38. doi: 10.1371/journal.ppat.1005042.

Saphire, E. O. *et al.* (2001) 'Crystal structure of a neutralizing human IgG against HIV-1: A template for vaccine design', *Science*, 293(5532), pp. 1155–1159. doi:

10.1126/science.1061692.

Saunders, K. O. *et al.* (2019) ‘Targeted selection of HIV-specific antibody mutations by engineering B cell maturation’, *Science*, 1215(366). doi: 10.1126/science.aay7199.

Scanlan, C. N. *et al.* (2002) ‘The carbohydrate epitope of the neutralizing anti-HIV-1 antibody 2G12’, *Adv. Exp. Med. Biol.*, 535(14), pp. 205–218. doi: 10.1007/978-1-4615-0065-0_13.

Scheepers, C. *et al.* (2015) ‘Ability to develop broadly neutralizing HIV-1 antibodies is not restricted by the germline Ig gene repertoire’, *J. Immunol. Res.*, 194(9), pp. 4371–4378. doi: 10.4049/jimmunol.1500118.

Scheepers, C. *et al.* (2020) ‘Antibody isotype switching as a mechanism to counter HIV neutralization escape’, *Cell Rep.*, 33(8), p. 108430. doi: 10.1016/j.celrep.2020.108430.

Scheid, J. F. *et al.* (2012) ‘Sequence and structural convergence of broad and potent HIV antibodies that mimic CD4 binding’, *Science*, 333(6049), pp. 1633–1637. doi: 10.1126/science.1207227.Sequence.

Scheid, J. F. *et al.* (2016) ‘HIV-1 antibody 3BNC117 suppresses viral rebound in humans during treatment interruption’, *Nature*, 535(7613), pp. 556–560. doi: 10.1038/nature18929.

Schief, W. R., Jardine, J. and Menis, S. (2021) ‘eOD-GT8 60mer, a self-assembling nanoparticle of engineered HIV Env proteins linked to a spherical protein structure.’, in *Understanding the results from IAVI G001 presented at HIV R4P // Virtual 2021*.

Schoofs, T. *et al.* (2019) ‘Broad and potent neutralizing antibodies recognize the silent face of the HIV envelope’, *Immunity*, 50(6), pp. 1513-1529.e9. doi: 10.1016/j.immuni.2019.04.014.

Shapiro, M. B. *et al.* (2020) ‘Single-dose bNAb cocktail or abbreviated ART post-exposure regimens achieve tight SHIV control without adaptive immunity’, *Nat. Commun.*, 11(1), pp. 1–13. doi: 10.1038/s41467-019-13972-y.

Shields, R. L. *et al.* (2001) ‘High resolution mapping of the binding site on human IgG1 for FcγRI, FcγRII, FcγRIII, and FcRn and design of IgG1 variants with improved binding to the FcγR’, *J. Biol. Chem.*, 276(9), pp. 6591–6604. doi: 10.1074/jbc.M009483200.

Shingai, M. *et al.* (2013) ‘Antibody mediated immunotherapy of macaques chronically infected with SHIV suppresses viremia’, *Nature*, 503(7475), pp. 277–280. doi: 10.1038/nature12746.ANTIBODY.

Sips, M. *et al.* (2016) ‘Fc receptor-mediated phagocytosis in tissues as a potent mechanism for preventive and therapeutic HIV vaccine strategies’, *Mucosal Immunol.*, 9(6), pp. 1584–1595. doi: 10.1038/mi.2016.12.

Slatko, B. E., Gardner, A. F. and Ausubel, F. M. (2018) ‘Overview of next generation sequencing technologies’, *Curr. Protoc. Mol. Biol.*, 122(1), pp. 1–15. doi: 10.1002/cpmb.59.Overview.

Smith, K. *et al.* (2009) ‘Rapid generation of fully human monoclonal antibodies specific to a vaccinating antigen’, *Nat. Protoc.*, 4(3), pp. 372–384. doi: 10.1038/nprot.2009.3.Rapid.

Smith, S. A. *et al.* (2019) ‘VH1-69 utilizing antibodies are capable of mediating non-neutralizing Fc-mediated effector functions against the transmitted/founder gp120’, *Front. Immunol.*, 10, pp. 1–19. doi: 10.3389/fimmu.2018.03163.

Smyth, R. P. *et al.* (2010) ‘Reducing chimera formation during PCR amplification to ensure accurate genotyping’, *Gene*, 469(1–2), pp. 45–51. doi: 10.1016/j.gene.2010.08.009.

Sok, D. *et al.* (2016) ‘Priming HIV-1 broadly neutralizing antibody precursors in human Ig loci transgenic mice’, *Science*, 353(6307), pp. 1557–1560. doi: 10.1126/science.aah3945.

Stamatatos, L. *et al.* (2009) ‘Neutralizing antibodies generated during natural HIV-1 infection: Good news for an HIV-1 vaccine?’, *Nat. Med.*, 15(8), pp. 866–870. doi: 10.1038/nm.1949.

Stapleton, N. M. *et al.* (2011) ‘Competition for FcRn-mediated transport gives rise to short half-life of human IgG3 and offers therapeutic potential’, *Nat. Commun.*, 2(1). doi: 10.1038/ncomms1608.

Stavnezer, J. and Schrader, C. E. (2014) ‘IgH chain class switch recombination: mechanism and regulation’, *J. Immunol. Res.*, 193(11), pp. 5370–5378. doi: 10.4049/jimmunol.1401849.

Steichen, J. M. *et al.* (2019) ‘A generalized HIV vaccine design strategy for priming of broadly neutralizing antibody responses’, *Science*, 366(6470). doi: 10.1126/science.aax4380.A.

de Taeye, S. W. *et al.* (2020) ‘FcγR binding and ADCC activity of human IgG allotypes’, *Front. Immunol.*, 11, pp. 1–16. doi: 10.3389/fimmu.2020.00740.

de Taeye, S. W., Rispens, T. and Vidarsson, G. (2019) ‘The ligands for human IgG and their effector functions’, *Antibodies*, 8(2), p. 30. doi: 10.3390/antib8020030.

Tay, M. Z. *et al.* (2016) ‘Antibody-mediated internalization of infectious HIV-1 virions differs among antibody isotypes and subclasses’, *PLoS Pathog.*, 12(8), pp. 1–25. doi: 10.1371/journal.ppat.1005817.

Tay, M. Z., Wiehe, K. and Pollara, J. (2019) ‘Antibody-dependent cellular phagocytosis in antiviral immune responses’, *Front. Immunol.*, 10, pp. 1–18. doi: 10.3389/fimmu.2019.00332.

Taylor, M. E. and Drickamer, K. (2003) *Introduction to glycobiology*. Third. Oxford University Press.

Thommesen, J. E. *et al.* (2000) ‘Lysine 322 in the human IgG3 CH2 domain is crucial for antibody dependent complement activation’, *Mol. Immunol.*, 37(16), pp. 995–1004. doi: 10.1016/S0161-5890(01)00010-4.

Tomaras, G. D. *et al.* (2008) ‘Initial B-cell responses to transmitted Human Immunodeficiency Virus type 1: virion-binding immunoglobulin M (IgM) and IgG antibodies followed by plasma anti-gp41 antibodies with ineffective control of initial viremia’, *J. Virol.*, 82(24), pp. 12449–12463. doi: 10.1128/jvi.01708-08.

Tsuchiya, S. *et al.* (1980) ‘Establishment and characterization of a human acute monocytic leukemia cell line (THP-1)’, *Int. J. Cancer Res.*, 176(2), pp. 171–176. doi: 10.1002/ijc.2910260208.

Tudor, D. *et al.* (2012) ‘Isotype modulates epitope specificity, affinity, and antiviral activities of anti-HIV-1 human broadly neutralizing 2F5 antibody’, *Proc. Natl. Acad. Sci. U.S.A.*, 109(31), pp. 12680–12685. doi: 10.1073/pnas.1200024109.

UNAIDS (2021a) *AIDSinfo: New HIV infections - young people (15-24)*. Available at: https://aidsinfo.unaids.org/ (Accessed: 21 April 2021).

UNAIDS (2021b) *South Africa*. Available at: https://www.unaids.org/en/regionscountries/countries/southafrica (Accessed: 21 April 2021).

Valenzuela, N. M., Hickey, M. J. and Reed, E. F. (2016) ‘Antibody subclass repertoire and graft outcome following solid organ transplantation’, *Front. Immunol.*, 7. doi: 10.3389/fimmu.2016.00433.

Vidarsson, G., Dekkers, G. and Rispens, T. (2014) ‘IgG subclasses and allotypes:

From structure to effector functions', *Front. Immunol.*, 5, pp. 1–17. doi: 10.3389/fimmu.2014.00520.

Vincents, B. *et al.* (2004) 'Enzymatic characterization of the streptococcal endopeptidase, IdeS, reveals that it is a cysteine protease with strict specificity for IgG cleavage due to exosite binding', *Biochemistry*, 43(49), pp. 15540–15549. doi: 10.1021/bi048284d.

Wagh, K. *et al.* (2016) 'Optimal combinations of broadly neutralizing antibodies for prevention and treatment of HIV-1 clade C infection', *PLoS Pathog.*, pp. 1–27. doi: 10.1371/journal.ppat.1005520.

Wagh, K. *et al.* (2018) 'Potential of conventional & bispecific broadly neutralizing antibodies for prevention of HIV- 1 subtype A , C & D infections', *PLoS Pathog.*, 14(3), pp. 1–24. doi: 10.1371/journal.ppat.1006860.

Walker, L. M. *et al.* (2009) 'Broad and potent neutralizing antibodies from an African donor reveal a new HIV-1 vaccine target', *Science*, 326(5950), pp. 285–289. doi: 10.1126/science.1178746.Broad.

Walker, L. M. *et al.* (2011) 'Broad neutralization coverage of HIV by multiple highly potent antibodies', *Nature*, 477(7365), pp. 466–470. doi: 10.1038/nature10373.Broad.

Wang, L. *et al.* (2019) 'Glycoengineering of antibodies for modulating functions', *Annu. Rev. Biochem.*, 88(5), pp. 139–148. doi: 10.1146/annurev-biochem-062917-012911.Glycoengineering.

Warrender, A. K. and Kelton, W. (2020) 'Beyond allotypes: the influence of allelic diversity in antibody constant domains', *Front. Immunol.*, 11, pp. 1–9. doi: 10.3389/fimmu.2020.02016.

Washburn, N. *et al.* (2015) 'Controlled tetra-Fc sialylation of IVIg results in a drug candidate with consistent enhanced anti-inflammatory activity', *Proc. Natl. Acad. Sci. U.S.A.*, 112(31), p. E4339. doi: 10.1073/pnas.1512309112.

Wei, X. *et al.* (2002) 'Emergence of resistant human immunodeficiency virus type 1 in patients receiving fusion inhibitor (T-20) monotherapy', *Antimicrob. Agents Chemother.*, 46(6), pp. 1896–1905. doi: 10.1128/AAC.46.6.1896-1905.2002.

Wibmer, C. K. (2016) *Identification, isolation, and characterisation of HIV-1 neutralising antibodies*. University of the Witwatersrand. Available at: https://wiredspace.wits.ac.za/handle/10539/22284.

Wibmer, C. K. *et al.* (2016) ‘Structure of an N276-dependent HIV-1 neutralizing antibody targeting a rare V5 glycan hole adjacent to the CD4 binding site’, *J. Virol.*, 90(22), pp. 10220–10235. doi: 10.1128/jvi.01357-16.

Wibmer, C. K. *et al.* (2017) ‘Structure and recognition of a novel HIV-1 gp120-gp41 interface antibody that caused MPER exposure through viral escape’, *PLoS Pathog.*, 13(1), pp. 1–30. doi: 10.1371/journal.ppat.1006074.

Williams, G. (1999) ‘RevSeq’. Cambridge: EMBOSS. Available at: http://emboss.sourceforge.net/apps/release/6.3/emboss/apps/revseq.html.

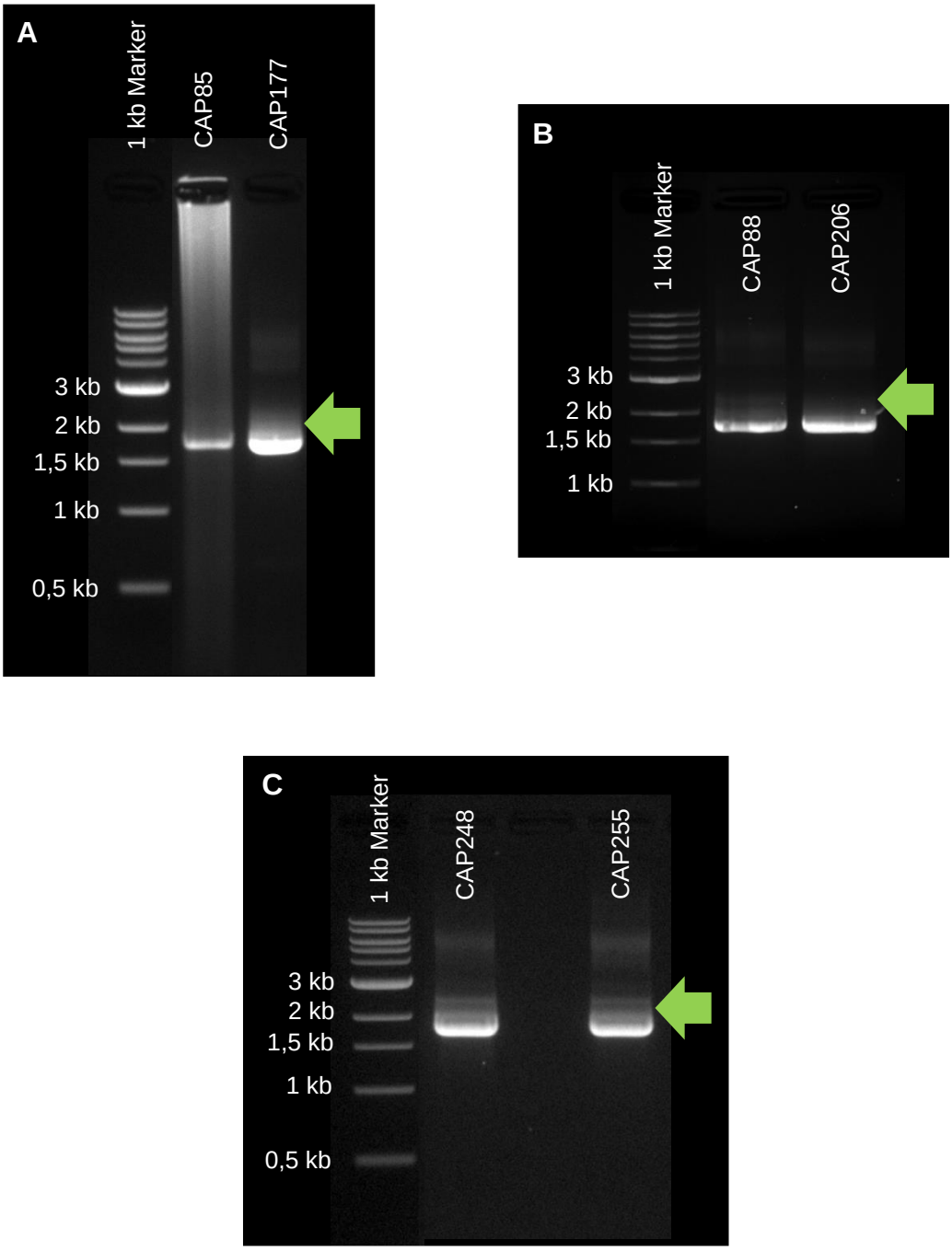
Yacoubi Loveslati, B. *et al.* (2001) ‘A study of Gm allotypes and immunoglobulin heavy gamma IGHG genes in Berbers, Arabs and sub-Saharan Africans from Jerba Island, Tunisia’, *Eur. J. Immunol.*, 28(5), pp. 531–538. doi: 10.1046/j.1365-2370.2001.00254.x.

Yates, N. L. *et al.* (2011) ‘Multiple HIV-1-specific IgG3 responses decline during acute HIV-1’, *Aids*, 25(17), pp. 2089–2097. doi: 10.1097/QAD.0b013e32834b348e.

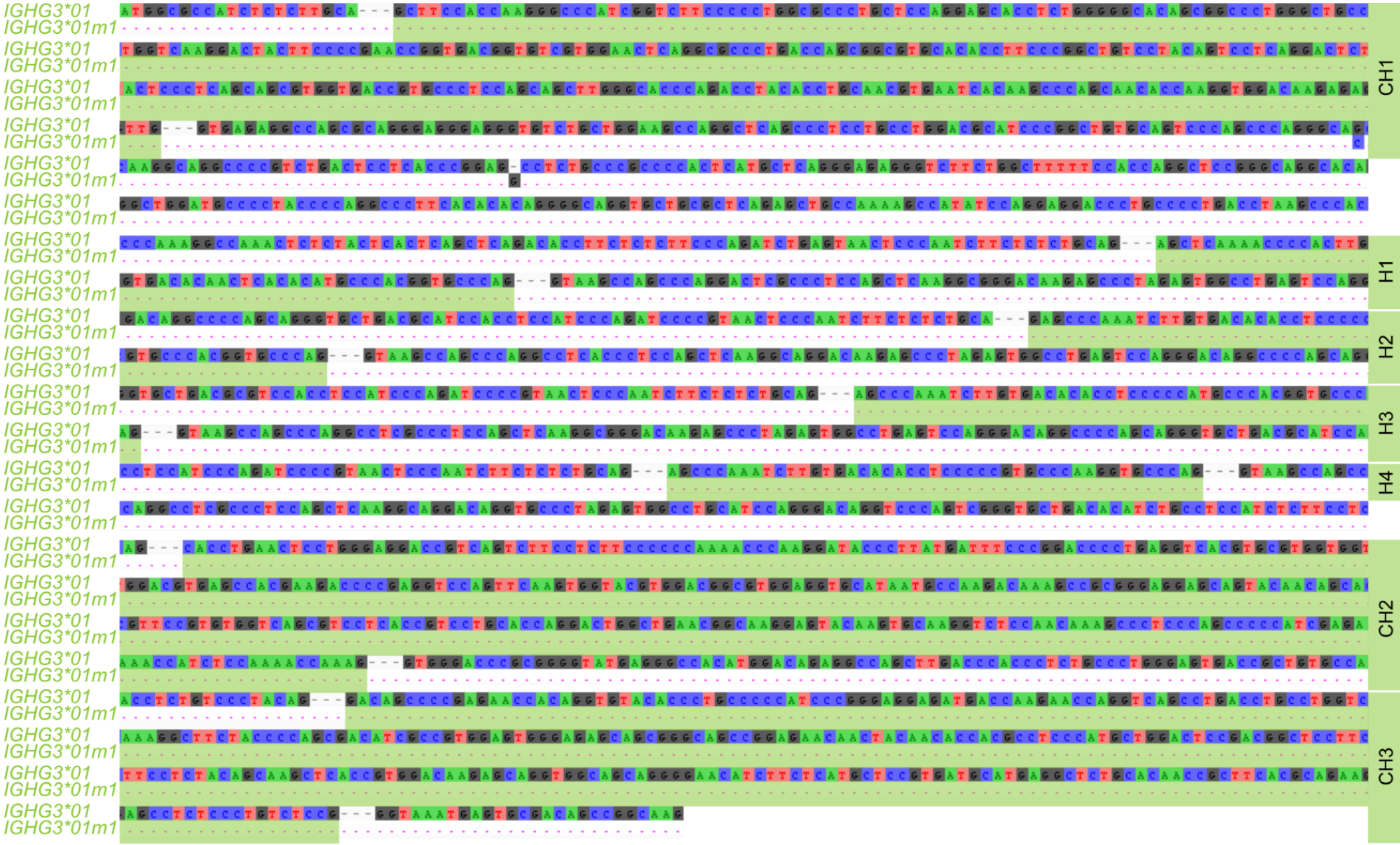
Yates, N. L. *et al.* (2014) ‘Vaccine-induced Env V1-V2 IgG3 correlates with lower HIV-1 infection risk and declines soon after vaccination’, *Sci. Transl. Med.*, 6(228), pp. 1–23. doi: 10.1126/scitranslmed.3007730.

Zhou, T. *et al.* (2018) ‘A neutralizing antibody recognizing primarily N-linked glycan targets the silent face of the HIV envelope’, *Immunity*, 48(3), pp. 500-513.e6. doi: 10.1016/j.immuni.2018.02.013.

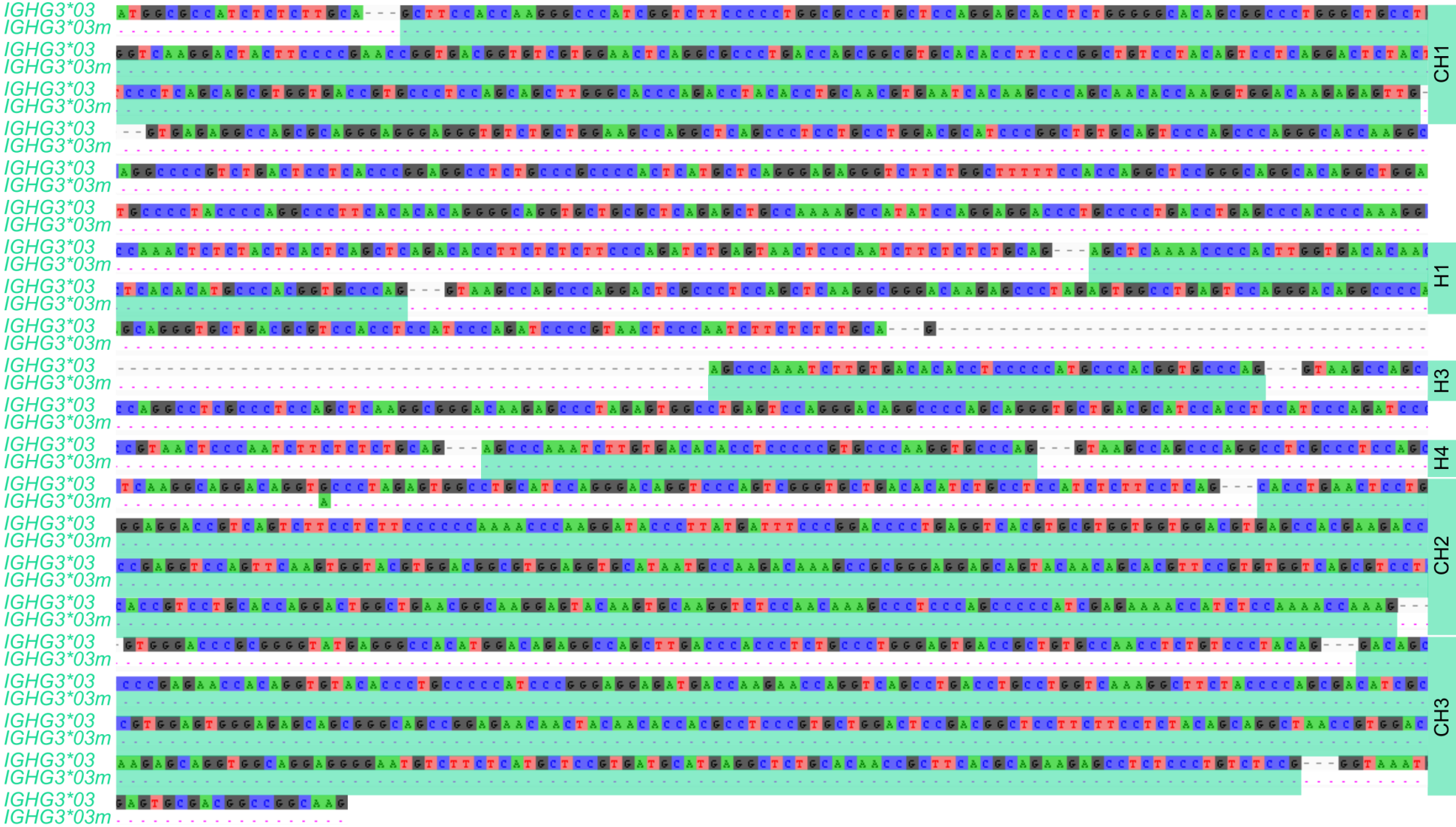
Supplementary



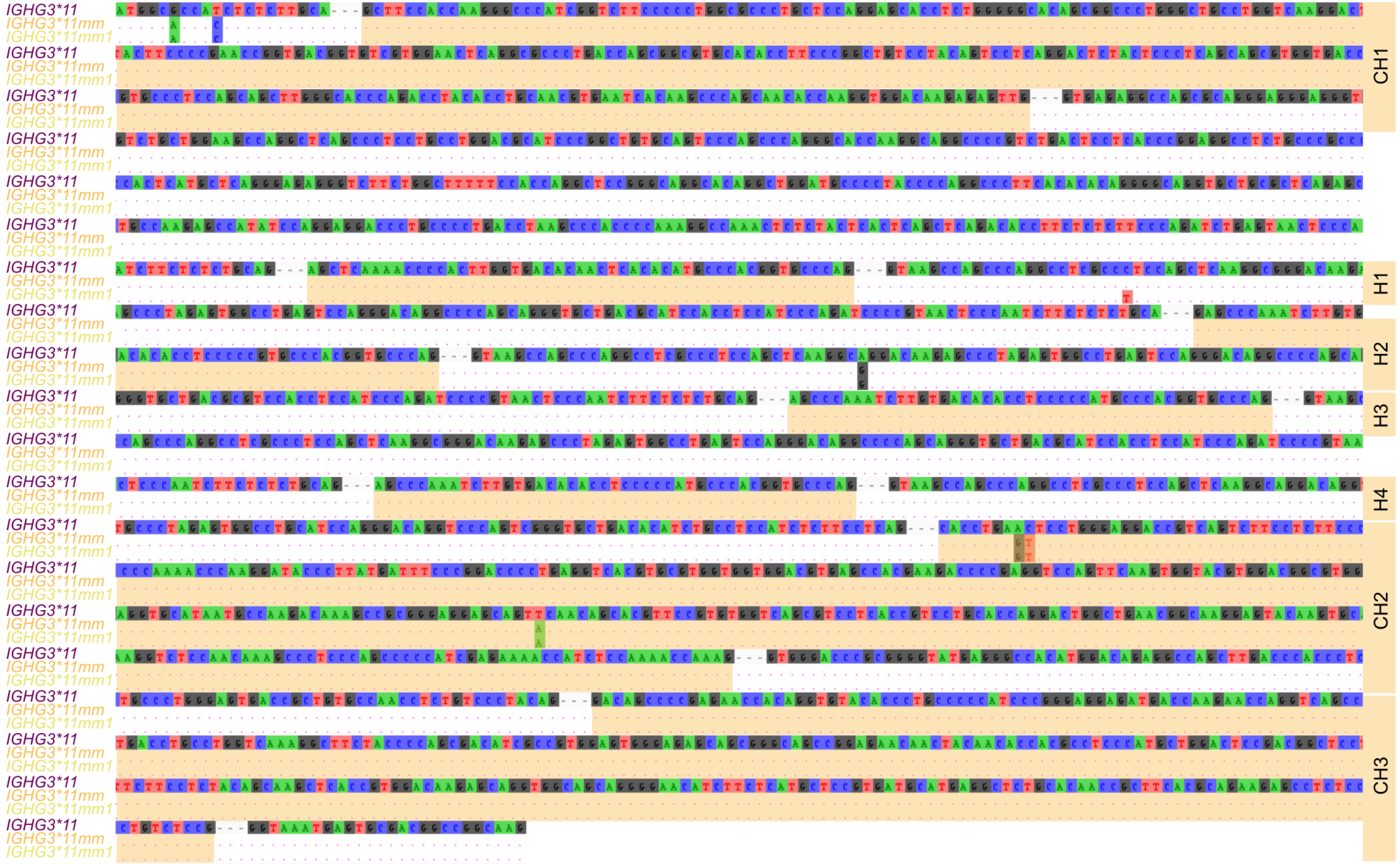
Supplementary Figure 1. The gels generated during Sanger sequencing for the remaining 7 participants. All seven PCRs shown used primer set 1 (F1 and R2). A) CAP85 and CAP177 PCRs. Despite smearing indicating DNA degradation, CAP85 yielded colonies containing *IGHG3.* B) CAP88 and CAP206 PCRs. C) CAP228, CAP248 and CAP255 PCRs.



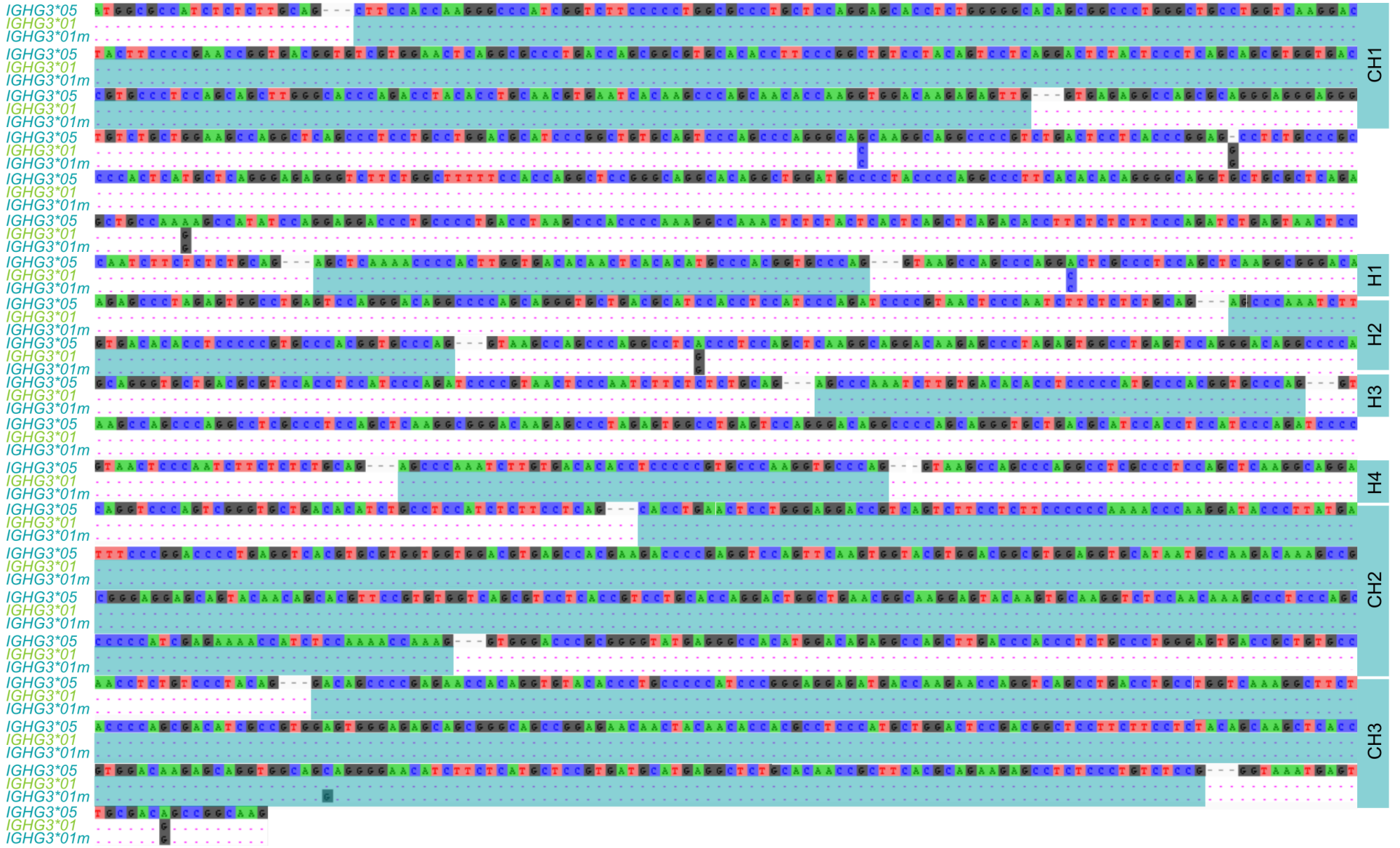
Supplementary Figure 2. The nucleotide sequence of the novel *IGHG3*01m1* aligned to the reference *IGHG3*01*. This allele was identified in CAP177. Exons are shaded in green and labelled on the right of the alignment.



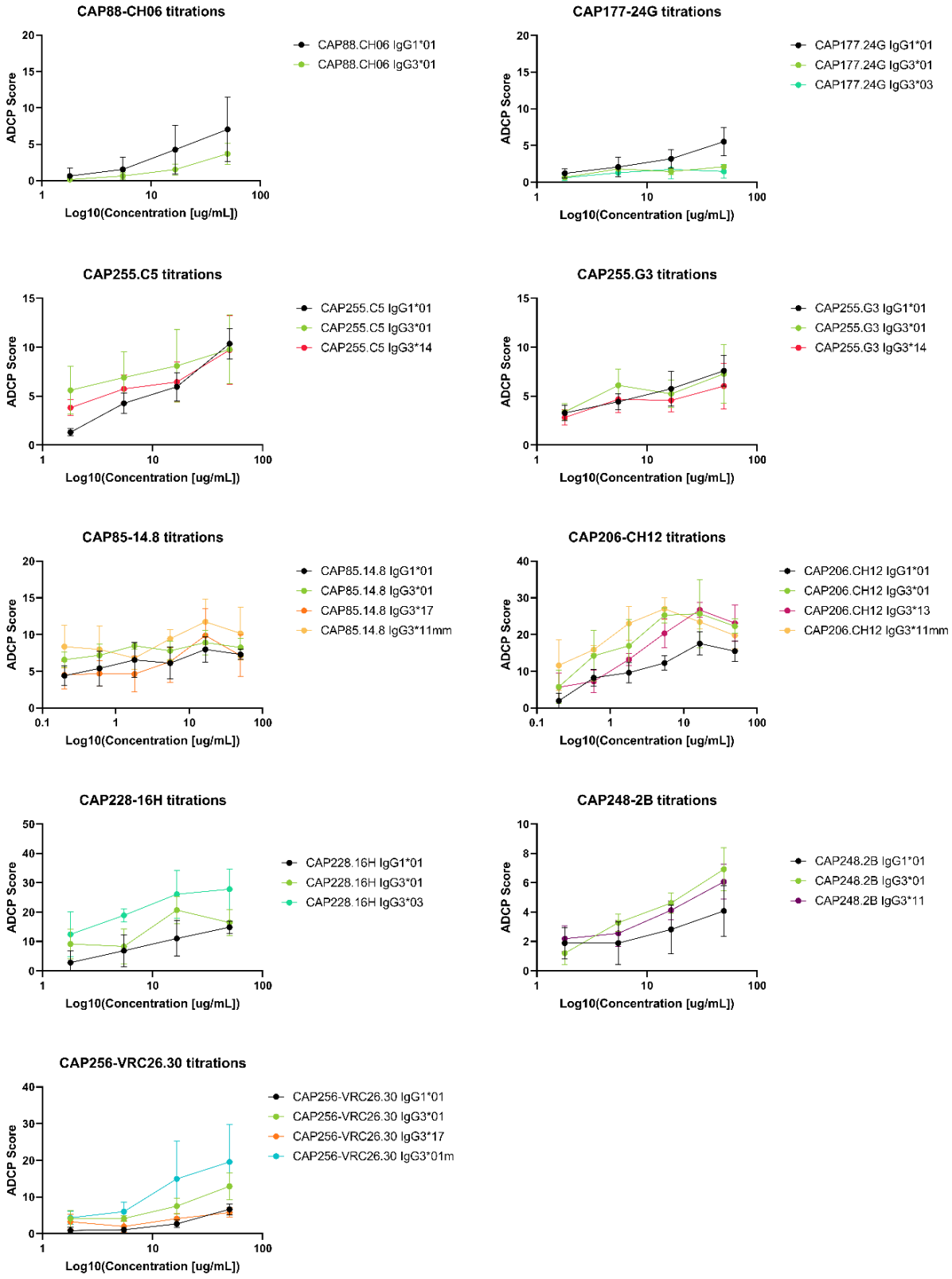
Supplementary Figure 3. The nucleotide sequence of novel allele *IGHG3*03m* aligned to the wildtype *IGHG3*03*. This allele was identified in CAP257. Exons are shaded in teal and labelled on the right of the alignment. *IGHG3*03* is a three-hinge allele, missing hinge 2.



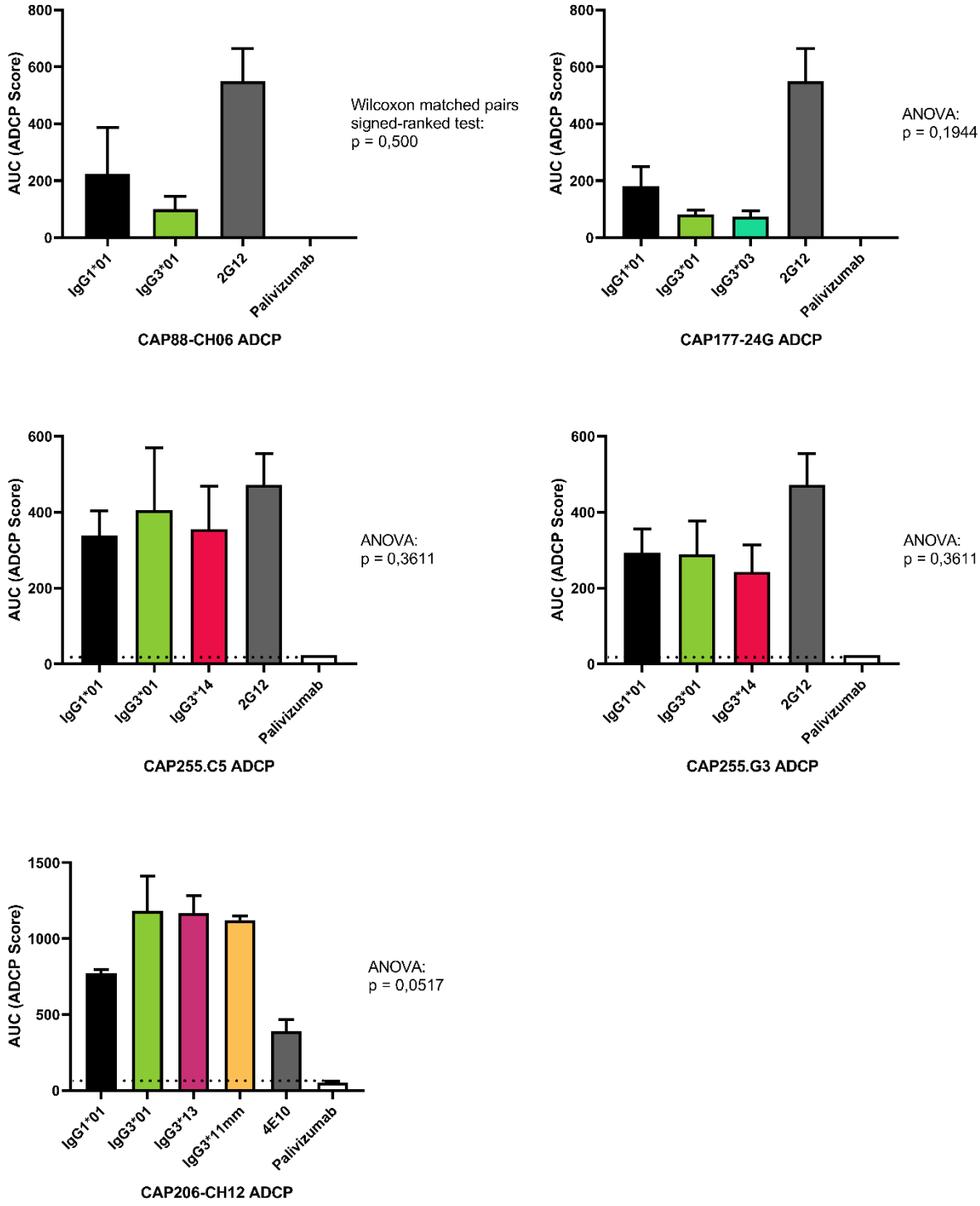
Supplementary Figure 4. The nucleotide sequence of *IGHG3*11mm* and *IGHG3*11mm1* aligned to the closest matching documented allele in IMGT - *IGHG3*11*. *IGHG3*11mm* was identified in CAP85, and *IGHG3*11mm1* in CAP206. Exons are shaded in orange and labelled on the right of the alignment.



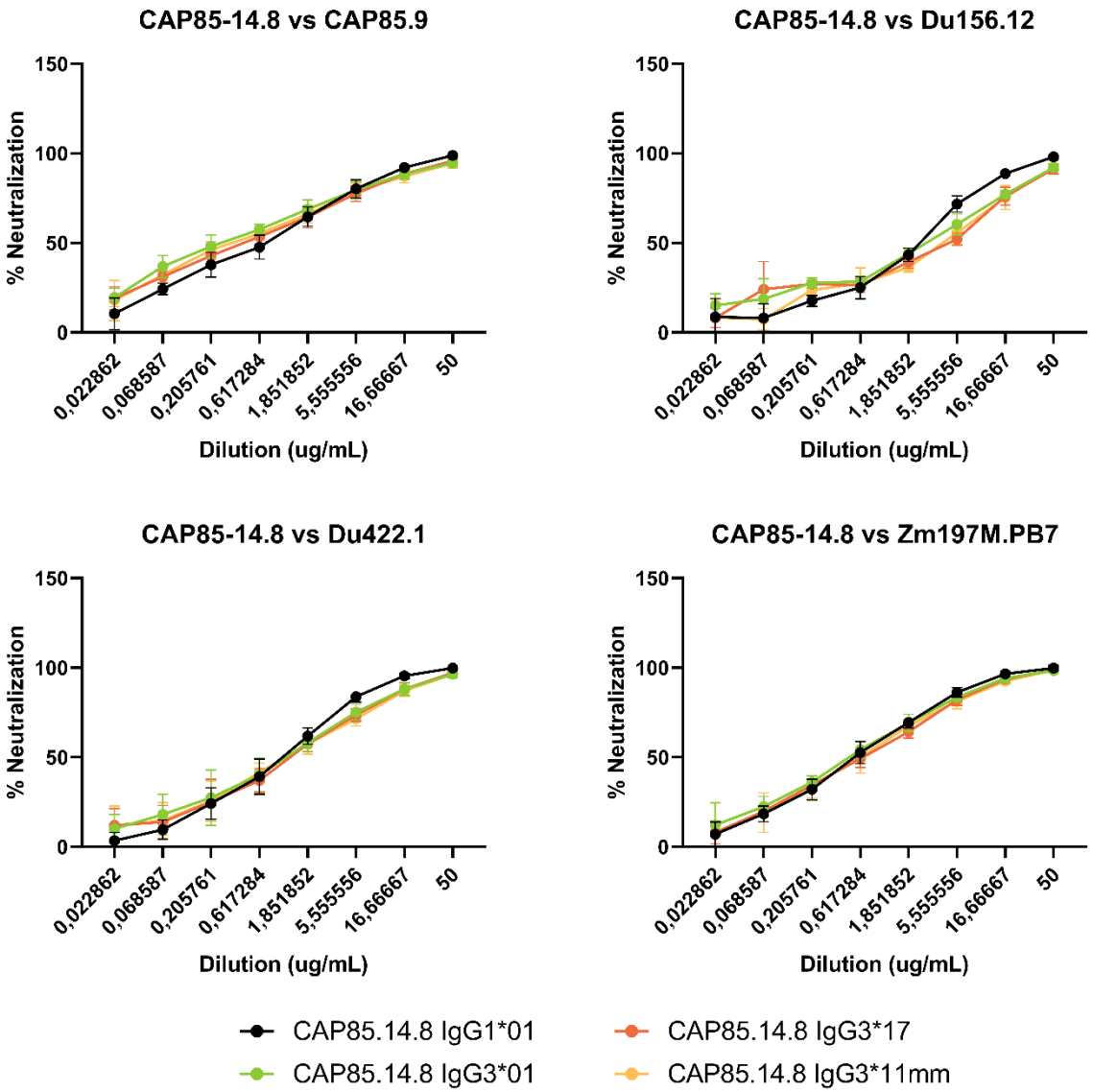
Supplementary Figure 5. The nucleotide sequence of *IGHG3*01m* aligned to the closest matching documented allele in IMGT - *IGHG3*05*. *IGHG3*01m* was named based on its similarity to the documented antibody protein sequences. It's closest matching coding sequence is IgG3*01, however based on nucleotide sequence, *IGHG3*01m* is more similar to *IGHG3*05.*



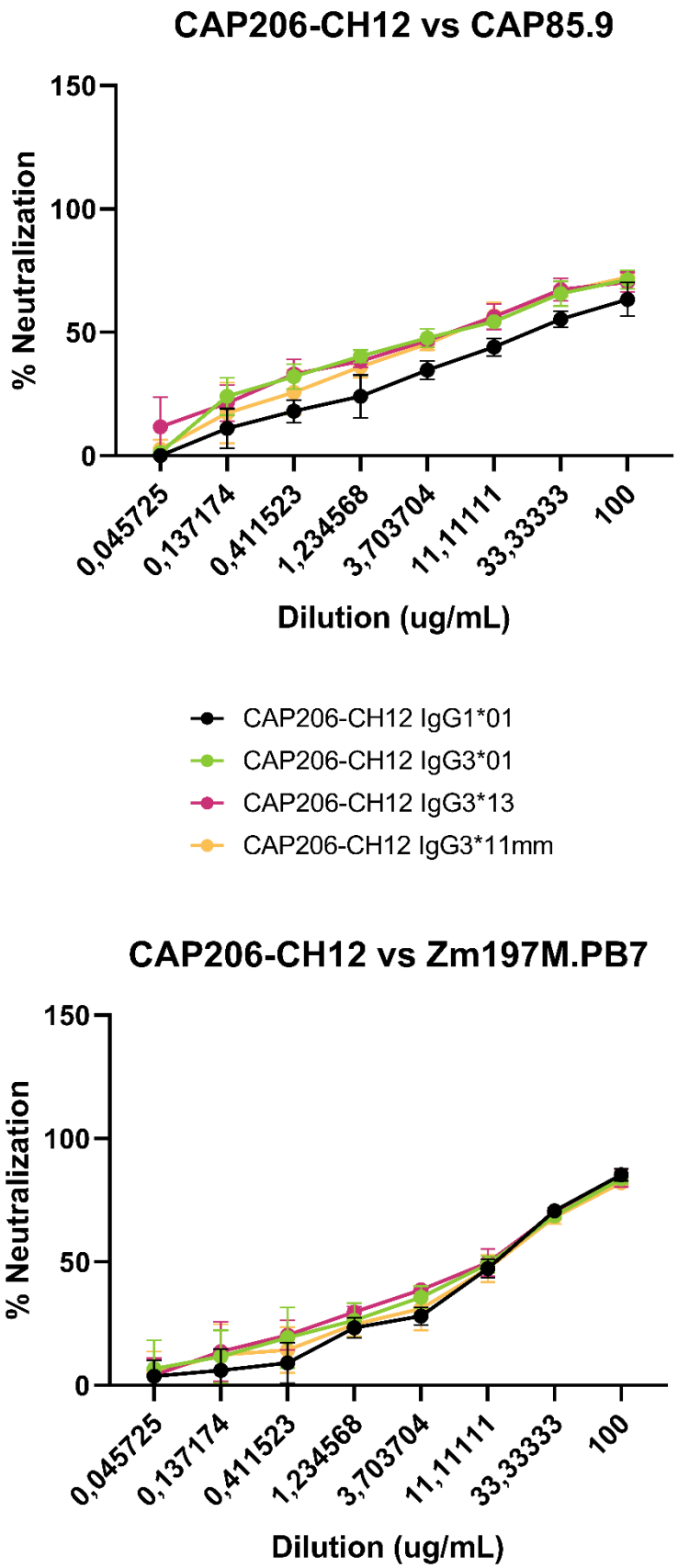
Supplementary Figure 6. A logarithmic graph of each of titration curves for all sets of antibodies in the ADCP assays.



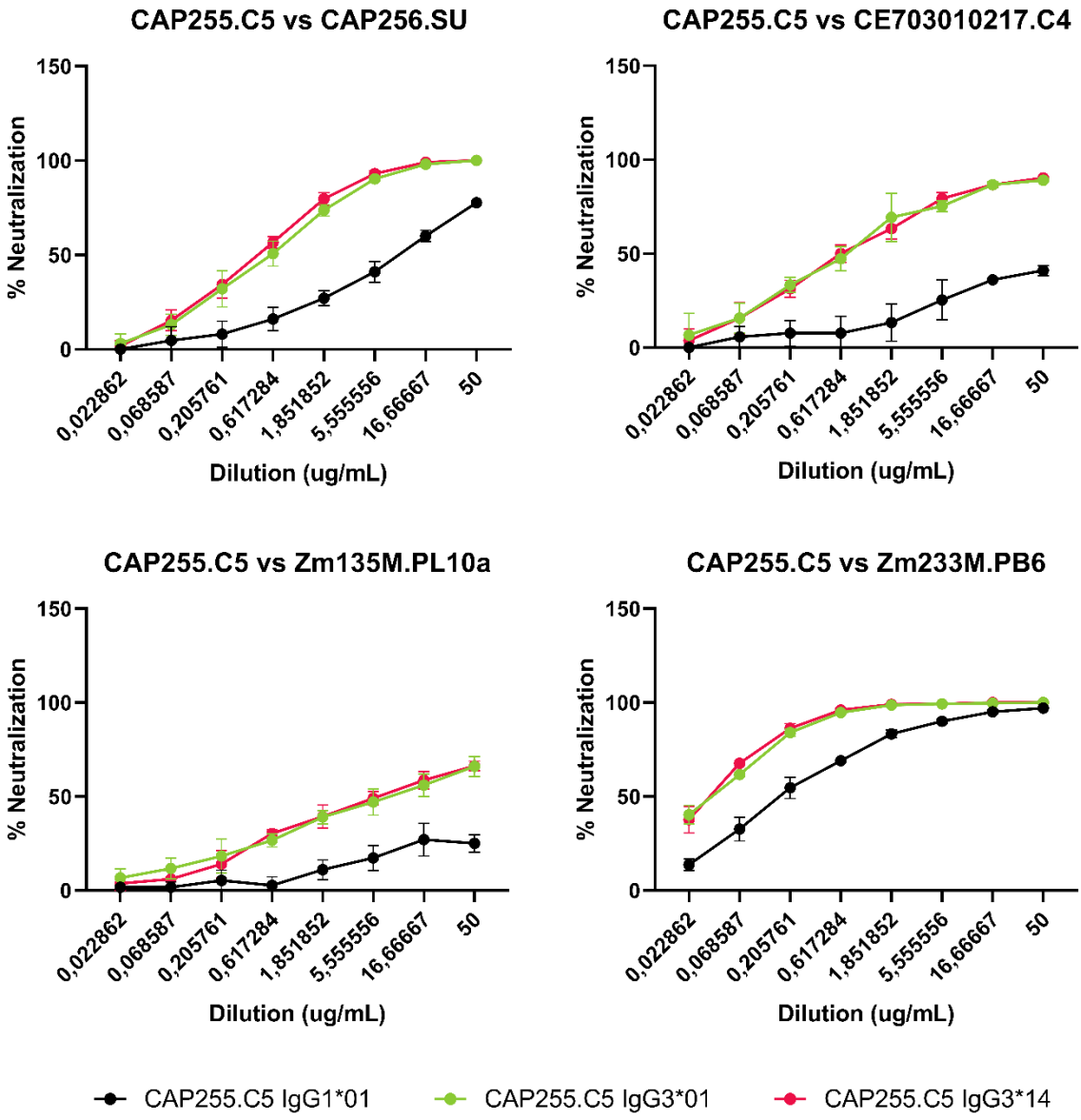
Supplementary Figure 7. The AUC ADCP scores for the five assays that did not demonstrate statistical significance.



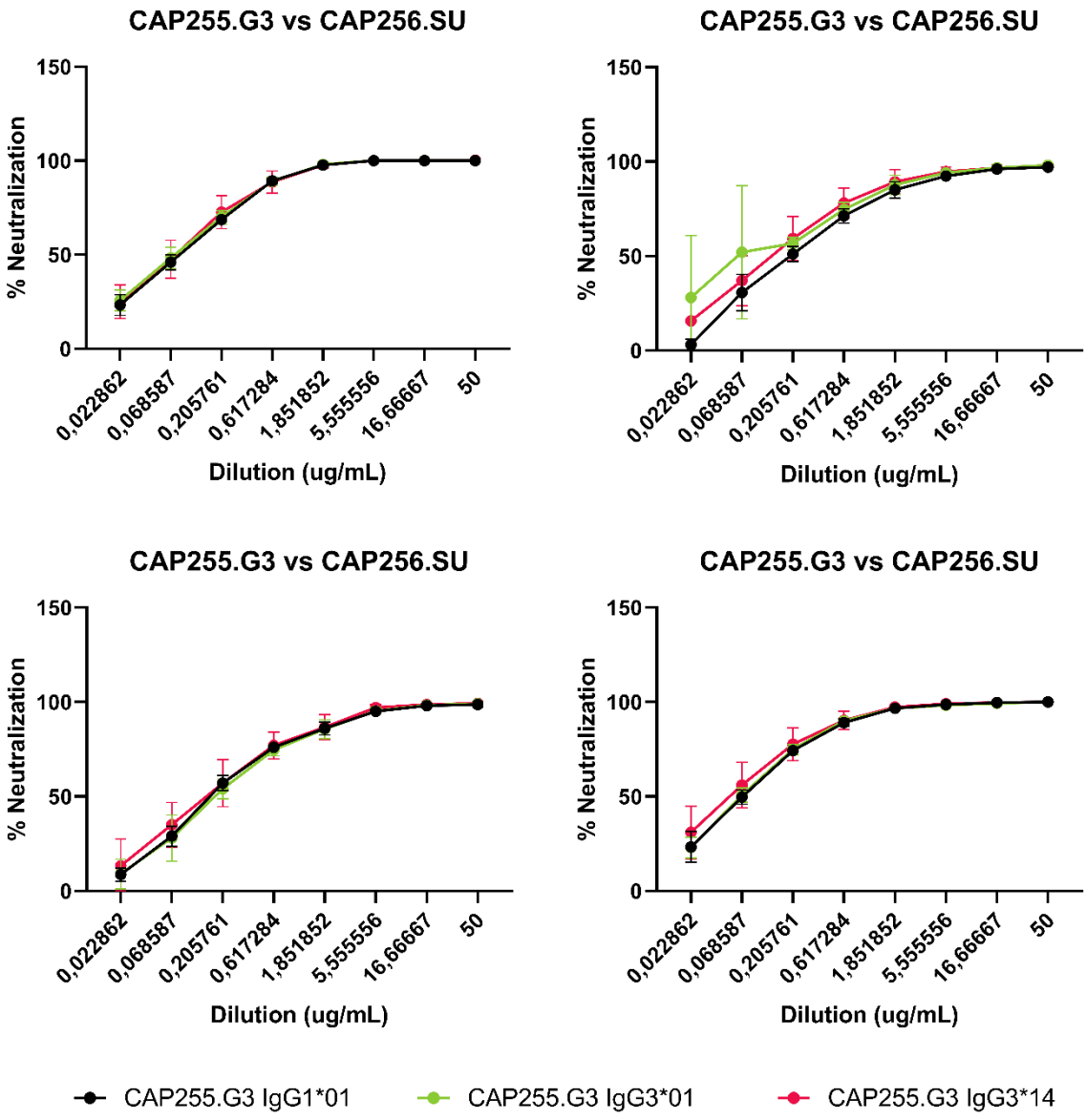
Supplementary Figure 8a. The titration curves of the CAP85-14.8 TZM-bl neutralization assays. CAP85-14.8 antibodies were tested against four viruses, the names of which are above each graph. Each graph is the average of at least three repeats.



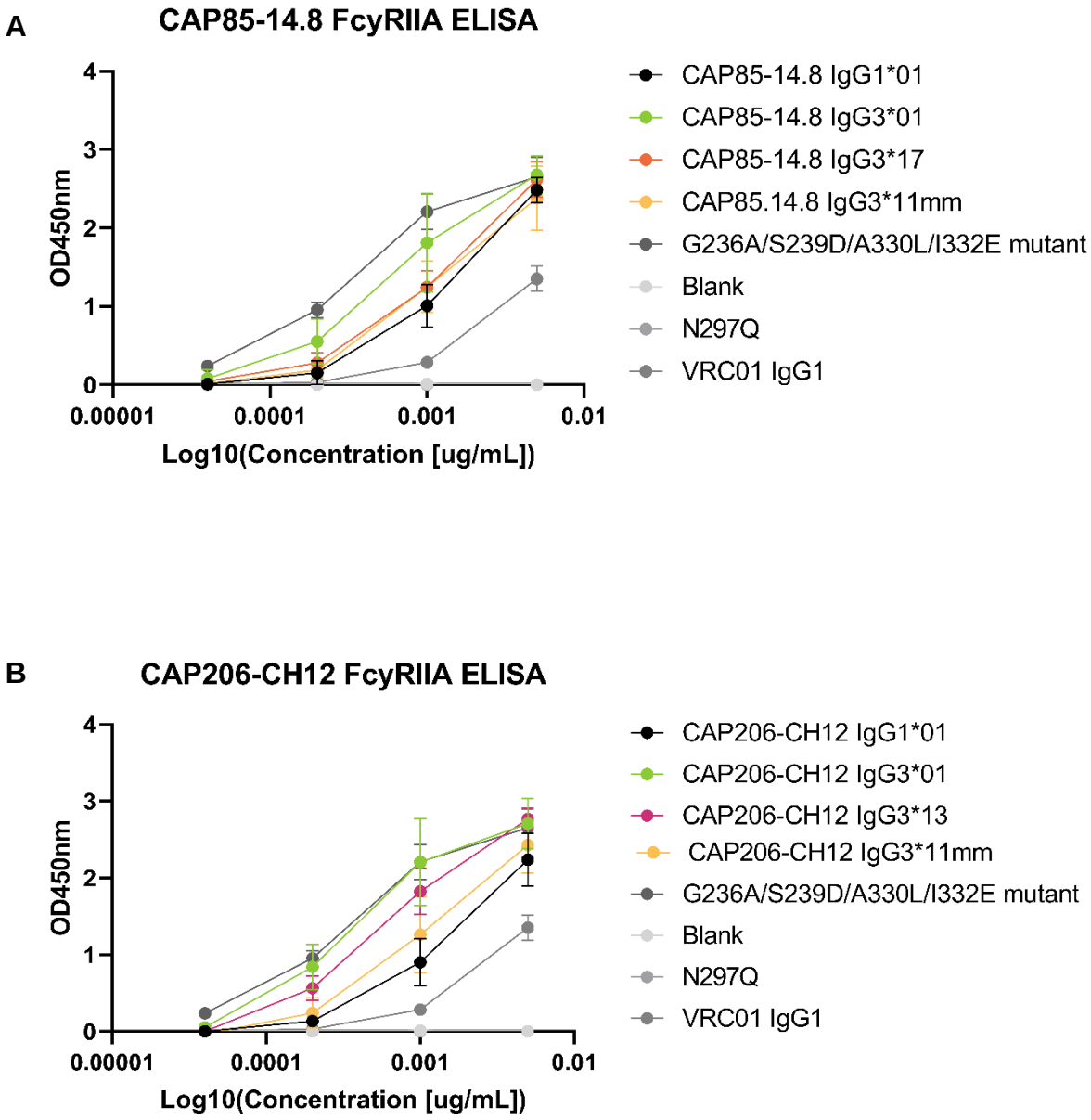
Supplementary Figure 8b. The titration curves of the CAP206-CH12 TZM-bl neutralization assays. CAP206-CH12 antibodies were tested against two viruses, the names of which are above each graph. Each graph is the average of at least three repeats.



Supplementary Figure 8c. The titration curves of the CAP255.C5 TZM-bl neutralization assays. CAP255.C5 antibodies were tested against four viruses, the names of which are above each graph. Each graph is the average of at least three repeats.



Supplementary Figure 8d. The titration curves of the CAP255.G3 TZM-bl neutralization assays. CAP255.G3 antibodies were tested against four viruses, the names of which are above each graph. Each graph is the average of at least three repeats.



Supplementary Figure 9. The titration curves of the FcyRIIA ELISA. A) The CAP85-14.8 antibody affinity for FcγRIIA. B) The CAP206-CH12 antibody affinity for FcγRIIA. Each graph is the average of two repeats, with two replicates each.

Appendix A: CAPRISA Letter of Permission

CAPRISA
CENTRE FOR THE AIDS PROGRAMME OF RESEARCH IN SOUTH AFRICA
Generating Knowledge - Impacting Health

Doris Duke Medical Research Institute (2nd floor), 719 Umbilo Road, Private Bag X7, Congella, 4013, Durban, South Africa
tel: +27 31 2604555 | **fax**: +27 31 2604549 | email: **caprisa@caprisa.org** | www.caprisa.org

02 May 2019

Prof Clement Penny
Chairperson: Human Research Ethics Committee (Medical)
Phillip V Tobias Health Sciences Building
29 Princess of Wales Terrace
Parktown, Johannesburg 2193
South Africa

Dear Prof Penny,

Re: Holly Spencer's MSc study "Functional Impact of Immunoglobulin Heavy Constant Gamma 3 Genetic Variation in Human Immunodeficiency Virus-1 Infection"

In my role as Head of Vaccine and Pathogenesis Research at the Centre for the AIDS Programme of Research in South Africa (CAPRISA) and Co-Chair of the CAPRISA 002 Acute Infection Study, I write to confirm that Ms Holly Spencer will have access to stored samples from the CAPRISA 002 cohort study to carry out the above study for a MSc degree.

Participants in the CAPRISA 002 and 004 studies have consented to stored specimens being used for additional studies. The CAPRISA 002 Informed Consent Form for Specimen Storage: Phase V - Antiretroviral therapy (V4.00) approved by the University of KwaZulu-Natal Biomedical Research Ethics Committee and attached here, states that: "*We may test your cells, proteins, other chemicals in your body and genes (DNA). Some of the samples will also be tested to see how your nutritional status may be interacting with HIV infection. Your samples may be analysed in laboratories outside of South Africa".*

Ms Holly Spencer's study will be supervised by Dr Cathrine Scheepers, Prof Penny Moore and Dr Simone Richardson and represents a continuation of our successful collaboration with Profs Moore and Morris' laboratory at the National Institute for Communicable Diseases, Johannesburg.

Please do not hesitate to contact me if there are any queries.

Yours sincerely,



Dr Nigel Garrett
MBBS, MRCP, MSc, PhD
Head of Vaccine and Pathogenesis Research, CAPRISA
Honorary Lecturer in Public Health, University of KwaZulu-Natal
Doris Duke Medical Research Institute (2nd Floor)
Nelson R Mandela School of Medicine, University of KwaZulu-Natal
Durban, South Africa Tel: +27 31 655 0617 (ECRS) +27 31 260 4453 (DDMRI)
Email: nigel.garrett@caprisa.org

CAPRISA hosts a DST-NRF Centre of Excellence in HIV Prevention
CAPRISA is the UNAIDS Collaborating Centre for HIV Research and Policy
CAPRISA hosts a MRC HIV-TB Pathogenesis and Treatment Research Unit

Partner Institutions:

Board of Control: B Ntuli (Chair) · M Rajab (Deputy Chair) · Q Abdool Karim · SS Abdool Karim · AC Bawa · D Clark · JM Frantz · LP Fried (US) · S Madhi · K Naidoo · N Padayatchi · RM Phakeng · D Ramjugernath · ZM Yacoob
Scientific Advisory Board: F Barré-Sinoussi (Chair) · T Quinn (Vice Chair) · SM Dhlomo · P Godfrey-Faussett · R Hayes · G Hirnschall · J Mascola · Y Pillay · S Swaminathan

Registration number: 2002/024027/08 • PBO number: 930 018 155

Appendix B: Ethics Clearance Certificate

UNIVERSITY OF THE WITWATERSRAND, JOHANNESBURG

R14/49 Ms Holly Spencer et al

HUMAN RESEARCH ETHICS COMMITTEE (MEDICAL)

CLEARANCE CERTIFICATE NO. M190564

NAME: (Principal Investigator)	Ms Holly Spencer et al
DEPARTMENT:	Virology National Institute for Communicable Diseases (NICD) Centre for HIV and STIs
PROJECT TITLE:	Functional impact of immunoglobulin heavy constant gamma 3 genetic variation in Human Immunodeficiency Virus-1 Infection
DATE CONSIDERED:	31/05/2019
DECISION:	Approved unconditionally
CONDITIONS:	
SUPERVISOR:	Dr Cathrine Scheepers
APPROVED BY:	CB Penny Dr CB Penny, Chairperson, HREC (Medical)
DATE OF APPROVAL:	24/07/2019

This clearance certificate is valid for 5 years from date of approval. Extension may be applied for.

DECLARATION OF INVESTIGATORS

To be completed in duplicate and **ONE COPY** returned to the Research Office Secretary on the Third Floor, Faculty of Health Sciences, Phillip Tobias Building, 29 Princess of Wales Terrace, Parktown, 2193, University of the Witwatersrand. I/we fully understand the conditions under which I am/we are authorized to carry out the above-mentioned research and I/we undertake to ensure compliance with these conditions. Should any departure be contemplated, from the research protocol as approved, I/we undertake to resubmit the application to the Committee. **I agree to submit a yearly progress report**. The date for annual re-certification will be one year after the date of convened meeting where the study was initially reviewed. In this case, the study was initially reviewed in **May** and will therefore be due in the month of **May** each year. Unreported changes to the application may invalidate the clearance given by the HREC (Medical).

Principal Investigator Signature Date

PLEASE QUOTE THE PROTOCOL NUMBER IN ALL ENQUIRIES

Appendix C: Turnitin Report Cover Page

Turnitin Originality Report

Processed on: 13-Sep-2021 10:08 AM SAST
ID: 1647255313
Word Count: 23263
Submitted: 1

HollySpencer_MSc_Dissertation_Final.docx By Holly Spencer

Similarity Index	Similarity by Source
16%	Internet Sources: 13% Publications: 10% Student Papers: 5%

1% match (Internet from 06-Apr-2021)
http://wiredspace.wits.ac.za/bitstream/handle/10539/23160/PhD%20thesis_Sonwabile%20Dzanibe.pdf?isAllowed=y&sequence=1

< 1% match (Internet from 06-Apr-2021)
http://wiredspace.wits.ac.za/bitstream/handle/10539/5705/Research%20Report%20Binder.pdf?isAllowed=y&sequence=1

< 1% match (Internet from 06-Apr-2021)
http://wiredspace.wits.ac.za/bitstream/handle/10539/2117/MSc%28Med%29%20Dissertation.pdf?isAllowed=y&sequence=3

< 1% match (Internet from 06-Apr-2021)
http://wiredspace.wits.ac.za/bitstream/handle/10539/5604/Stoyan_Stoychev%20PhD_thesis_%26_appendix.pdf?isAllowed=y&sequence=1

< 1% match (Internet from 25-Jul-2020)
https://journals.plos.org/plospathogens/article?id=10.1371%2Fjournal.ppat.1008064

< 1% match (Internet from 16-Feb-2020)
https://journals.plos.org/plosntds/article?id=10.1371%2Fjournal.pntd.0005330

< 1% match (Internet from 22-Jul-2019)
https://journals.plos.org/plosone/article?id=10.1371%2Fjournal.pone.0198629

< 1% match (Internet from 25-Jul-2019)
https://journals.plos.org/plosone/article?id=10.1371%2Fjournal.pone.0200080

< 1% match (Internet from 09-Sep-2020)
https://journals.plos.org/plospathogens/article?id=10.1371%2Fjournal.ppat.1006987

< 1% match (Internet from 11-Mar-2019)
https://journals.plos.org/plospathogens/article?id=10.1371%2Fjournal.ppat.1005989

< 1% match ()
Wibmer, Constantinos Kurt. "Identification, isolation, and characterisation of HIV-1 neutralising antibodies", 2016

< 1% match ()
Mostert, Ilani. "Genetic diversity and identification of putative recombination events in Grapevine rupestris stem pitting-associated virus", Stellenbosch : Stellenbosch University, 2017

< 1% match ()
Kanhayuwa, Lakkhana. "Development of silencing vectors for Aspergillus fumigatus based on mycoviruses and short interspersed nuclear elements", Life Sciences, Imperial College London

< 1% match ()
Tekiner, Tuğçe Ayça. "Regulation Of Pi3k/akt Signalling Pathway In Pediatric Acute Myeloid Leukemia (aml): A Novel Tumour-suppressor Phlpp", Institute of Science and Technology, 2009

< 1% match ()
Breaux, Breanna Laine. "The Florida Manatee Adaptive Immune Receptor Genes Reveal Novel Patterns in Mammalian Evolution", 2019

< 1% match ()
Bhiman, Jinal Nomathemba. "Defining virus-antibody interplay during the development of HIV-1 neutralization breadth to inform vaccine design", 2016

< 1% match ()
Gumede, Nomathemba Michell. "Molecular detection of atypical bacteria and viruses linked to community-acquired pneumonia", 2009

< 1% match ()
Oellermann, Michael. "Blue Blood on Ice: Cephalopod haemocyanin function and evolution in a latitudinal cline", Bremen University, 2015

< 1% match (Internet from 18-Jul-2021)
https://www.frontiersin.org/articles/10.3389/fdata.2021.672460/full

< 1% match (Internet from 19-Jul-2021)
https://www.frontiersin.org/articles/10.3389/fimmu.2021.702705/full

< 1% match (Internet from 19-Feb-2020)
https://www.frontiersin.org/articles/10.3389/fimmu.2019.02415/full